DIPARTIMENTO DI SCIENZE CARDIOLOGICHE, TORACICHE E VASCOLARI

UNIVERSITÀ DEGLI STUDI DI PADOVA

SCUOLA DI DOTTORATO DI RICERCA IN SCIENZE MEDICHE, CLINICHE E SPERIMENTALI

INDIRIZZO: METODOLOGIA CLINICA, SCIENZE ENDOCRINOLOGICHE, DIABETOLOGICHE E NEFROLOGICHE

XXVIII CICLO

GLUCOTOXICITY, PROTEIN GLYCATION AND ADIPOSE TISSUE DYSFUNCTION

DIRETTORE DELLA SCUOLA: CH.MO PROF. GAETANO THIENE
COORDINATORE D'INDIRIZZO: CH.MO PROF. ROBERTO VETTOR
SUPERVISORE: CH.MO PROF. ROBERTO VETTOR

DOTTORANDA: ALESSIA FAGGIAN

Non esiste vento favorevole

per il marinaio che non sa dove andare

[Seneca]

ABSTRACT

Introduction: Glycation is a non-enzymatic reaction between a sugar and a free-amino group contained in molecules such as proteins, amino acids, DNA, RNA, and lipids. In the initial phase, the carbonyl group of the reducing carbohydrate condenses with the free-amino group on the biomolecule to form a reversible glycosylamine, which is then converted to a more stable Amadori product. Once formed, these products can with time undergo to dehydration, cyclization, oxidation, and rearrangements forming a polymorphic group of compounds collectively referred as Advanced Glycation End-products (AGEs). The accumulation of AGEs *in vivo* is considered the most important link between diabetes and oxidative disease. The rate of glycation could account for the long-term diabetic complications. Nevertheless, the role of AGEs is yet to be determined and it is, still nowadays, an important and challenging field of study. Little is known about their presence and their consequences on adipose tissue; in particular, the role of AGEs on adipogenesis and fat cell functionality remains fully unexplored.

Methods: In this project, 3T3-L1 cell line and stromal vascular fraction cells isolated from human adipose tissue were used. The purpose was to set up an *in vitro* model for investigating the effects of a chronic exposure to a glycation-inducing environment on the adipogenetic process. Morphological analyses, E.L.I.S.A. assay for AGEs, expression analysis of lipid and glucose metabolism genes, glucose uptake, and immunofluorescence for RAGE, GLP1r, GLUT4 and AGEs, were performed on mature adipocytes. Moreover, the gene expression profile obtained *in vitro*, was compared to that of subcutaneous and visceral adipose tissues obtained from 64 obese subjects with type 2 diabetes or with normal glucose tolerance underwent to bariatric surgery. In collaboration with the Mass Spectrometry Service (CNR – IENI Padova), the use of mass spectrometry to characterize post-translation modifications induced by glycation was evaluated.

Results and conclusions: Following an exposition to a glycation-inducing environment, an increase of intracellular AGEs both by immunofluorescence and E.L.I.S.A. was observed in our *in vitro* model. Preliminary analysis on cell cultures suggested that a glycation-inducing environment importantly impacts on gene expression profile. In glycating conditions, an increased expression of *Glut4* and, on the contrary, an insulin-induced glucose uptake reduction was observed. These results allow us to hypothesize an influence of AGEs on GLUT4 translocation to the plasma-membrane and/or on its functionality. Finally, although mass spectrometry represents a high potential technique was shown that it has several disadvantages and technical challenges. In particular, several post-translational modifications can affect simultaneously the same protein,

thus the total mass increase will reflect the sum of all modifications. Furthermore, spectra analysis of a whole cellular or tissue lysates resulted excessively complex to underline small differences. Multiple steps in which proteins of a specific molecular weight range would be isolated, concentrated and separately assayed are therefore required in order to simplify the analysis by mass spectrometry.

SOMMARIO

Introduzione: La glicazione è una reazione non enzimatica tra uno zucchero e un gruppo amminico contenuto in molecole come proteine, aminoacidi, DNA, RNA e lipidi. Nella fase iniziale, il gruppo carbonilico del carboidrato riducente condensa con il gruppo amminico libero delle biomolecole formando una glicosil-ammina reversibile, la quale verrà poi convertita in un prodotto più stabile, detto prodotto di Amadori. Nel tempo, tali prodotti possono subire processi di disidratazione, ciclizzazione, ossidazione e riarrangiamenti formando un gruppo polimorfico di composti indicati come prodotti di glicazione avanzata (AGEs). L'accumulo degli AGEs *in vivo* è considerato il più importante collegamento tra il diabete e la malattia ossidativa. In particolare, il tasso di glicazione potrebbe spiegare le complicanze diabetiche a lungo termine. Tuttavia, la loro presenza a livello del tessuto adiposo ed il loro ruolo nell'adipogenesi e nella funzionalità dell'adipocita, non sono ancora stati del tutto determinati e sono a tutt'oggi un importante e stimolante campo di ricerca.

Metodi: In questo progetto, sono state utilizzate cellule 3T3-L1 e cellule della frazione vasculo-stromale isolate dal tessuto adiposo umano allo scopo di costruire un modello *in vitro* per indagare gli effetti indotti sul differenziamento adipogenico dovuti da una esposizione cronica ad un ambiente inducente la glicazione. Sugli adipociti maturi ottenuti *in vitro* sono stati eseguite: analisi morfologiche, saggi E.L.I.S.A. per gli AGEs, analisi di espressione di geni coinvolti nel metabolismo lipidico e glucidico, misurazione della capacità di captazione del glucosio ed analisi di immunofluorescenza per RAGE, GLP1r, GLUT4 ed AGEs. È stata inoltre confrontata l'espressione genica ottenuta *in vitro*, con quella misurata nelle biopsie di tessuto adiposo viscerale e sottocutaneo di 64 soggetti obesi con diabete di tipo 2 o con normale tolleranza al glucosio sottoposti ad intervento di chirurgia bariatrica.
In collaborazione con il servizio di Spettrometria di Massa (CNR – IENI, Padova), è stato valutato l'utilizzo della spettrometria per la caratterizzazione delle eventuali modifiche post-traduzionali indotte dalla glicazione.

Risultati e conclusioni: È stato osservato, sia mediante immunofluorescenza, sia mediante test E.L.I.S.A., che un ambiente inducente alla glicazione porta effettivamente ad un aumento degli AGEs intracellulari. Analisi preliminari delle colture cellulari, inducono ad ipotizzare che possano esistere alcuni effetti indotti dall'ambiente glicante sull'espressione genica. In condizioni glicanti, è stata osservata un'aumentata espressione di *Glut4* e una ridotta captazione di glucosio che suggerisce una probabile influenza degli AGEs sulla traslocazione e/o sulla funzionalità del trasportatore del glucosio. Tale osservazione suggerisce che possa esistere una probabile

influenza degli AGEs sulla traslocazione /o sulla funzionalità del trasportatore del glucosio.

Nonostante la spettrometria di massa sia una metodica molto sensibile ed abbia alte potenzialità, ha anche alcuni svantaggi: modifiche post traduzionali, siano esse enzimatiche o non-enzimatiche, possono essere contemporaneamente presenti sulla stessa proteina; pertanto, l'incremento di massa totale rifletterà la somma di tutte le modifiche. Lo spettro di un lisato intero, si è dimostrato eccessivamente complesso per poter apprezzare piccole differenze. Risulta pertanto necessaria un'analisi composta da più passaggi in cui, in prima istanza verrà isolata e concentrata una frazione di proteine caratterizzate da uno specifico range di peso molecolare che solo in seguito verrà analizzata mediante spettrometria di massa; suddividendo in questo modo l'intero spettro in piccole parti.

TABLE OF CONTENTS

ABBREVIATIONS

AGER	See RAGE
AGEs	Advanced Glycation End-products
ALEs	Advanced Lipoxidation End-products
AT	Adipose Tissue
BAT	Brown Adipose Tissue
BMI	Body Mass Index
BSA	Bovine Serum Albumin
BSA-AGE	BSA Advanced Glycation End-products
BSA-MGO	BSA Glycated with Methylglyoxal
BSA-neg	BSA Negative control/not glycated
cAMP	Cyclic Adenosine Monophosphate
cDNA	Complementary DNA
DAPI	4',6-diamidino-2-phenylindole
DIO	Diet-Induced Obesity
DMEM	Dulbecco's Modified Eagle Medium
DMSO	Dimethyl Sulfoxide
DNA	Deoxyribonucleic Acid
dNTPs	Deoxy-Nucleotides Triphosphates
DPP4	Dipeptidyl Peptidase-4
EDTA	Ethylenediaminetetraacetic
ESI	Electrospray Ionization
FBS	Fetal Bovine Serum
FFAs	Free Fatty Acids
FWHM	Full Width at Half Height
GDP	Guanosine Diphosphate
GIP	Glucose-dependent Insulinotropic Polypeptide
GLO1	Glyoxalase 1
GLP1	Glucagon-like Peptide-1
GLP1r	Glucagon-like Peptide-1 receptor
GLUT4/ SLC2A	Glucose Transporter 4/ solute carrier family 2 member 4
GPCR	G protein-coupled receptors
GTP	Guanosine Triphosphate
HbA1c	Glycated Haemoglobin
HFCS	High fructose corn syrup
hSVF	human Stromal Vascular Fraction

ABBREVIATIONS

IBMX	Isobutilmetilxantina
IF	Immunofluorescence
IL	Interleukin
LEP	Leptin
LPL	Lipoprotein Lipase
m/z	Mass/charge
MAF	Fraction of mature adipocytes
MALDI	Matrix-Assisted Laser Desorption Ionization
MAPK	Mitogen-activated protein kinase
MGO	Methylglyoxal
miRNAs	Small non-coding RNAs
MMP	Matrix Metallopeptidase
MS	Mass Spectrometry
MTT	3-[4,5-dimethylthiazol-2-yl]-2,5 diphenyl tetrazolium bromide
NAFLD	Non-alcoholic fatty liver disease
NF-kB	Transcription Nuclear Factor-Kb
PBS	Phosphate buffered saline
PCG1α	Proliferator-activated receptor coactivator 1 alpha
PCR	Polymerase chain reaction
PPARγ	Peroxisome proliferator-activated receptor γ
RAGE	Receptor of AGEs
RNA	Ribonucleic acid
RNS	Reactive nitrogen species
ROS	Reactive oxygen species
RPMI 1640	Roswell Park Memorial Institute
SAT	Subcutaneous adipose tissue
SIRT	Sirtuin
T1DM	Type 1 diabetes mellitus
T2DM	Type 2 diabetes mellitus
TNF α	Tumor necrosis factor α
TOF	Time of Flight
UCP1	Uncoupling protein-1
VAT	Visceral adipose tissue
WAT	White adipose tissue
WHO	World Health Organization

1. INTRODUCTION

1.1 ADIPOCYTE AND ADIPOSE TISSUE

Energy homeostasis and reproduction are arguably the two most important biological function of any organism; the adipose tissue is inextricably entwined with both.

The main role of adipose tissue, or fat, is to store energy, although it also cushions and insulates the body; other functions are to give mechanic protections for organs, insulation and streamlining in aquatic mammals. Maintaining an appropriate amount of adipose tissue is essential for optimal health. Outside healthy levels lead to adverse consequences having too little amount results in anorexia or cachexia, an inappropriate redistribution of adipose tissue results in lipodystrophy and too much results in obesity (1). The major constituent of adipose tissue is called adipocyte, this cell type is proposed to share a common precursor with osteoblasts, chondrocytes and myocytes. The adipocytes are surrounded by a basement membrane, composed of collagen, laminin and heparan sulfate proteoglycans The fat cells are adapted for their main function, to store and release energy; them are among the largest cells of the body and can increase in size by storing the surplus of energy by incorporating more triglycerides in the lipid droplet during periods of energy excess, while during conditions of fasting, hypocaloric diets and exercise, lipolysis becomes crucial, releasing energy-rich free fatty acids (FFAs) and glycerol.

Adipose tissue mass increases by two mechanisms the hyperplasia in which the cells number increase and the hypertrophy in which enlarge the lipid deposition. Genetic and diet affect the relative contributions of these two mechanisms to the growth of adipose tissue in obesity.

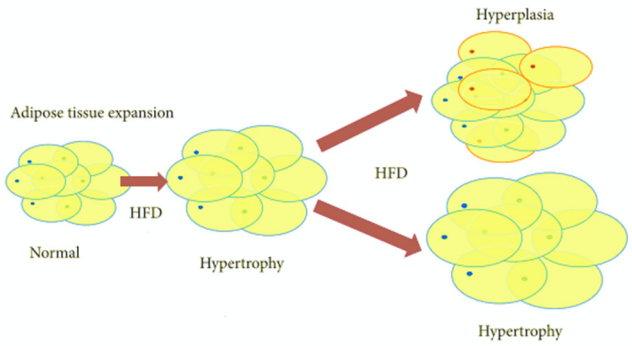

Figure 1.1: Comparison between hyperplasia to hypertrophy adipose tissue expansion

The size can influence secretion, human adipocytes can change about several thousand-fold in volume and as adipocytes grow larger, they become dysfunctional. While the smaller adipocytes are insulin sensitive, large adipocytes become insulin resistant and contribute to the metabolic problems associated with obesity. Adipocytes can rapidly reach the diffusional limit of oxygen due to the inability of the neo-vasculature to keep pace with tissue expansion. Hypoxia is therefore an early determinant for adipose tissue dysfunction.

Adipose tissue is not all the same, in fact there is no single type of adipocytes. (2)

There are two major categories of adipose tissue, white adipose tissue or white fat (WAT) and brown adipose tissue or brown fat (BAT), so comprise two types of fat cells: white adipocytes and brown adipocytes.

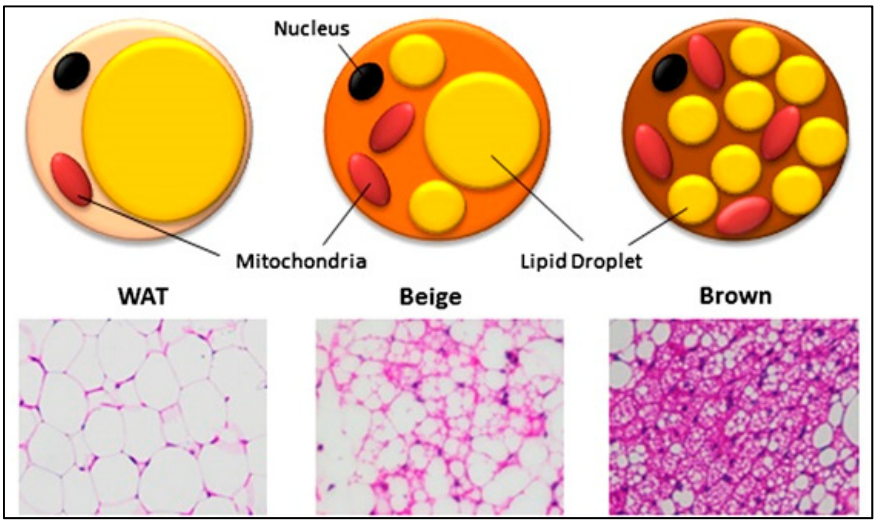

Figure 1.2: Morphological differences between WAT, beige and brown adipose tissue (BAT) adipocytes as shown by cartoon and hematoxylin/eosin staining (3)

White adipocyte organelles are poorly developed; in particular mitochondria are small, elongated and have short, randomly organized cristae and a single huge large lipid droplet occupying about 90% of the cell volume. From a cellular point of view, the adipogenic process consists essentially in two phases, the first, called the "determination", during which the pluripotent cell is gradually "committed" in the adipogenic lineage becoming pre-adipocyte, morphologically similar to a fibroblast; and the second phase called the "terminal differentiation", the process that bears pre-adipocyte to acquire the morphological and functional characteristics a mature adipocyte. In addition to the drastic cellular morphological changes that mainly consist in training lipid vacuoles, terminal differentiation is characterized by a marked increase of lipo-neo-genesis through the induction of specific enzymes involved in the metabolism lipids (e.g. fatty acid synthase, glycerol-3-phosphate acyltransferase) and proteins adipose-specific, such as the fatty acid binding protein (aP2 or FABP4) and the perilipin (protein associated with lipid droplets). Furthermore, WAT display

differences between adipose tissue present in subcutaneous areas (SAT) and visceral adipose tissue (VAT) present in the abdominal cavity. The distribution of SAT and VAT shows person-to-person variations, that is dependent from several factors such as age, nutrition, sex and energy homeostasis. Difference between depots include anatomical, cellular, molecular, physiological, clinical and prognostic differences. The SAT it is the first to receive excess of lipids, it contains about 80% of all body fat, and the major subcutaneous depots are deep abdominal, superficial abdominal, and gluteus-femoral adipose tissue and is recognized as the safest triacylglycerol depot. The VAT, in which deposition occurs only after SAT capacity has been exceeded, can anatomically be divided into omental, mesenteric, and retroperitoneal depots.

VAT has a greater capacity to generate free fatty acid and to glucose- uptake, while SAT is more avid in the absorption of circulating free fatty acids and triacylglycerols. (4)
Other depots are founded in intermuscular fat, gonadal fat, epicardial fat or gluteus-femoral fat (5).

Totally different is the BAT, because it has a fundamental thermogenic function. It takes its name from its macroscopic color. Brown adipocytes are smaller than white adipocytes, their cytoplasm contains several lipid droplets, a roundish nucleus and numerous, large, spherical mitochondria with laminar cristae well developed that extend from end to end. These cells express the Uncoupling Protein-1 (UCP-1) protein that dissipates the proton electrochemical gradient of the internal mitochondrial membrane producing heat. From an embryological point of view, the brown adipocytes derive from precursors expressing the genes Paired Box 7 (Pax7) and Myogenic Factor 5 (Myf5), considered up to few years ago muscle-specific genes. In rodents, BAT is located interscapularly. Human depots of BAT are found in the supraclavicular and the neck regions with some additional paravertebral, mediastinal, para-aortic, and suprarenal localizations (6).

Most recently, the presence of beige adipocytes with a gene expression pattern distinct from either white or brown adipocytes has been described. Date back to the 80's the first evidence of the presence of cells multi-vacuolated UCP1 positive in the context of some of the white adipose tissue deposits, in particular following the exposure to the cold or to the stimulus β -adrenergic. At first these adipocytes were considered simple brown adipose tissue cells "infiltrated" the WAT.

Assuming that are halfway between white and brown adipocytes, they were called adipocytes beige or brite (brown in white) or brown adipose tissue "recruitable": they occur *in vivo* as multi-vacuolated cells able to induce the expression of UCP1 and other genes involved in mitochondrial biogenesis (PRDM16, PGC1α) in response to various stimuli at levels comparable to those of brown cells. In the light of their localization within the WAT depots, they have been formulated two

hypotheses for the origin of the beige adipocytes: according to a line of thinking, they derive at least in part for trans-differentiation of mature white adipocytes in response to a stimulus; the alternative idea is that beige cells derive from de novo adipogenesis of residents precursors in WAT depots recruited as needed. (1) (7) (8)

A third type of adipocyte, less well known, the pink adipocyte, has recently been characterized in mouse subcutaneous fat depots during pregnancy and lactation. Pink adipocytes are mammary gland alveolar epithelial cells whose role is to produce and secrete milk. Emerging evidence suggests that they derive from the transdifferentiation of subcutaneous white adipocytes. (9)

1.1.1 Adipose tissue: an endocrine organ

Adipose tissue is composed of several types of different cells: the lipid storing one is the adipocytes and the stromal-vascular compartment that contains stem cells, macrophages, endothelial cells, fibroblasts, and leukocytes; its multifarious composition renders fat an important mediator of metabolism and inflammation. Being directly involved with its expansion in the onset and exacerbation of obesity in response to overfeeding, and the main organ involved in long term energy storage, the adipose tissue is seen as a central player in the onset of the various comorbidities associated with obesity itself; so, fat is not only a passive storage tissue, but an authentic effective dynamic organ. The first to suggest a role beyond a repository for lipids for adipose tissue was von Gierke, who in 1905 recognized a role for adipose tissue in glycogen storage. In addition, the mature adipocytes secrete several substances some of which are considered true hormones. e.g.: leptin, whose effects can range from increased satiety, energy expenditure and insulin sensitivity, or adiponectin that induces oxidation of fatty acids in the liver, improving the function of β-cells and the peripheral insulin sensitivity. The adipose tissue can communicate both with the brain and peripheral tissues through a wide array of adipokines such as leptin, IL-6, adiponectin, MCP-1 and TNF-α; they are implicated in a wide variety of processes such as appetite and energy balance, lipid metabolism, homeostasis of glucose levels and insulin sensitivity, inflammation and immunity, angiogenesis and regulation of blood pressure, cell division and signal transduction; producing also proinflammatory and anti-inflammatory factors.

1.2 OBESITY AND METABOLIC DISEASES

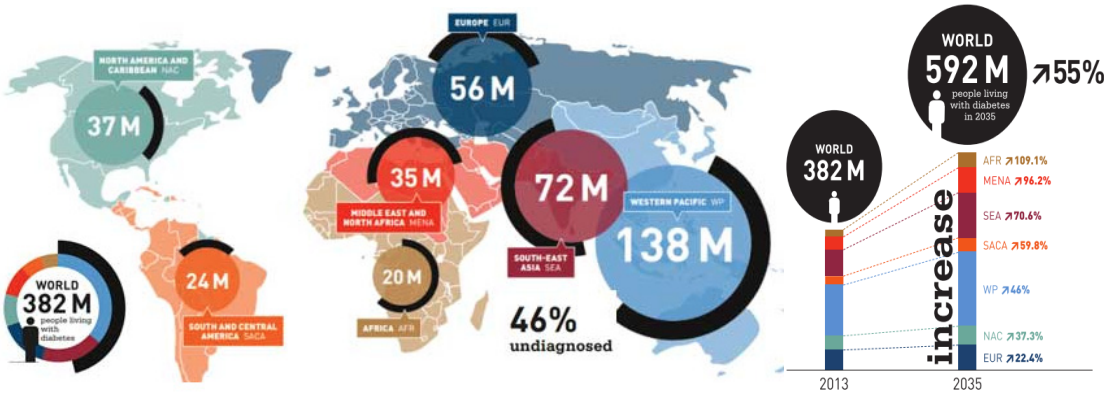

Figure 1.3: Distribution of diabetes in the world, growth estimate of diabetes in next 20 years (IDF)(10)

"Globesity", I.e. the global epidemic of overweight and obesity, paradoxically coexisting with undernutrition in developing countries, is rapidly becoming a major public health problem in many parts of the world; the number of people with diabetes mellitus has increased massively, raising prevalence worldwide, and it is not focused on western societies.

Obesity is associated with the increased risk of numerous metabolic complications, such as insulin resistance, dyslipidemia, hypertension, and various cancers. While insulin resistance and endothelial dysfunction are risk factors for all of these metabolic diseases the precise molecular mechanisms that may explain the associations between obesity and its co-morbidities is, as yet, poorly understood.

Although not a direct measure of adiposity, the most widely used method to gauge obesity is the body mass index (BMI), which is equal to weight/height^2 (in kg/m^2). World Health Organization (WHO) defines obesity as BMI equal to, or greater than 30 kg/m^2. A BMI≥25 is a risk factor for metabolic, cancer, and cardiovascular morbidity.

Classification	**BMI kg/m^2**	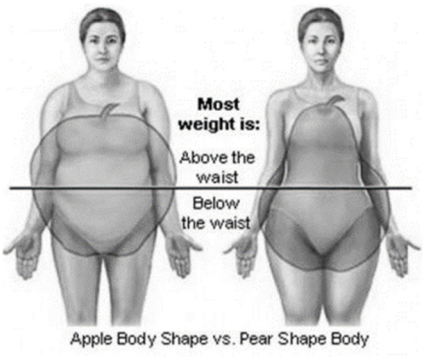
Underweight	<18.4	
Normal	18.5-25	
Overweight	25-30	
Obese	≥30	
Obese class I	30-35	
Obese class II	35-40	
Obese class III	≥40	

Table 1.1 Classification of body mass index (BMI) and body shape

The use of BMI is not the optimal way to calculate the ideal weight of a person, because slender but very muscular individuals may be overweight with BMI calculations without having increased adiposity. Accordingly, to both BMI and metabolic profile, individuals may be classified in the following phenotypes: 1) lean and healthy, 2) lean and unhealthy (also known as “thin outside but fat inside”), 3) obese and unhealthy and 4) obese and healthy.

A classical paradigm has been the fact that the more adipose tissue, the higher the prevalence of metabolic diseases; but certain inconsistencies have been found. The distribution of fat between these depots seems to be more important than the total adipose tissue mass for the risk of developing obesity-associated diseases. Lipid surplus may accumulate ectopically, in non-adipose tissues, e.g. in the liver, skeletal muscle, heart, and the β-cells, increasing insulin resistance and impairing insulin secretion.

The distribution of adipose tissue in different anatomic depots also has substantial implications for morbidity and complications, those are more strongly linked with upper body fat than overall adiposity. Specifically, intra-abdominal and abdominal visceral fat have more significance than subcutaneous fat present in the buttocks and lower extremities, a ratio waist-to-hip ≥0.9 in women and ≥1 in men is abnormal.

Obesity has become a real concern worldwide due to the associated cluster of chronic diseases that reduce life quality and expectancy. The major comorbidity of obesity is Type 2 diabetes mellitus (T2DM); approximately half of the individuals with T2DM are obese and therefore the terms ‘diabesity’ and ‘obesity-dependent diabetes’ are often used (11). With around 350 million cases in 2014 (10), T2DM is one of the most frequent diseases throughout the world. This number is predicted to increase dramatically in the upcoming years, resulting in serious health and economic challenges; the cost of treating diabetic complications might double from the current total of £ 7.7 billion to £ 13.5 billion by 2035. The WHO defines the current diagnostic criteria for diabetes as a fasting plasma glucose concentration ≥ 7.0 mmol/L and a level of ≥ 11.1 mmol/L 2 h after a 75g oral glucose load.

Obesity is associated with several other comorbidities such as metabolic syndrome, an increased risk of developing insulin resistance, fatty liver disease, hypertension, dyslipidemia and hyperlipidemia, cardiovascular complications, nonalcoholic fatty liver disease (NAFLD) many cancers and in women hyperandrogenism even though there are metabolically healthy obese patients without any of these obesity-related complications. (12)

The metabolic syndrome, according to the definition of WHO is a constellation of metabolic abnormalities that confers a predisposition to cardiovascular diseases with a cluster of diabetes

mellitus, hyper-glycaemia, hypertension and low HDL cholesterol. The key predictor is central obesity that can highlight the relationship between waist circumference and adiposity, however some people have a standard weight, they are insulin resistant but they have that syndrome. The second predictor factor for the metabolic syndrome is a sedentary lifestyle; that is as dangerous as smoking. (13)

Obesity is associated with low-grade inflammation in both clinical and experimental settings, increased adiposity has been related to elevated systemic inflammation. Several studies have found that macrophages in adipose tissue are increased in the obese subjects and, together with the adipocytes, they are responsible for the majority of the proinflammatory adipokines production in WAT in the obese state. T-lymphocytes in visceral adipose tissue contribute both to the initiation and perpetuation of adipose tissue inflammation and the development of insulin resistance. Macrophages can be characterized as M1-type (involved in proinflammatory processes such as TNF-α, IL-6, and IL-12) or M2-type involved in immunomodulatory and tissue remodeling.

It has been established that the diet-induced obesity(DIO) leads to a shift in the activation state of adipose tissue macrophages from an M2-type to an M1 proinflammatory state that contributes to insulin resistance (14-16).

Chronic inflammation and hyperglycaemia trigger endothelial damage and dysfunction (so loses its physiological properties), starting the release of E-selectin, a marker of endothelial activation; in humans, E-selectin levels are increased in insulin-resistance states and they are linked with glycaemic control and extension of vascular diseases. E-selectin is glucose and TNF-α induced, and inversely proportional to SIRT1. (17) Moreover, it is well known that incubation in high glucose *per se* can drive the differentiation of uncommitted stem cells into adipocytes (18). The damaging effects of hyperglycemia can also generate high reactive oxygen species (ROS) levels and they can induce huge oxidative stress. (19) In diabetes and its complications, oxidative stress results from an overproduction of ROS, generated by glucose autoxidation, mitochondria dysfunction, polyol pathway, and protein glycation. Hyperglycemia is shown to be correlated to several age-related diseases and the controlling of such condition prolonged life span in experimental animals, creating a vicious loop: the higher the blood sugar, the greater damage to the β-cells and the greater damage to βcell higher goes the sugar; high sugar is toxic to βcell. (20) Finally, recent studies highlighted that pregestational diabetes mellitus enhances the risk of fetal neurodevelopmental defects, the mechanism of hyperglycaemia-induced neurodevelopmental defects is not fully understood, but it is clear that maternal hyperglycaemia has a crucial role in inducing neurodevelopmental defects. (21)

1.2.1 Types of diabetes and treatments

Diabetes mellitus (DM) is probably one of the oldest diseases known to man. Diabetes was first recognized around 1500 a.C. by the ancient Egyptians; who considered it a rare condition in which a person urinated excessively and lost weight. The term diabetes mellitus, reflecting that the urine of those affected had a sweet taste, was first used by the Greek physician Aretaeus, who lived from about 80 to 138 d.C. No effective treatment was available at the time, and diabetes was uniformly fatal within weeks to months after its diagnosis. In the intervening years, major fundamental advances have been made in our understanding of the underlying causes of diabetes and the approach to its prevention and treatment. The major forms of diabetes are T1DM, T2DM, and gestational diabetes mellitus. As a general treatment, patients with diabetes receive an education about nutrition, exercise and medication, with daily self-monitoring levels of glucose and regular control of Hb1Ac.

T1DM diabetes or insulin sensitive, that affects 5-10% of the total of patients, is characterized by a cellular-mediated autoimmune destruction of the pancreatic β-cells, usually leading to absolute insulin deficiency. T1DM, generally considered to be caused by genetic predisposition, normally occurs in childhood and adolescence although it could happen at any age, treatment of patients is by the injection of insulin. Insulin was discovered 1921 and it is the most important anabolic hormone with profound effects on glucose and lipid metabolism. Insulin is synthesized in the endoplasmatic reticulum and it is stored in vesicles released from the β-cell of the pancreatic islets of Langerhans in the pancreas in response to increased blood glucose concentration. The glucose-induced initial increases of [$Ca2^{+}$] triggers fusion of these insulin-containing vesicles with the plasma membrane followed by insulin release via an exocytotic process (22). Insulin stimulates glucose up-take in adipose tissue and skeletal muscle, and it suppresses the endogenous glucose production in the liver. Insulin resistance is an inability of peripheral target tissues, e.g. adipose tissue, liver and muscle to respond properly to insulin stimulation. (16)

Otherwise, for the T2DM or diabetes mellitus or insulin insensitive, a major type of diabetes accounting for approximately 90-95% of total cases, the causes are not clearly defined. This type of diabetes usually develops fairly slowly and patients are often undiagnosed for many years; indeed, T2DM develops with increasing age but it is now being diagnosed more frequently in children and young adults. DM produces a wide range of symptoms and signs that include: polyuria, polydipsia, weight loss, fatigue, weakness, blurry vision, frequent infections and slow healing of skin lesions even in minor trauma. It is characterized by insulin resistance, impaired insulin secretion, increased glucose production and abnormal fat metabolism. At the early stages, as insulin resistance appears, a healthy pancreas is able to compensate by increasing insulin

secretion and β-cell mass. However, as the disease advances, loss of the compensatory mechanism leading by a progressive decline in β-cell function and mass, resulting from increased β-cell death by apoptosis and decreased β-cell proliferation, leading for a hyperglycemia. Under hyperglycemic conditions, the ability of the kidney to reabsorb glucose is exceeded and it spills over into the urine, this causes an osmotic diuresis (polyuria) followed by increased drinking (polydipsia). Muscles and other insulin-sensitive cells become unable to take up glucose results in the metabolism of fat which induces muscle breakdown due to proteins degradation and weight loss, which in turn, leads to increased eating (polyphagia). Long-term diabetes is virtually always associated with the development of secondary complications and comorbidities including macrovascular diseases (e.g. coronary artery disease and peripheral artery disease) and microvascular diseases (e.g. nephropathy, neuropathy and retinopathy) which is a result of microvascular changes. T2DM is treated with oral hypoglycaemic agents for example metformin, sulfonylureas (23), thiazolidinedione and α-glucosidase inhibitors. (24, 25)

Other specific types of diabetes result from causes such as genetic defects in insulin action, exocrine pancreas dysfunction and drug or chemical-induced side effects, gestational diabetes mellitus that happens during pregnancy and a hypothetical type 3 of diabetes or “metabolic cognitive syndrome” that will be a risk factor for Alzheimer disease. (26)

Despite accessing to a variety of treatment regimes, diabetes is the leading cause of blindness, damage to nerves throughout the body (neuropathy) resulting in loss of feeling, ulceration of extremities that will lead to amputation and kidney failure while cardiovascular disease accounts for 50–80% of deaths amongst the diabetic population. (27) That highlights the inadequacy of current therapeutics and the need for alternative and improved treatment regimes.

1.2.2 The glyco-oxidation: glucotoxicity and lipid-oxidation

Lipotoxicity and glucotoxicity may both be implicated in the pathogenesis of type 2 diabetes. (28) Excess circulating fat, glucose, or both, act on diverse cells and tissues to counteract insulin-mediated glucose uptake, hepatic regulation of glucose output, and insulin secretion. Many metabolic pathways in this array of diseases become aberrant, which is accompanied by a variety of post-translational protein modifications that in turn can reflect diabetic glucotoxicity. Exploring the nature of these modifications should ease our understanding of the pathological mechanisms of diabetes and its associated complications. Protein modifications are strategies routinely used by cells to expand their function, but they can also be the status quo of struggled cellular functions under stressed condition. Changes can be classified into two categories: irreversible and reversible. Irreversible protein ones include carbonylation, nitration, and glycation, and reversible

protein ones include nitrosylation, acetylation, sumoylation, O-GlcNAcylation, ADP-ribosylation, and succination. (29)

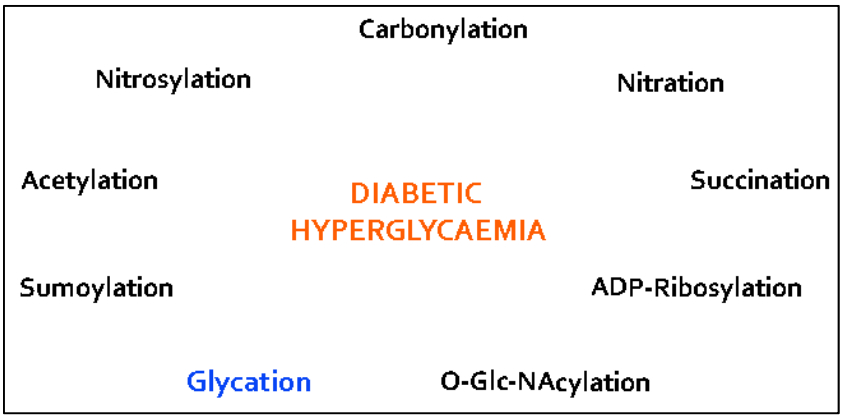

Figure 1.4: Protein modifications that can manifest glucotoxicity in diabetes.

When blood glucose level is persistently high, the body will attempt to mobilize all the possible pathways involved in glucose clearance. One such significant pathway is the polyol pathway; this pathway involves two reactions, catalyzed by aldose reductase and sorbitol dehydrogenase, respectively, making an excess of NADH by consuming NADPH, hence breaking the redox balance between NADH and NAD+. The excess NADH can overload the mitochondrial electron transport chain and drive overproduction of reactive oxygen species (ROS), which can attack proteins and induce protein modifications. (30) Moreover, diabetic hyperglycemia can also activate other metabolic or signaling pathways; eventually elevate cellular ROS levels might start, hence further aggravating cellular redox imbalance and oxidative stress.

Lipids encompass a wide variety of molecules such as fatty acids, sterols, phospholipids and triglycerides. Those molecules represent a highly efficient energy resource and they can act as structural elements of membranes, or as signaling molecules that regulate metabolic homeostasis through many mechanisms. While lipids are pivotal for these homeostatic processes, they can also contribute to detrimental metabolic outcomes. When metabolic stress becomes chronic and adaptive mechanisms are overwhelmed, as occurs during prolonged nutrient excess or obesity, lipid influx can exceed the adipose tissue storage capacity, leading to accumulation of harmful lipid species at ectopic sites such as liver and muscle. It is now well established, that immuno-metabolic pathways are highly responsive to lipid and linked to lipotoxicity, alterations in lipids metabolism and signaling converging on common immune and stress responses. (31, 32) Moreover, under some conditions, fatty acids may have the primary effect of impairing pancreatic islet insulin secretion: low levels of circulating free fatty acids in the range of physiologic postprandial values actually enhance glucose-induced insulin secretion. However, marked

accumulation of lipids within islets impairs insulin secretion, causing glucose increasing; thereby creating a deleterious self-powered mechanism.

1.3 THE GLYCATION

1.3.1 Differences between glycation and glycosylation

From a chemical point of view, AGEs represent a quite complex class of compounds that are formed by different mechanisms, from heterogeneous precursors and they can be formed either exogenously or endogenously; that was termed glycation to be distinguished from enzymatic glycosylation. Glucose has a dual activity: it is a source of energy and carbons for cell survival but it is nevertheless a toxic agent.

The first one, glycosylation, is an important biological process which occurs in endoplasmic reticulum and Golgi, that serves a number of key functions and it is required for getting functional proteins; these include, but are not limited to, proper protein folding, increased protein stability, and overall diversification of the proteome, it is a carefully regulated and essential process; but at the same time, it may be a sign of glucotoxicity as glycation but with a lot of differences. Many glycans are on the outer surface of cellular and secreted macromolecules, they are in a position to modulate or mediate a wide variety of events in cell–cell, cell–matrix, and cell–molecule interactions critical to the development and function of a complex multicellular organism, in addition they are abundant within the nucleus and cytoplasm, where they can serve as regulatory switches. This posttranslational modification is a reversible modification occurring on serine or threonine residues. As glucose level becomes higher in diabetes, more glucose will be fluxed into the hexosamine pathway, resulting in elevated levels of uridine diphospho-N-acetylglucosamine that can be attached to proteins. O-GlcNAcylation of forkhead box O1 (FoxO1) in hepatocytes can increase its transcriptional activity that then upregulates the expression of glucose 6-phosphotase, leading to hyperglycemia by increasing hepatic glucose production. (33) The second one is as follows: the glycation, on the other hand, is a time-consuming cascade of chemical reactions and non-enzymatic process, not mediated by the organism and happens "by itself" (that means spontaneously) out of control; it is one of the most important unwanted post-translational modifications. Sugars and sugar degradation products covalently and irreversibly modify the proteins; it is a form of protein damage, as glycated proteins have reduced and impaired functionality. So, in a way, they are the extreme opposites.

1.3.2 Sources

Figure 1.5: Examples of exogenous source of AGEs.

AGEs (Advanced Glycation End products) are ubiquitous substances. AGEs found in the organism have two origins: exogenous (dietary (19), smoke (34)) or endogenous. The diabetic patients, in particular those with diabetic nephropathy are moreover prone to a further accumulation of circulating mechanism of AGEs, since in these subjects the renal clearance of these compounds is reduced. This creates a gradual and inevitable vicious circle, in which the growing pools of plasma circulating AGE alters the structure and function of glomerular proteins, associated with further impairment in renal function and then clearance of AGE. Hyperglycaemia also creates a vicious circle: the higher the blood sugar, the greater damage to the beta cells, and greater damages to beta-cells higher is sugar.

AGEs are also made of non-oxidative mechanisms in anaerobic glycolysis and from oxidative decomposition of polyunsaturated fatty acids or catabolism of ketone bodies (35). AGEs are naturally present in uncooked animal-derived food that is high in fat and protein, especially red meat. Cooking methods that apply high temperatures to brown or char foods, such as grilling, roasting, searing, frying and broiling propagate and accelerate new AGEs formation. While carbohydrate-rich food such as fruits, vegetables, and whole grains will keep low AGEs levels after cooking. The global food industry is expected to have increased more than US $ 7 trillion by 2014/5. This rise in processed food sector shows that more and more people are diverging towards modern processed foods. As modern diets (fig. 1.5) are largely heat processed, they are more prone to contain high levels of AGEs. (36) Sugary food, highly processed, convenience food, such as packaged snacks and ready-to-eat meals (fig. 1.5) are very awash in AGEs and have the largest impact on the amount of AGEs consumed. The findings from animal and human studies suggest that avoidance of smoke and dietary AGEs in food will help delay chronic diseases and aging in animals and, possibly, in human beings. (37) In food industry, glycating reaction is engaged for reasons of safety and to enhance flavor, aroma, coloring, and texture; but at the same time

results in loss of protein quality and formation of harmful compounds with mutagenic, carcinogenic and genotoxic properties.

AGEs-modified proteins are partially resistant to proteolysis and their nutritive value is reduced because dietary AGEs are only poorly digested and absorbed, the absorption has been estimated at between 10 and 30% of ingested, suggesting that the digestive barrier limits bioavailability of food-derive AGEs, the 70% of absorbed are stored in tissues. Restriction of food-derived AGEs can lower AGE concentrations in serum (37, 38). Furthermore, it was shown that a high-AGE diet causes decreased insulin secretion and increased cell death in rats. (19). Chronic exposure to a diet with a high content in dietary AGEs promotes chronic inflammation and insulin-resistance. A cross-sectional study, in which subjects were categorized by both presence or absence of metabolic syndrome's criteria, recording the dietary calories composition and AGEs intake, suggests that although over-all serum AGEs were not associated with markers of fat mass, in the presence of obesity and one or more metabolic syndrome's criteria, serum AGEs levels were markedly higher, as was dietary AGEs introduced by diet, even after adjusting for nutrient consumption. Beyond over-nutrition, the high dietary AGEs consumption may link healthy obesity to risk obesity. (39) (40) Unfortunately, there is a lack of well-designed studies concerning the bioactivity of dietary AGEs.

1.3.3 Protective not-synthetic compounds

Naturally occurring compounds, especially polyphenols, are of great interest, because they are considered potential candidates to prevent the formation of AGEs, especially given their proven safety and efficacy (compared to synthetic compounds) in the prevention of cancer, hyperglycemia, heart disease and aging. Some examples of food are: green tea, whole apple, cereal bran, ginger, ginseng, curcumin, chili-capsaicin-containing. (41, 42). Generally, indications say that Mediterranean diet reduces oxidant AGEs and increases antioxidant defenses in the fasting and postprandial states, having protective effects against oxidative stress and inflammation. (43)

1.3.4 The kinetics of formation of AGEs, initial-intermediate-late stage

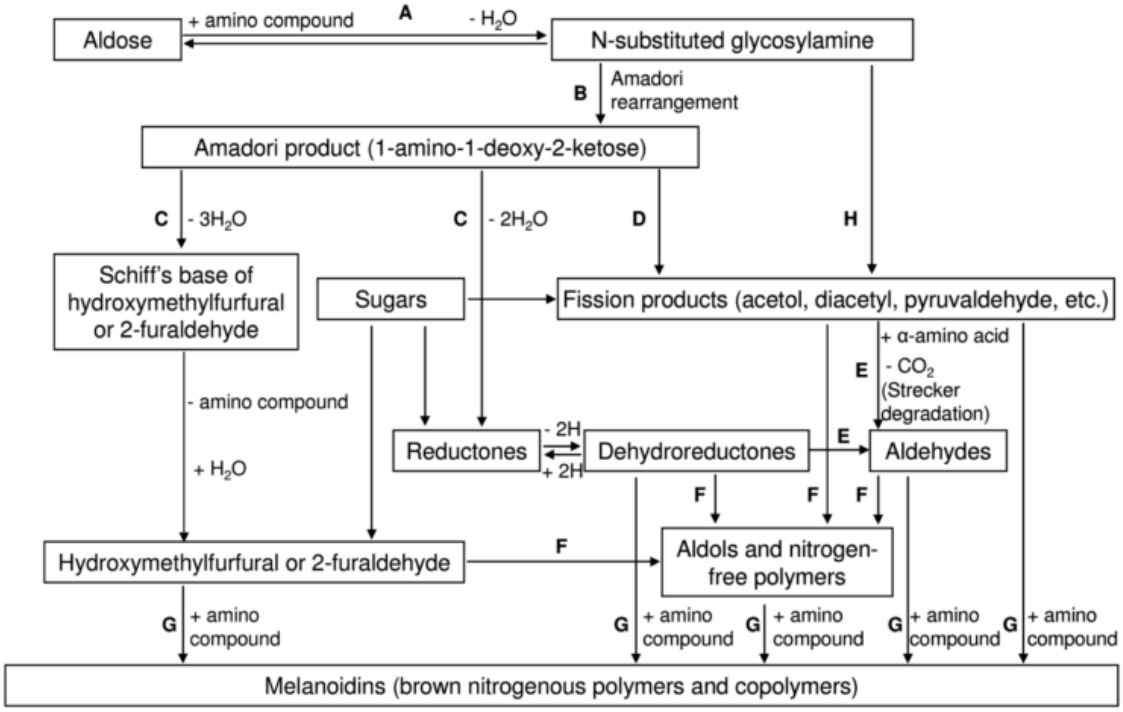

Figure 1.6: Hodge Diagram (44) of process summarized in seven steps A) The initial reaction between a reducing sugar and amino group forms an unstable Schiff base; B) The Schiff base slowly rearranges to form the Amadori product; C) Degradation of the Amadori product; D) Formation of reactive carbonyl and dicarbonyl compounds; E) Formation of Strecker aldehydes of amino acids and aminoketones; F) Aldol condensation of furfurals, reductones, and aldehydes produced in Steps C, D, and E without the intervention of amino compounds; G) Reaction of furfurals, reductones, and aldehydes produced in Steps C, D, and E with amino compounds to form melanoidins; H) Free radical-mediated formation of carbonyl fission products from the reducing sugar

The formation of AGEs intracellularly is part of normal metabolism, where they may contribute to several normal intracellular functions. The glycation time line started during the first years of 20th Century. Louis Camille Maillard first studied condensation, a non-enzymatic reaction and reversible step, between the carbonyl group of a reducing sugar and the amino group-containing molecule such as proteins, peptides or amino acids in early ears of the 20th Century. Amino groups on protein vary widely in their rate and extent of glycation; moreover, the pattern of glycation reactivity is quite different among peptides, this is determined by both the structure of the protein and endogenous ligands, and both acidic and basic neighboring groups affect the specificity of glycation of protein, either through effects on the pKa of the amino group, which enhances its nucleophilicity and the kinetics of formation of the Schiff base, or through catalysis of the Amadori rearrangement, which is the rate limiting step in glycation. (45)

This glycation reaction results in the formation of an unstable Schiff base (aldimine) that spontaneously rearranges to form the more stable 1-amino-1-deoxy-2-ketose (ketoamine), which is also known as the Amadori product. Mario Amadori demonstrated two structurally different isomers in condensation of D-Glucose with aromatic amines in 1929. (46) These products are

degraded via various pathways leading to the formation of furfurals, reductones and fragmentation products producing of high reactive compounds as dicarbonyl contents. These lasts are potent glycating agents, 200–50000-fold more reactive than glucose (47). The reaction of amino acids with glyoxal derivatives was found by Takahashi in 1977 and free radical degradation of Maillard intermediates were investigated by Namiki in 1986. (44, 48) The dicarbonyl compounds have a relatively long half-life and easy cross the plasma membrane, reacting with nucleophilic groups of macromolecules, thereby acting far away from the site of production and they can modify molecules both inside and outside, moreover they can be accumulated in tissues giving a carbonyl stress. (19) (49) The final product of this reaction is a polymorphic group of compounds collectively referred to AGEs, which is formed through the interaction between intermediates stages. Gradually several AGEs like Nε-carboxymethyl-lysine (CML), Nε-(carboxyethyl)lysine (CEL), pentosidine, pyrraline, fructosamine and modification of arginine or lysine were discovered. AGEs can also cross-interact with each other, forming super-aggregates and very complex structures that have nothing in common with the starting proteins.

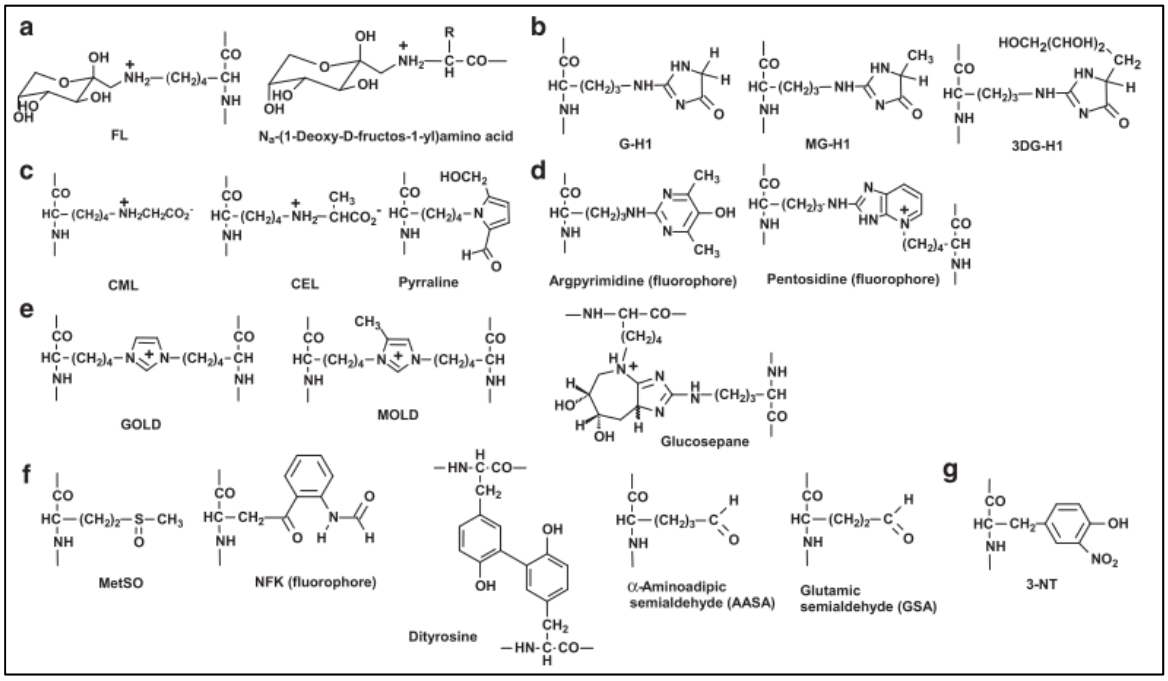

Figure 1.7: Some examples of protein glycation, oxidation and nitration adduct residues in physiological systems. a. Early glycation adducts — FL and Nα-(1-deoxy-D-fructos-1yl) amino acid residues.b. Hydroimidazolones, c. Monolysyl d. Fluorophores, AGEs, e. Non-fluorescent crosslinks, f. Oxidation adducts, and g. Nitration adduct. (50)

The effects of AGEs in tissue destruction and in the pathogenesis of health disorders happen through three major mechanisms: by cross linking pathways, by activation of several inflammatory signaling pathways, activating cell signaling and leading to the production of ROS and inflammatory factors, thought the crosslink of proteins on the extracellular matrix such as collagen with other matrix components, leading to the loss in their stability and function. AGEs are

considered the most important links between diabetes and oxidative disease, they are still nowadays an important and challenging field of studies. It is important to note that all intracellular and extracellular proteins, lipoproteins and tissue that contain long lived proteins (i.e. crystalline or lens or collagen of the extracellular matrix of connective tissues) are prone to AGEs formation.

Proteins misfolding and aggregation are important problems in the research world, because the accumulation of their constructs is toxic and it interferes with cell biological function accounts the molecular basis of conformational disease.

1.3.5 Biological Effects of glycation and protein dysfunction

The most significant effects of AGEs have been observed in T2DM where they are ultimately correlated with multi-organs complications. Glycation and AGEs induce misfolding, native change and protein aggregation provoking stochastic conformational changes and failure in any protein biological function. Intra- and extra-cellular accumulation of misfolded and aggregation protein are seen as molecular basis of the conformation diseases, as these compounds are toxic and they interfere with cell function. (51) Cellular clearance of AGEs metabolites is inefficient and they accumulate in our tissues and organs as we grow older with pathogenic effects. Since molecular alterations induced by AGEs are permanent, normalization of glucose levels does not completely prevent elevated plasma methylglyoxal levels and late complications in diabetic patients. This can lead to the concept of "*metabolic memory*".

That aforementioned phenomenon has been reported in animal models of diabetic complications: retinopathy continued to progress for a considerable period even after hyperglycemia was corrected; the inclination of protein to be glycated was free from its actual glycation-inducing environment glucose level because it was an auto-sustainable phenomenon. (52)

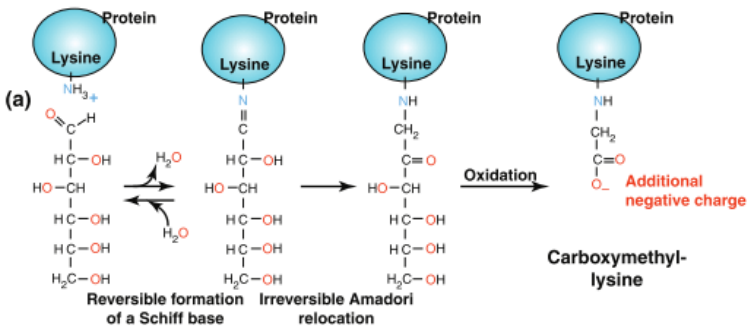

Figure 1.8: Example of protein glycation – exemplifying cartoon

Several intracellular proteins modified by glycation are found to have altered activities and stabilities; AGEs formation does not only alter the activity of intracellular proteins, but it can also affect the functional properties of important molecules on extracellular matrix such as various

types of collagens. Classical targets of glycation in the plasma are proteins with commonly have a low turn-over haemoglobin and albumin, while in ECM, there are proteins like collagen, vitronectin, laminin or elastin. AGEs are very slowly degraded and they can be around for a long time in diabetic vessels even after glycaemic control has been improved. The damaging potential of AGEs results from direct alterations on protein structures and functions due to AGEs per se or the cross-linking effect of some AGEs. AGEs can initiate a wide range of responses in cells and tissues, such as inappropriate expression of growth factors, alterations in growth dynamics, accumulation of extracellular matrix, start of vasoregulatory dysfunction, and initiation of death pathways.

Excessive presence of AGEs is the most dangerous mechanism involved in the pathophysiology of chronic diabetic complications and in particular for microvascular complications, in the onset of coronary artery disease and aortic stiffness. (53-57) Although insulin has a very short half-life and it is not a typical target for modification, glycation sites on insulin have been found *in vivo* in cells as well as islets when they were cultured under hyperglycemic conditions in the phenylalanine position in the amino terminus of the insulin β chain. This leads to suppose that there may be a direct insulin glycation and that was a contributory cause to insulin resistance. (58). Reaffirming that, AGEs contribute to diseases such as diabetes, cardiovascular disease, arthritis, and neurodegenerative disorders. Failure to remove these highly reactive metabolites can lead to protein damage, aberrant cell signaling, increased inflammatory responses, increased oxidative damage, changes in extracellular matrix composition, and decreased genetic fidelity.

AGEs can also act as neo-antigens to trigger proinflammatory cellular immune responses; in fact, recently, an association between high levels of IgM has been highlighted against methylglyoxal-modified apolipoprotein B100 and reduced coronary artery calcification in patients with type 2 diabetes. It suggested that IgM against the methylglyoxal-modified protein may be protective in diabetic vasculopathy. However, the linkage between AGEs and innate immunity, has never been studied that well. (59) Moreover, the accumulation of AGEs has been implicated as strong contributors to many progressive diseases including diabetic complications, aging and Alzheimer's disease. Aβ is a suitable substrate for glycation, producing one form of the AGEs, Li et al. group speculated that Aβ-AGE formation may exacerbate neurotoxicity. (26, 60-62) Finally, because intracellular accumulation of AGEs alters cytoplasmic and nuclear factors including the proteins involved in regulating gene transcription (63); it has been proposed that aberrant AGE accumulation may represent a metabolic susceptibility difference that contributes to cancer disparity. (64)

1.3.6 Cellular defense mechanisms and antioxidants

Modified proteins alter the 20S proteasome subunit, decreasing proteasome activity, and it decrease any activity of the protein quality control pathway. Several mechanisms tend to limit the level of cellular AGEs-modified proteins by scavenging and metabolizing carbonyl compounds: glutathione peroxidase, reductase and S-transferase; superoxide dismutase, catalase. (65) Recently, a few AGEs breakers have been discovered in order to fight back deleterious protein cross-links. Dietary antioxidants are substances found in food that can decrease the damage of ROS, and restore physiological function in humans. Vitamin C is a powerful antioxidant, as it can neutralize harmful free radicals and sustain neutralization of pollutants and toxins. Although the direct antioxidant protection afforded by vitamin C is limited to water-soluble environments, vitamin E (tocopherol) plays an antioxidant role in lipids through its regeneration of the fat-soluble antioxidant. (66) Some antioxidants are able to fight against the effects of glycation end-products acting either by preventing cellular action of AGEs or by inhibiting AGEs formation (scavenging of reactive carbonyl intermediates) e.g. some nucleophilic compounds such as pyridoxamine, tenilsetam, 2,3-diaminophenazone, OPB-9195 or aminoguanidine. It is only when the overall levels of AGEs in the extracellular and the intracellular spaces exceeds the ability of the native antioxidant defenses that they pose a problem. Glycation is a major cause of spontaneous damage to cellular and extracellular proteins in physiological systems, affecting 0.1–0.2% of lysine and arginine residues. For some proteins with limited protein turnover, such as lens fiber cells, the extent of protein glycation may be up to 10-fold higher. (67) (68) Oxidative stress has long been associated with diabetic complications and more recent studies indicate that oxidative stress can cause the development of cell dysfunction and insulin resistance, the two hallmarks of T2DM. Increased formation of AGEs and ALEs occurs in diverse settings, such as diabetes and aging. In the complex pathways of AGEs/ALEs formation, hyperlipidemia, hyperglycemia and oxidative stress, all characteristic features of obesity, play an important role. (69)

β-cell dysfunction and insulin resistance occur long before blood glucose levels reach the amount defined as pre-diabetes. The first link between glycated proteins and diabetes was made in 1968 with the discovery of an altered form of haemoglobin (known as HbA1c) in red blood cells of patients with diabetes. It became clear that it is formed by non-enzymatically in a reaction which was before only known to take place in food. Increased concentrations of glyoxal, methylglyoxal as well as 3-deoxyglucosone have been found in plasma of patients with T2DM. The complexity and diversity of AGEs formation makes clear why substances belonging to the group of AGEs are so heterogeneous regarding their chemical and physical properties: some are florescent, some others not, some can induce protein cross-linking, some other not, finally some are both some

other either. Taken together, AGEs are proposed to play a role in the development and progression of T2DM as well as in diabetic complications. (70)

In cells, AGEs can be degraded by the endosomal-lysosomal system and that is linked with sirtuin 1 (SIRT1 a major deacetylase with anti-inflammatory and metabolic functions) expression, that inhibits activity per NADPH oxidase; the deacetylation of NFkB by SIRT1 suppresses its proinflammatory processes. However, long term exposure to AGEs at high levels, can entail high quantity of these in serum AGEs depleting SIRT1 expression oxidative stress and inflammation increase. (71)

Any aforementioned disparity between adipose tissues depots, can be involved in reaction against hyperinsulinemia and it can also reflect the ability to react to AGEs.

BAT is commonly associated with non-shivering thermogenesis, lipolysis, fatty acid oxidation, insulin sensitivity, and improved serum lipid profile; and for this reason, it was thought to be a good therapeutic target. Recent studies report that not only diet-induced obesity leads to BAT inflammation and insulin resistance; but hyperinsulinemia itself reduces insulin sensitivity of brown adipocytes by decreasing brown adipocyte-specific characteristics such as expression of UCP1, PGC1α, mitochondrial biogenesis, and spare respiratory capacity. Inducing the UCP1 overexpression it is possible to prevented hyper glycaemia induced ROS and methylglyoxal modified proteins, RAGE, S100A8, S100A12 calgranulins and HMGB1 expression (72, 73)

1.3.7 Beneficial effects of reactive carbonyl species

Although excessive reactive carbonyl species may lead to pathological disorders and accelerate aging, that species may also exert beneficial effects at very low levels. Defining how much is “low” and “excessive” is a challenge, since concentration may differ in different cellular compartment and tissues and there are not standard techniques to measure carbonyl species. These species will play a central role as a host defense mechanism against invading pathogens (74); but if the level is excessive they will induce apoptosis of neutrophils and enhanced expression of the adhesion molecule Mac-1 resulting in increased formation of platelet-neutrophil aggregates. (75) Moreover, at low concentration MGO was found to effectively kill Gram positive and negative bacteria; the exact mechanism by which MGO kills bacteria is still unknown but is also thought to interfere with the structural proteins in the flagella causing reduced motility and adherence.

1.4 *RAGE: ITS RECEPTOR AND ITS PATHWAY*

Cellular interactions with AGEs proteins are known to induce several biological responses, not only endocytic uptake and degradation, but also induction of cytokines and growth factors. Several different receptors for AGEs have been discovered: SR-AI (scavenger receptor type I), SR-BI, LOX-1, FEEL-1, FEEL-2, OST-48 (also known as AGE-R1), p90 (also known as AGE-R2), galectin-3 (also known as AGE-R3), PRKCSH, INSR, MSR1, LGALS3, DDOST, SRA, CD36 and AGER (also known as RAGE). (76) Any expression of these receptors depends on cell/tissue types and is regulated in response to metabolic changes for instances during aging, diabetes and hyperlipidemia. Whether AGEs are originating from exogenous or endogenous sources, there compounds have to be removed; so, they first need to be taken up by the cell. AGEs receptor which are believed to be involved in detoxification are: OST-48, galectin-3, p90 and further scavengers. These receptors can compete with RAGE.

A lesser-known soluble receptor which is essential in "detoxification" of AGE is lysozyme. Lysozyme is a member of the human immune defense system and it exhibits high AGE-binding affinity, recognizing at least two structurally distinct AGEs, CML and methylglyoxal derivatives. Exposure to AGE-modified proteins inhibits the enzymatic and bactericidal activity of lysozyme, and it blocks the bacterial agglutination and bacterial killing activities of lactoferrin; that is another tile leading to why diabetes is associated with abnormally high susceptibility to infection. (77)

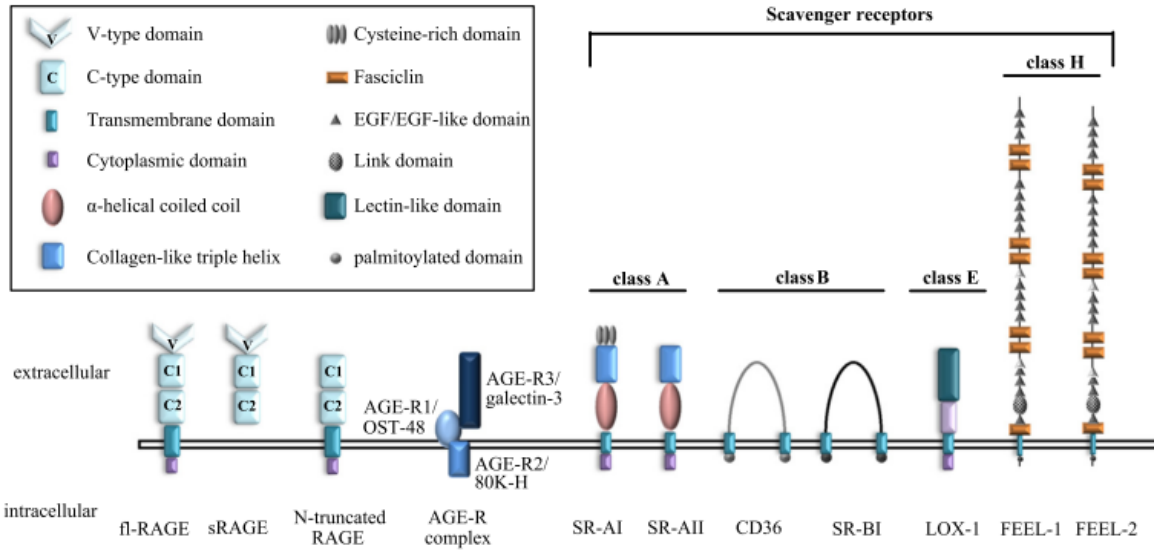

Figure 1.9: Structure of AGE receptors and scavenger receptors family. (76)

The most important receptor for advanced glycation end products RAGE was first characterized in 1992 by Neeper (78) from bovine lung endothelial cells, this multi-ligand cell surface receptor that is only present in mammals, belonging to the immunoglobulin (Ig) super-family, which is a cell surface receptor with a broad variety of ligands including AGEs, members of S100/calgranulin

family, amphoterin, HMGB1 and amylogens. The physiological role of RAGE is largely undefined: its pathway is very complex and not yet understood. Each ligand would promote a different receptor complex: at the same time, different ligands can induce the same signal pathway and, on the opposite, the same ligand can steer different pathways. There is not a general scheme for cellular response upon RAGE activation, in fact there are many factors that affect such cell type, identity and concentration of ligand, the presence of co-receptors, the surface concentration of receptor itself and so on.

The receptor is weakly expressed in almost all adult tissues, while it is highly expressed in the lung, where it is correlated with development, organogenesis, alveolarization and gas exchange (79); the second tissue by quantity of expression is the bone, where it is associated with the biomechanical strength, the third in the neuronal system in which is finally regulated and it is responsible of neuronal differentiation. It is expressed in the immune system: in particular, in T and B lymphocytes, as well as neutrophils, or dendritic cell in which is involved in the differentiation of T cells along the Th1 phenotype representing as well a new link between the innate and adaptive immune system. (80, 81) It has got an important function in central nervous system in which it is expressed in almost all cells, in particular during development.

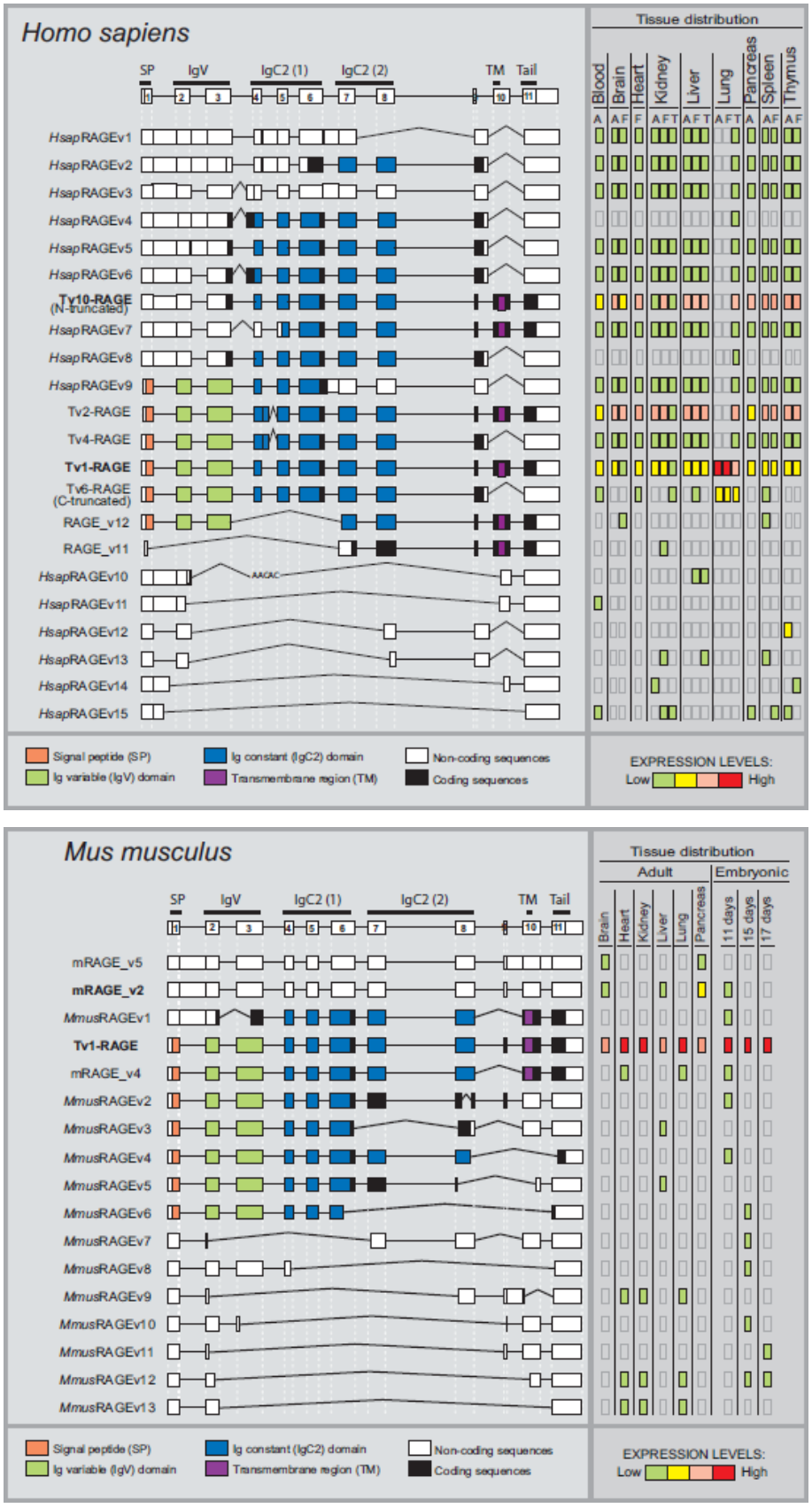

Figure 1.10: Representation of RAGE splice transcript variants and their relative expression levels in Homo sapiens and in Mus musculus tissues. A: adult, F: fetal, T: tumor. Non-coding sequence are show in white, alternative junctions in open tangle. Splice variants result in changes that might affect the extracellular ligand-binding domain. Relative abundance of each splice variants show differences in expression levels among all the analyzed tissues. (82)

The canonical full-length isoform of RAGE exists as a cell surface 45-50kDa protein and it consists of 404 amino acids. The full receptor is made of11 exons and 10 introns od variable length and a 3'UTR region that spans over 4 kbp, which is located within the gene-dense major histocompatibility class III region on chromosome 6. Globally it is made of 5 domains and it is composed of highly-charged and hydrophobic cytosolic domain (amino acids 362-404), which is responsible for signal transduction, single transmembrane domain (amino acids 340-361) which anchors the receptor in the cell membrane, and the extracellular ligand-binding region (amino acids 1-339). This one is made of one N-terminal V type variable domain and two C-type constant domains. The ligand binding site is reported to be on the V type which secondary structure consists of two β-sheet, an α-helix and a random coil domain. The cytoplasmic portion of RAGE is a critical domain for RAGE ligand signaling inside the cell. In 2010, studies of crystallography of RAGE, revealed a highly basic surface based on Arg and Lys residues in the V-C1 domain the accounted for the ligand binding characteristic. Thus, the entire V domain and a major part of C1 form a large area of electropositive surface that fits well to the acidic (negative) feature character of the diverse RAGE ligands, including AGE-modified proteins, amyloid-b, S100 proteins, dsRNA and dsDNA, consisting in the major driving force of in formation of the complex.
RAGE expresses several splice variants, at least 20 in humans, however nearly of 40% of the total transcripts are noncoding ones and they have tissue specific patterns. (82).
Alternative promoters, polyadenylation sites and alternative splicing play an important role in expanding transcriptomic and proteomic diversity that are expressed by a wide variety of cell types. Studies have shown that extensive genetic variability occurs within the RAGE gene, with several SNPs characterized to-date. Promoter RAGE polymorphisms -429T>C (rs1800625), -374T>A (rs1800624) and 63 bp deletion (-345to -407 bp) are associated with an increase in RAGE expression and immune-related diseases, like systemic lupus erythematosus, Crohn's disease and T1DM. The resulting proteins from these transcripts have different binding properties, including the total absence of ligand-binding sites (i.e., N-terminal truncated), or the absence of the transmembrane domain with a distinct C-terminal sequence. It is estimated that 20-60% of the total transcripts, depending on species, are noncoding ones and they are only in specific tissues. The derived protein from an alternative splicing of dis-functional RAGE represents a powerful signal regulator of the isoform complete. (82-84)

RAGE exists in four main forms: i.e. as a trans-membrane signaling receptor, as a N-truncated form, as circulating soluble forms (cRAGE, esRAGE) and as a dominant negative form (dnRAGE). (fig. 1.11) It was shown that RAGE can form oligomers on the plasma membrane, the preassembly has substantial implications for the mechanism of RAGE activation. Although preassembly of RAGE

might facilitate ligand binding and increase its efficiency in signaling, preassembled receptors could promote nonspecific activation with adverse consequences (85). dnRAGE can form hetero-complexes with full-length RAGE, resulting in nonfunctional assemblies. It has been proposed that soluble alternative splice products of RAGE can act as decoy receptors, decreasing the concentration of available ligands. (82-84, 86) However, the molecular basis for RAGE activation by its diverse set of ligands has remained enigmatic.

RAGE is able to bind a large plethora of ligands of different origin, that will vary in structure, size, and molecular organization, including not only AGEs and β-sheet fibrils, but also several members of the S100 protein family (S100B, S100P, S100A4, S100A6, S100A8/9, S100A12, S100A11–13), high mobility group box-1 (HMGB1) and prions, with a so-called PRR domain. RAGE ligands are predominantly negatively charged molecules. All RAGE ligands are characterized by a strong negative net charge that can extend over a single domain as in HMGB1 or over the entire molecule, as in native S100 proteins or in AGE-modified proteins. (87, 88)

The high resolution 1.5 Å crystal structure of the first two domains of RAGE lead to propose that RAGE employs at least two completely different mechanisms for ligand binding: the first mechanism involving hydrophobic interaction; the second one involving AGE-RAGE recognition occurs primarily through binding negatively charged regions of AGE-modified proteins rather than interaction with distinct glycation moieties on the amino acid side chains of proteins. (89)

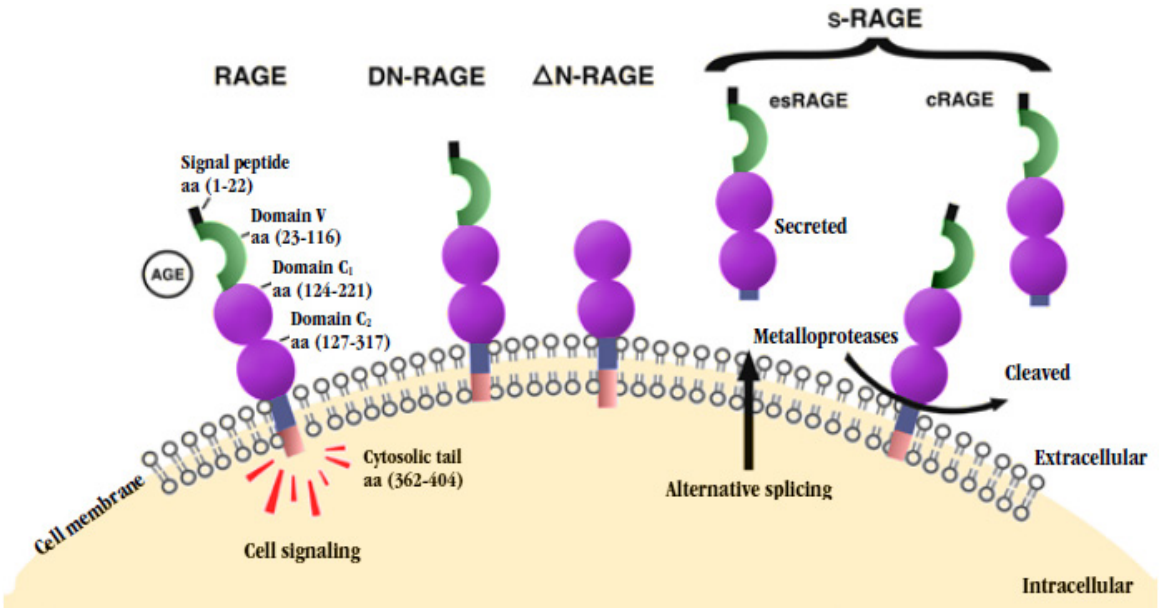

Figure 1.11: the main form of RAGE: a trans-membrane signaling receptor, a N-truncated forms, as circulating soluble forms (cRAGE, esRAGE) and as a dominant negative form (dnRAGE).

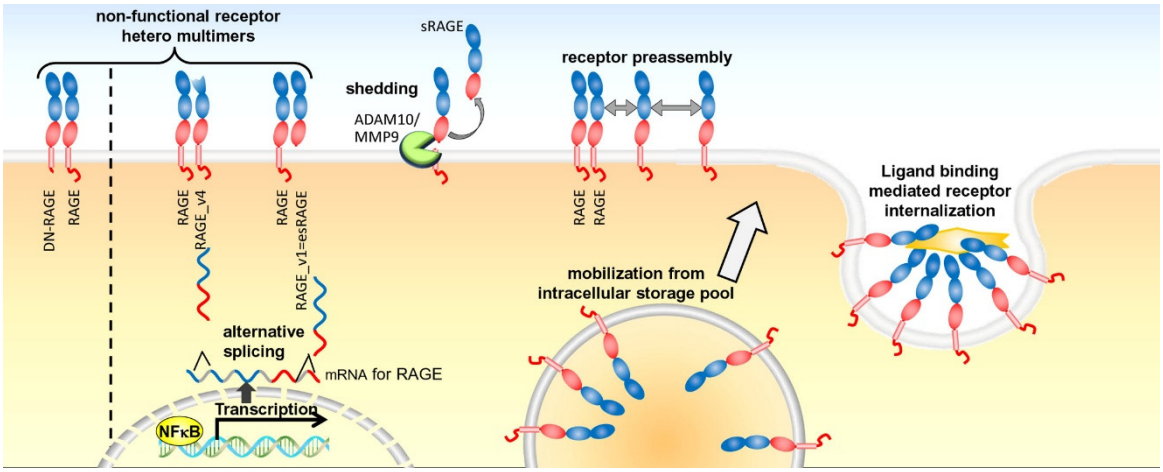

Figure 1.12: Alternative splicing of RAGE mRNA results in two major variants of RAGE: RAGE_v1 (es-RAGE) and RAGE_v4, which are signaling-incompetent. Full-length RAGE is cleft by metalloproteases ADAM10 and MMP9, leading to the release of sRAGE. The surface concentration of RAGE is regulated by receptor export and ligand-induced internalization. Assembly of full-length RAGE with sRAGE/esRAGE or RAGE_v4 will result in heterocomplexes that can bind extracellular ligands but are not signaling-competent. (80)

Ligand-binding activates the receptor though phosphorylation or ubiquitination on the cytoplasmatic side stimulating the receptor endocytosis. The endocytosis of the complex undergoes to a regulated mechanism both clathrin dependent or independent. These vesicles are transported to endosome, where AGEs have been dissociated from receptor; this last been transferred back to membrane, while AGEs are fragmented by an unknown mechanism, then processed and released. Assembly of hetero-complexes of RAGE can bind extracellular AGEs ligands but results are non-signaling-competent. See fig. 1.12 (76, 80, 85, 88)

On the other end the link between the RAGE and its ligands triggers a cascade of intracellular events, followed by the transcription of a range of genes involved in different biological systems, as well as other reactions such as the formation of oxidative stress. AGE-s-RAGE interaction stimulates a various number of signaling pathways, depending on the identity of the ligand and the cell type, the concentration of ligand, the presence of other ligands and the concentration of RAGE on the cell surface. RAGE interactions stimulate a various number of cascades signaling including Jak/Stat, NADPH oxidase, mitogen activated protein kinase (MAPK), p38, extracellular regulated ERK-1/2, c-Jun, activation of transcription of the nuclear factor Nf-kB, AP-1, or IFN stimulated response elements (ISRE) followed by a consequent upregulation of cytokine, growth factors or inflammatory pathways. Moreover, that can activate signal pathways such as those of protein kinase C, triggers NADPH-oxidase, chemo-attractive and proinflammatory gene expression, VCAM-1, or intercellular adhesion molecules-1 (ICAM-1). It has been shown that in patients with coronary artery disease, serum levels of secreted MMPs, such as MMP-2, MMP-8 and MMP-9, are higher in patients accompanied by type 2 diabetes than in nondiabetics, indicating a role of MMPs in the pathogenesis of coronary atherosclerosis complicated with T1D;

analysis showed a significant positive correlation between AGEs accumulation and MMP-9 expression in all aortic and coronary specimens from both diabetics and non-diabetics. (90)

RAGE has also got a crucial role in the development and progression of nephropathy (91), atherosclerosis (92), functional changes in peripheral nerves, neurodegenerations, retina damage and lung homeostasis (93). Under physiological conditions, RAGE is expressed at low levels on several cell types (monocytes/macrophages, T-lymphocytes, endothelial cells, dendritic cells, fibroblasts, smooth muscle cells, neuronal cells, glia cells, chondrocytes, keratinocytes), on the opposite In pathophysiological settings, such as diabetes, chronic inflammation, cancer or neurodegenerative disorders, RAGE expression is increased drastically.(76) RAGE induces inflammation through persistent activation of the proinflammatory transcription factor, NF-kB (94) with a pathway mediated by Jak/Stat; also AGEs have been reported to activate serine-threonine protein kinases in the mitogen-activated protein kinase (MAPK) pathways. C jun N terminal kinase (JNK) and p38 MAPK are the two major subfamilies of MAPKs that participate in apoptosis. Activation of NF-kB increases the expression of proinflammatory cytokines such as IL-6 and monocyte chemoattractant peptide 1 (MCP-1) as well as RAGE itself thus intensifying the inflammatory response. Blockage of RAGE causes a retarded inflammatory response (95). Moreover, recent studies showed that RAGE-deficient mice are resistant to DIO and insulin resistance, this kind of protection resulted from increased metabolic rate (96)

Recent studies have identified microRNAs (miRNAs) involved in the regulation of AGEs-RAGE signaling in the context of diabetic micro- and macro-vascular complications. Only a few studies explored the role of miRNAs in AGE/RAGE signaling and their relationship with diabetes, e.g. miR-214 is up-regulated after exposition of primary monocytes to various AGEs delaying apoptosis. mi-RR-221/miR-222 cluster has also been shown to be increased where RAGE is stimulated resulting in proliferation of smoot muscle cells exposed to AGEs. (97)

1.4.1 The cross talk between AGEs -RAGE axis and DPP4-incretins

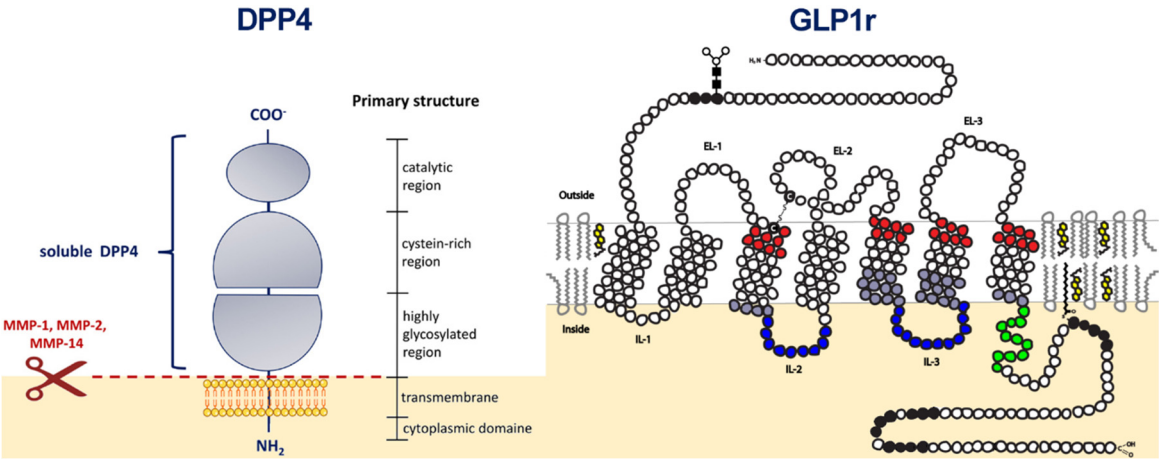

Figure 1.13: Schemes of structures of DDP4 (edited from: (98)) and GLP1r.

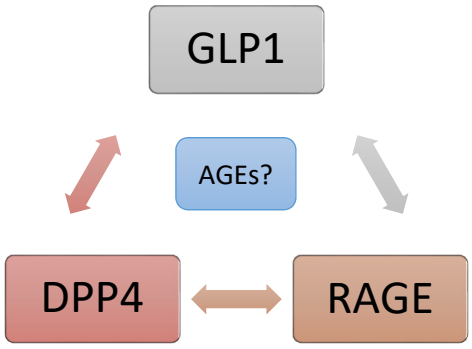

The incretin hormones account for approximately 50% of the insulin secretion after a meal, they are involved in multiple functions and in particular they ease the disposal of glucose trough the stimulation of insulin secretion from the endocrine pancreas. (99, 100) It has been known for many years that intravenous glucose will not stimulate insulin secretion to the same extent of a glucose given orally, those hormones were called incretins. Those hormones are secreted from intestine after a meal, their name was proposed by "La Barre" in 1932. The incretin hormones account for about 70% of the total insulin secretion after the administration of oral glucose. The two major incretins are GLP1 and GIP.

↳ *GLP1/GIP*

The main gut hormones are Glucose-dependent Insulinotropic Polypeptide (GIP) and Glucagon Like Peptide-1 (GLP1), which will lower blood glucose levels and increase the insulin secretion. GIP found by Brown and colleagues in 1970, is a 42 amino acids peptide synthesized in enteroendocrine K cells in the proximal small bowel. It was reported that GIP has the ability to stimulate insulin secretion at physiological doses in a glucose-dependent manner (101). GIP is released from K-cells in the proximal small intestine and targets the GIP receptor (GIPR). However, more than 50% of the incretin effect remains after removal of GIP.

The second incretin hormone, GLP1 that is the greatest incretin, was discovered in 1985. It is a 30-residue peptide long hormone that derives from the transcription product of the pro-glucagon gene which is expressed in the pancreas, intestine, and brain. It is released from L-intestinal cells;

cells in the distal ileum and colon and it exists in two molecular forms GLP1 (7-37) and GLP1 (7-36) amide; it has been recognized that the post-translational processing of preproglucagon differs in a tissue specific manner: GLP1 (1-36) amine is predominantly secreted in the plasma, GLP1 (1-37) in the ileum and hypothalamus. Normal plasma levels of GLP-1 in the fasted state are 5–10 pmol/L and 15–50 pmol/L after eating. The release occurs in a biphasic pattern with the first phase occurring at 10–15 min after oral food ingestion and the second phase occurring at 30–60 min. GLP1 release is mainly regulated via a glucose-sensing mechanism, both metabolizable sugars and non-metabolizable sugars can trigger GLP1 release by closure of K_{ATP} channels and stimulation of sodium-glucose co-transporters (SGLTs); moreover, it is released to respond to lipids amides which in turns activate GPCRs.

GLP1 has got multiples effects: it stimulates β-cells survival, transcription of proinsulin, enhancing insulin biosynthesis and secretion from pancreatic β-cells in a glucose-dependent manner, inhibition of glucagon secretion from pancreatic α-cells. (102, 103) GLP1 also increases the expression of GLUT-2 and glucokinase, enhancing the efficacy of glucose on insulin secretion. Therefore, GLP-1's may contribute to the enhancement of insulin secretion and biosynthesis. Moreover, it has got other functions: in stomach and intestine it will inhibit gastric emptying and delay absorption of food while in the hypothalamus it can regulate appetite interacting with other hormones as leptin and gherlin. GLP1 may also be neuroprotective, via activation of anti-apoptotic signaling pathways in specific neurons; in liver, muscles and adipose tissue also increase insulin sensitivity. Finally, GLP1 regulates preadipocytes differentiation significantly promoting the expression of adipocyte specific markers aP2, PPARγ and LPL. (104) Treatments *in vitro* of 3T3-L1 cells or human primary cultures show that GLP1 stimulates in adipocytes differentiation, production of a major number of smaller lipid dropplets and lipolysis; GLP1 also suppresses AGEs induced RAGE gene expression (105-108).

The C-terminal regions of the peptide-1 binds to the N terminus of the 7-helix transmembrane guanine nucleotide-binding protein-coupled receptor GLP1 receptor (GLP1R). The receptor, see fig. 1.13, consists of 463 amino acids and is a glycoprotein. Specifically, it is a G protein-coupled (GPCRs) belonging to family B; these receptors possess a unique extracellular N-terminal domain which is connected to the integral membrane core (or J domain) that is typical of all GPCRs.

To be totally functional, the GLP1R undergoes N-linked glycosylation and only the fully glycosylated form is present in the plasma membrane. Inhibition of the glycosylation prevents appropriate processing and cell surface positioning.

A complicating factor in understanding and determining the structure may be its tendency to form oligomers, but nowadays the structure of the receptor remains partially unknown. (109) As with

family, GLP1R predominantly couples with $G_{\alpha s}$ and activate adenylate cyclase to raise the intracellular cAMP levels and finally to insulin secretion. GLP1R is expressed at low grade in many tissues: lungs, pancreatic islands, stomach, hypothalamus, heart, intestine and kidney. Extensive studies have been done but the saga is not completed. The unambiguous identification of GLP1R expressing tissues and cells types both in humans and in animals constitute a critically important knowledge for fully understand the effects of GLP1 peptide and for create pharmacological compounds ad hoc.

GLP1 is susceptible to cleavage at position 2 (in alanine) by the ubiquitous dipeptidyl peptidase DPP4, which occurs almost immediately upon the secretion, rendering GLP1 a short half-life, of only two minutes. (110, 111)

↳ *DPP4 (o CD36)*

Dipeptidyl peptidase-4 (DPP4) or adenosine deaminase complexing protein 2 (ADCP 2) or T-cell activation antigen CD26 (EC 3.4.14.5), see fig. 1.13, is a type II glycoprotein ubiquitously expressed (lung, brain, pancreas, kidney, vessel, prostate, uterus, thymus, lymph nodes, spleen and adipose tissue) in a variety of cells. e.g. epithelial cells, fibroblasts, adipocytes, leukocytes and natural killers. Its expression is dysregulated in several disease states as inflammation, cancer, diabetes and obesity. (98)

DPP4 acts as a serine exopeptidase with a dipeptidyl peptidase activity that regulates various physiological processes by cleaving peptides in the circulation, including many chemokines, mitogenic growth factors, neuropeptides and peptide hormones as incretins. It removes N-terminal dipeptides sequentially from polypeptides having unsubstituted N-termini provided that the penultimate residue is proline. The soluble circulating form of DPP4 that lacks the transmembrane and cytoplasmic domains of the membrane-associated DPP4 is largely responsible for degradation of the majority of newly synthesized GLP1 and GIP. (111) Recent studies revealed a strong expression of this gene in human white adipocytes suggesting a possible role to the adipocytes differentiation process. Moreover, in adipose tissue DPP4 will have a strong impact: it stimulates lipid accumulation and PPARγ expression and it may be involved in remodeling and inflammation of adipose tissue. Importantly, its circulating form is augmented in obese and T2DM, and it may represent a molecular link between obesity and vascular dysfunction. Recapitulating, DPP-4 is involved in adipose tissue inflammation, which is associated with insulin resistance and diabetes progression, being a common pathophysiological mechanism in obesity-related complications. Several studies have been done to analyze the correlation between DPP4, glucose, lipids and differentiation many of which are conflicting. (112, 113). The observation that

GLP1 is rapidly degraded by DPP4 has fostered the development of specific protease inhibitors that prevent the rapid fall of GLP1 in circulating plasma after eating: some examples of drugs analogous of GLP1 are exenatide, liraglutide, lixsenatide or DPP4 inhibitors e.g. vidagliptin, sitagliptin or linagliptin. (114)

Nowadays DPP4 inhibitors are a class of anti-hyperglycemic agents indicated for improving glycemic control in patients with T2DM. The pleiotropic effects of DPP4 inhibitors, along with the control of glucose plasma concentrations, represent important mechanisms of action of these drugs, among which a potential cardiovascular protection activity appears to be of major importance, especially in T2DM. Moreover, DPP4 inhibitors have protective effect on the endothelium, anti-inflammatory and anti-oxidative effects; the binding of AGEs to RAGE results in a generation of ROS and subsequent activation of NF-kB which could promote monocyte chemoattractant protein 1 (MCP1) that plays an important role in early phases of atherosclerosis and inflammation (108, 115)

↳ *Medical Treatments*

Weight reduction is an important goal for many people with TM2D. Bariatric surgery is no longer considered a last resort treatment. GLP1 agonists given by injection are emerging as a useful treatment since they not only lower blood sugar but are associated with a modest weight reduction. The role of the oral DPP 4 inhibitors is emerging as second line of treatment due to a possible beneficial effect on the β-cell and weight neutrality. Nevertheless, insulin treatment still remains the cornerstone of treatment in many patients with TM2D. New treatments for diabetes are coming on line but prevention and treatment of obesity through increased exercise and reduced calorie intake still seems the best option in most patients with TM2D. (114)

1.5 MASS SPECTROMETRY

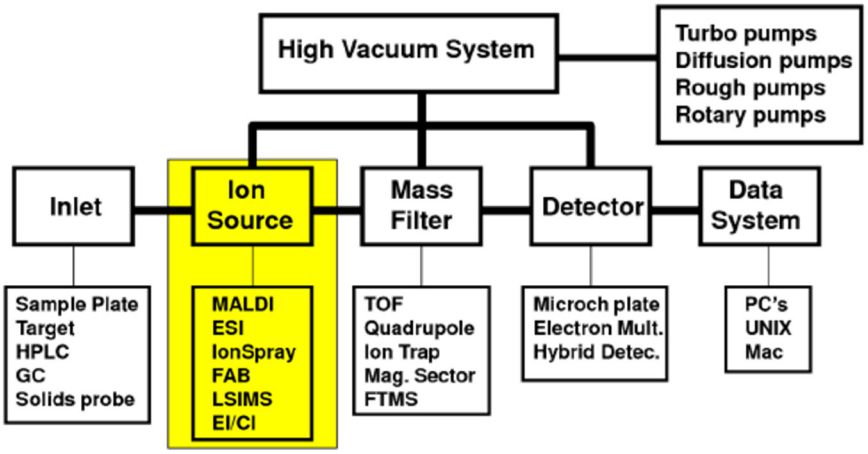

Figure 1.14: Configuration that characterizes mass spectrometers: INLET) system of sample insertion, which can be entered directly, or come from a separation system; ION SOURCE) an ionization source, which has the task to provide for the production of analyte ions in the gas phase; MASS FILTER) a mass analyzer, which purpose is the separation of the products in source ions according to their ratio m/z; DETECTOR) that receives the ion current generated by the ions from the analyzer; DATA SYSTEM) a processing system and data management, which deals with the transformation of the analog signal coming from the analyzer to a digital signal and the generation and storage of the mass spectrum and its data analysis

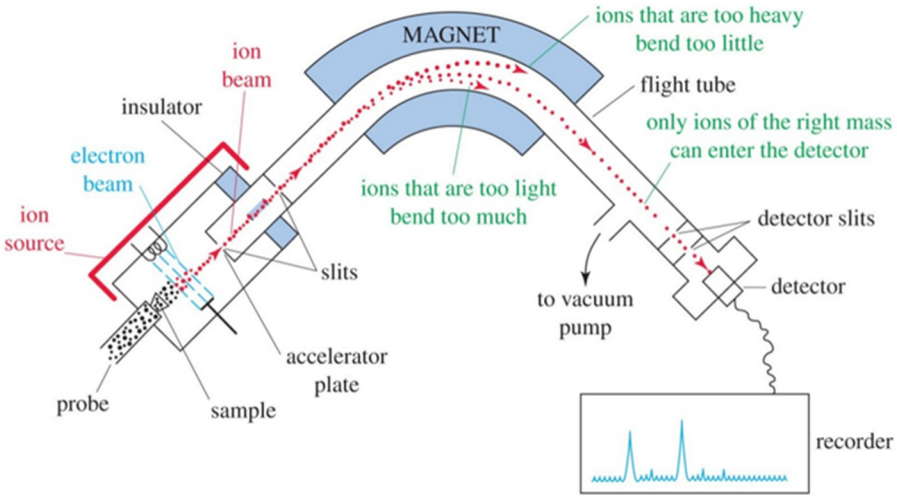

Figure 1.15: Simplified scheme of a mass spectrometer (116)

The genome is a fairly static system and is almost the same in every cell of the body; the proteome, instead, is highly dynamic since the type of protein, its abundance, its localization within a tissue, the type and amount of post-translational modifications, depend strongly from the environment and the physiological state in which cells are located. The proteome and the more highly dynamic metabolome can describe the environment of life in which the cell found itself, and spectrometry has a fundamental role in the analysis of both.

Spectrometry is generally recognized to have been started with the work of Sir. Joseph John "JJ"

Thomson. His work on conduction of electricity through ionized gasses lead to his being awarded the Nobel Prize for Physics in 1906, though his best-known work on mass spectrometry came later in 1911. There are more than one types of spectrometry. There is the infrared spectrometry that measures the bond vibration frequencies in a molecule and is used to determine the function groups. The nuclear magnetic resonance spectrometry, that analyzes the environment of the hydrogen atoms in a compound; the ultraviolet spectrometry that determines bonding patterns and finally the mass spectrometry (MS). (116)

Mass spectrometers consist of three main components: an ion source, a mass analyzer and a mass detector. The ion source is responsible for the ionization of the sample molecules, is concerned with applying a charge to a molecule. Once a molecule has been charged by the ion source, it now has a specific mass-to-charge ratio. The mass analyzer that is in many cases both physically and functionally the middle, is accountable for separation of ions based on their mass-to/charge ratio (*m/z*) and evaluate this ratio for ions passing through the mass spectrometer. The detector, whom records the incoming ions and thereby measuring their *m/z* ratio. It is responsible for counting the molecules at each mass-to-charge value reported by the mass analyzer. (117, 118) The first step in the analysis is the production of a gas phase ions of the compound, for example by electron ionization. These molecular-ions normally undergone into fragmentations. A radical cation with an odd number of electrons, can give either a radical and an ion with an even number of electrons, or give a molecule and a new radical cation. These two types of ions have different chemical properties. Each primary produced ion can, in turn, undergoes into fragmentation, and so on. All these ions are separated in the mass spectrometer according to their *m/z* ratio and are detected in proportion to their abundance. The output of the mass detector is the mass spectra. With this type of ionization, also, it has the production of mono-charge species, and therefore it is possible to determine directly the mass of the analyte. The ionization is based on desorption, the work of a laser beam, the analyte is embedded in a matrix suitably crystallized; the product ion is sent to the analyzer in TOF that measures the *m/z* according to the time taken to travel the distance between the source and the detector.

The methods commonly used in proteomics are “Matrix Assisted Laser Desorption Ionization” or MALDI introduced by Karas and Hillenkamp in 1988 and “Electrospray Ionization” also known as ESI. MALDI is more sensitive than other laser ionization techniques, it is a powerful tool to analyze many different structures almost independently of their chemical and physical properties; it is an analytical technique which allows the identification of unknown substances through the measurement of their molecular weight. This technique works physically measuring the accurate masses of either precursor ions or its fragmentation products. MALDI ionization allows the

production of intact ions (that is, not fragmented) in gas phase, starting from large molecules, non-volatile and thermally labile, such as proteins, oligonucleotides, polymers and other inorganic compounds with high molecular weight. If the MALDI is attached to a Time of Flight (TOF) mass analyzer these ions are then sent down the TOF tube (typically ~2m) and are separated according to their velocity (light ions hitting first). To obtain the protein identification, these data are used for querying protein databases for example MS-Fit, MOWSE, Prot-ID, Expasy tools, and Peptide search. The sequence with the highest score has the highest probability to individuate the protein of interest. (119)

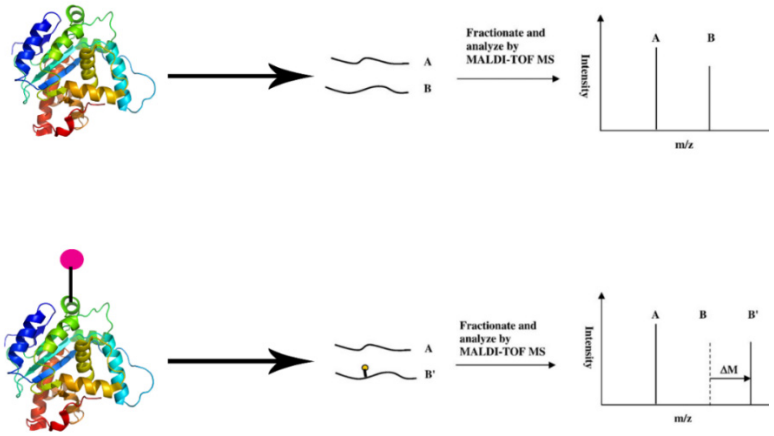

Figure 1.16: The cartoon described the scheme for the use of MALDI-TOF and peptide mapping for study modifications sites on a glycated protein. (image adapted from (120))

MS is characterized by a relatively simple and fast sample preparation and has sufficient tolerance to contamination by salts, buffers and detergents, but requires a sample fairly concentrated. The primary advantage of this approach is that the technique is very fast, is high sample throughput and sensitive; it requires very small amounts of analyte also it requires easy preparation of sample; but it is a destructive technique, that means that the sample cannot be recovered, furthermore a whole tissue lysate or a whole homogenate of cells contain also proteins in very small quantity and these last cannot be resolved without an enrichment. MS allows sophisticated and very in-depth investigations, the downside is the great influence of the pre-analytical phase, the environmental conditions of work and the processing of the sample that can lead to false positive results unreadable or unusable. In particular, post translation modifications (PTMs) are often thermally and chemically labile when removed from the physiological setting, particularly at high pH and temperature; pre-analytic processing may compromise MS analysis. (50, 121, 122). The analyses of PTMs modification with MS can be difficult, the level of difficulty is dependent on: the mass shift in the peptide molecular weight, the overall abundance of the modified peptide, the stability of the modification during MS and MS/MS analysis, and finally the effect of the

modification on the peptide's ionization efficiency (and therefore the sensitivity). PTMs may be detected in spectra by a rightward (that mean a mass increase) shift of specific peak in *m/z* due to peptide modification. (fig. 1.16)

1.5.1 Use in medicine

MS's characteristics have raised it to an outstanding position among analytical methods: unequalled sensitivity, detection limits, speed and diversity of its applications. The most recent applications are mostly oriented towards biochemical challenges such as investigate intact protein complexes, providing details about the complex composition, topology, stability and dynamics analysis of proteome, metabolome and into discovery of new drugs. Other analytical applications of MS are routinely applied in pollution control, food control, forensic science, natural products or process monitoring.

Forasmuch as the non-enzymatic reaction between proteins and sugars leads to glycated proteins which, depending on the number of glucose molecule condensed on them, would exhibit a different functionality; several studies and medical investigations start to use MS to measure the glycation of proteins in diabetes (50, 123-125). Quantitative measurement of protein oxidation and glycation adducts provides information on level of exposure to potentially damaging protein modifications, protein inactivation in ageing and disease, metabolic control, protein turnover, renal function and other aspects of body function. Nowadays, the measurement of the glycated haemoglobin (HbA1c) is widely used for the diagnosis and monitoring of diabetes mellitus and assessment of the mean glycation level present in the subject. Actually, considering that the half-life of haemoglobin is 120 days, the measurement of HbA1c can provide valid information on the "glycation stress" experienced by the subject during the protein life.

Past works MALDI/TOF-MS analysis of patient samples was used to demonstrate a method for quantitation of total glycation on the β-subunit of haemoglobin. The glycation levels were easily calculated by the abundance ratio of the peaks corresponding to the glycated and the un-glycated species. Recent studies shown that exists several types of glycated haemoglobin but MALDI-TOF MS cannot distinguish between isobaric and mono-glycated forms. (126) It is important to underline that HbA1c is not properly an AGEs although an Amadori product, so an intermediate product. The AGEs if compared with HbA1c have a longer life, so them will be a stronger glycation control, but, as further studies are needed, their use is not yet implemented.

Application of quantitative high resolution MS to studies of protein oxidation and glycation will facilitate measurement of extent of protein oxidation and glycation in proteome-wide analysis in

the future. It stands as the final goal, to obtain a fingerprint of the quantitative damage to cellular and extracellular. The levels of one or a combination of these adducts may provide a critical marker for disease diagnosis and progression monitoring. This will be applied to screening protein glycation, oxidation and nitration markers in plasma, red blood cells and leukocytes, urine, cerebrospinal fluid or tissues.

The use of this technique, and others such as immunoassay corroborated to it, will provide for robust assessment of protein oxidation and glycation markers in health and disease.

2. AIMS

Glycation is one of the most important unwanted post-translational modifications, which modifies protein three-dimensional structure and it can trigger the subsequent functional abnormalities. Diabetic subjects, besides the high blood levels, also have a characteristic dyslipidemia and high levels of plasma AGEs. It is well known that glycation and its products can cause a series of pathological conditions but their exact roles is still to be determined. In particular, little is known about their presence and their consequences on adipose tissue which is still fully unexplored.

Glycated proteins are characterized by changes in their function, therefore the rate of glycation could account for the long-term diabetic complications.

The pathophysiological cascades triggered by AGEs could play a crucial role in the hyperglycaemia-independent complications of diabetes. For this reason, prevention and treatment strategy should not only be focused on the early glycaemic control but also on reducing any factor related to glyco-oxidative stress.

In this study the aim was:

1) to build up an *in vitro* model in order to investigate the effects of a chronic exposure to a glycation-inducing environment on the adipogenetic process using a specific cell line or preadipocytes from the stromal vascular fraction obtained by adipose tissue abdominoplasties in obese patients.

2) to compare the gene expression as obtained *in vitro*, with data obtained in adipose tissue from obese subjects with type 2 diabetes or with normal glucose tolerance.

3) to evaluate the use of the method of mass spectrometry to examine and characterize post translation modifications induced by glycation. [In collaboration with Prof. Annunziata Lapolla and the Mass Spectrometry Service (dr. Roberta Seraglia – dr. Marco Roverso; CNR-IENI; Padova)]

2.1 EXPERIMENTAL PLAN

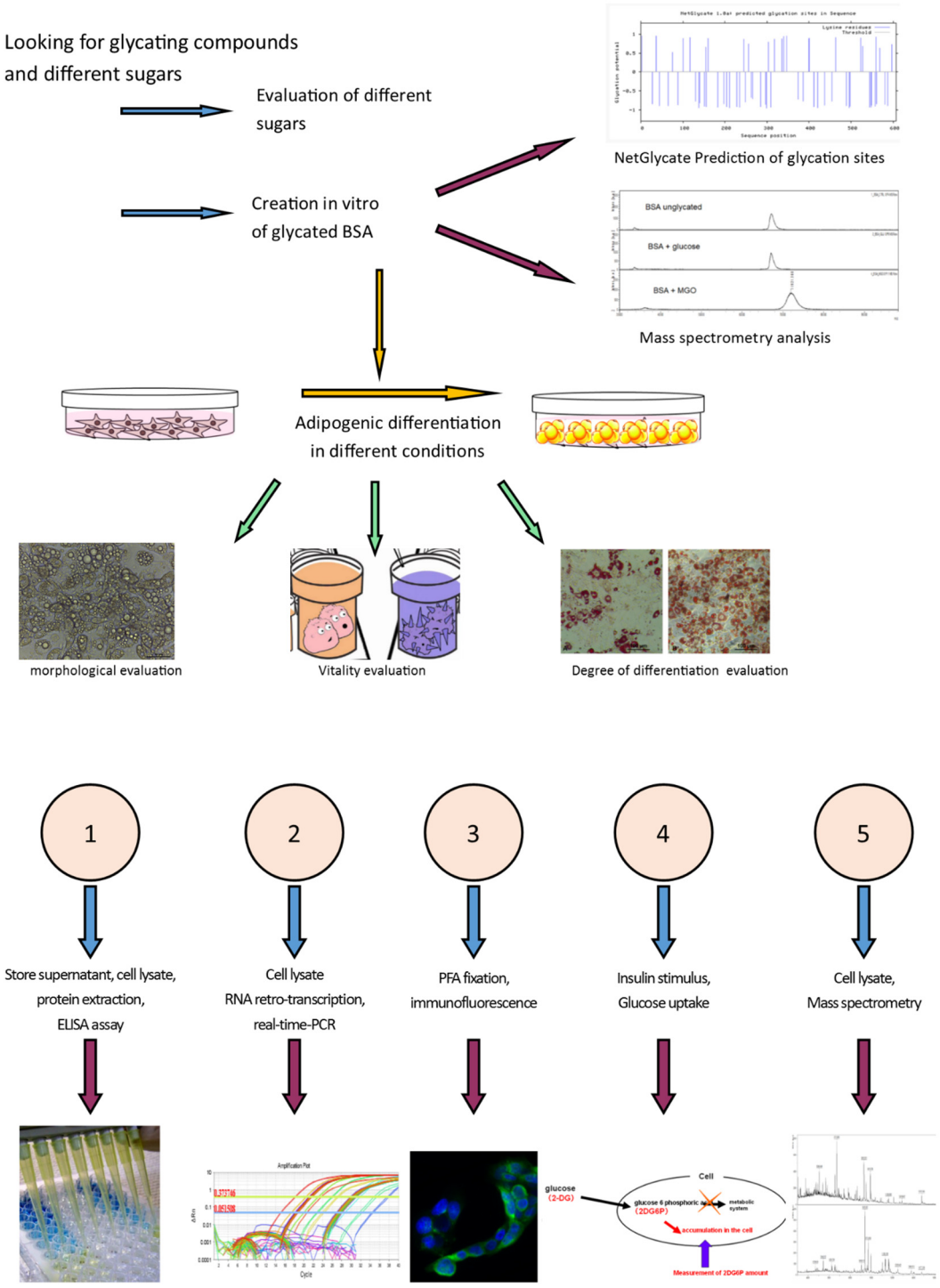

Figure 2.1: Cartoon of the construction of the reference model.

From both scientific and medical literature, it is known that one of the most abundant glycated protein into serum of diabetic patients is albumin. Glycated albumin was recreated *in vitro*, subsequently to characterize it and then, to apply it in cell cultures.

In the first part of the study, 3T3-L1 cell line, a stabilized cell line derived from murine fibroblasts and stromal vascular fraction cells isolated from human adipose tissue hSVF cells were applied.
To study the effects of glycation-inducing environment on the metabolic processes of these cells, a cell culture protocol was developed, providing for the chronic administration of methylglyoxal or glycated BSA. First of all, different substances use was tested: sugars, methylglyoxal, BSA and glycated-BSA in order to choose concentration, allowing both a good percentage of survival and a good differentiation. Following such treatments, some parameters were rated in order to understand the effects of these substances on cellular metabolic process. For this purpose, some tests were performed: immunoassay E.L.I.S.A. test, real-time qPCR, immunofluorescence, glucose uptake and mass spectrometry on mature adipocytes.

Subsequently, the presence of AGEs products with western blot and mass spectrometry in human adipose tissues was investigated. Moreover, were analyzed the gene expression profile for *GLP1R*, *RAGE* and *DPP4* in adipose tissues from 64 obese subjects with type 2 diabetes, pre-diabetes or with regular glucose tolerance. Then, the lipid composition of adipose tissues for 71 different species lipids in normal-glycaemic obese, diabetic obese and post-obese subjects was studied.

3. MATERIALS & METHODS

3.1 MATERIALS

3.1.1 Materials

- µ-Slide VI 0.1; Ibidi® Cell in focus, Ibidi USA Inc., Madison, Wisconsin.
- 2,5 dihydroxybenzoic acid
- 2-deossi- [3H] D-glucose (Amersham-Biosciences, Piscataway, NJ, USA)
- 3,3', 5-Triiodo-L-thyronine (T3) (Sigma®)
- Amersham ® ECL Western blotting, GE Healthcare (Little Chalfont, Buckinghamshire, UK)
- Anti-AGEs: ab23722 (AbCam ®)
- Anti-CML: ab 27684 (AbCam®)
- Anti-GLP1r: (#AGR-021) (Alomone)
- Anti-GLUT4: sc-1606 (Santa Cruz Biotechnology)
- Anti-RAGE: ab135513 (AbCam®)
- Bio-Rad DC ® Protein Assay
- Biotin (Biomedicals® Inc.)
- BSA (Sigma – Aldrich®)
- Cell Scraper (Falcon ®)
- Collagenase (Gibco™ – Life Technologies®)
- Complete Mini Protease Phosphatase inhibitors (Roche®)
- Coomassie blue: Bio-Rad ®
- CUSABIO ®: CSB-E09414m
- CXR Reference Dye (Promega ®, Madison, USA)
- Dithiothreitol (Fluka, St. Louis, MO)
- DMEM F12 (Gibco™ - Thermo Fisher®)
- DMEM high (4.5g/L) glucose: (Gibco™ - Thermo Fisher®)
- DMEM low (1g/L) glucose: (Gibco™ - Thermo Fisher®)
- DMEM NO glucose: (Gibco™ - Thermo Fisher®)
- dNTPs (Deoxy-nucleotides triphosphates) (Promega®)
- Donkey Serum
- EDTA: 60-00-4 (Sigma – Aldrich®)
- FBS (Gibco™ – life technologies®): inactivated by heating 30'-40' at 56°C
- Fluoroshiedl™ with DAPI (Sigma – Aldrich®)
- Fructose: 57-48-7 (Sigma – Aldrich®)
- Galactose: 59-23-4 (Sigma – Aldrich®)
- Glucose: 50-99-7 (Sigma – Aldrich®)
- Glycine: 56-40-6 (Sigma – Aldrich®)
- Goat Anti Rabbit IgG (H+L), Horseradish Peroxidase (HRP) Conjugate (Novex – Life Technologies ®)
- Goat Anti-Rabbit IgG Alexa Fluor® 488 (Gibco - Thermo Fisher®)
- GoTaq®qPCR Master Mix (Promega, Madison, USA)
- Human Leptin full length protein ab51273 (AbCam ®)

- Hyperfilm ECL (GE Healthcare ®, Little Chalfont, Buckinghamshire, UK)
- IBMX 3-Isobutil-1-metilxantina (Sigma – Aldrich®)
- Insulin – Humulin R (Lilly®)
- Isopropyl alcohol: 67-63-0 (Sigma – Aldrich®)
- Lactose: 63-42-3 (Sigma – Aldrich®)
- L-Glutamine (Gibco™ – life technologies®) 100x
- Menzel-Gläser Objektträger, Thermo Scientific ® (Saarbrűckener strasse, Braunschweig)
- Methanol: 67-56-1 (Sigma – Aldrich®)
- Methylglyoxal (MGO): (Sigma – Aldrich®)
- Millex ® Sterile Filter Unit 0.22µm Millipore ®
- M-MLV RT Buffer (Promega®)
- M-MLV RT Enzyme (Moloney Murine Leukemia Virus Reverse Transcriptase) (Promega®)
- MTT: (Sigma – Aldrich®)
- NH_4HCO_3 (Carlo Erba Reagenti)
- Nonfat dry Milk powder
- NP-40 -IGEPAL CA-630 (Sigma – Aldrich®)
- NuPAGE ® Bis-Tris 10% 1.0 mm Mini Gels (Novex ®- Life Technologies' ™)
- NuPAGE ® LDS Sample Buffer 4X (Novex ®- Life Technologies' ™)
- NuPAGE ® MOPS Buffer (25X) (Novex ®- Life Technologies' ™)
- NuPAGE ® Sample Reducing Agent (10X), Novex ®- Life Technologies' ™)
- Oil-Red O (Sigma – Aldrich®)
- Pantothenate (Biomedicals® Inc.)
- Penicillin/Streptomycin (Gibco™ - Thermo Fisher®)
- Peptide Calibration Standard (Bruker Daltonics ®, Bremen, Germany)
- PhosSTOP (Roche®)
- Ponceau S red
- Protran ® BA, Whatman Scheicher & Schuell, Germany
- QIAzol® Lysis Reagent
- Rabbit Anti-Goat IgG Alexa Fluor® 594 (Gibco - Thermo Fisher®)
- Random Primers (Promega®, Madison, WI, USA)
- RNAsin (Promega®)
- RNeasy ® Plus Mini Kit (Qiagen ®)
- Rosiglitazone
- Rox -CXR Reference Dye (Promega®)
- RPMI 1640 (Gibco - Thermo Fisher®)
- SeeBlue ® Plus2 Pre-Stained Standard (Novex ® Life Technologies' ™)
- Sharp Pre-Stained Protein Standard (Novex ® Life Technologies' ™)
- Sodium deoxycholate: 302-95-4 (Sigma – Aldrich®)
- Sodium dodecyl sulfate/SDS: (Sigma – Aldrich®)
- Syber green (Promega®)
- TFA – CF_3COOH: (Fluka Analytical®)
- transferrin (Biomedicals® Inc.)
- Tripsine: (Gibco™ - Thermo Fisher®)
- TRIS
- Turbo DNA-free (Ambion®, Austin, TX, USA).
- Tween 20

3.1.2 Cells lines

Cells were grown on plastic culture dishes or multi-plate wells and maintained at 37°C in an incubator at 5% CO_2 and 95% humidity.

- **3T3-L1** (ATCC® CL-173™): *Mus musculus* - mouse; Embryo, fibroblast-pre-adipocyte. Them derive from Swiss albino (3T3) mouse embryo tissue by Howard Green of Harvard Medical School, L1 is a continuous substrain developed through clonal isolation.
  Canonical grow medium is DMEM 25mM glucose supplemented with 10% Fetal Bovine Serum (FBS), L-glutamine 1% and Penicillin/Streptomycin 1%. To subculture: renew medium 2-3 times a week; ratio 1:10 - 1:15
- **Huh-7**: (kind gift from Dr. Claudia Radu, Department of Medicine DIMED, University of Padova) is an immortal epithelial-like tumorigenic human hepatic cellular carcinoma cell line. Derived from cellular carcinoma taken from a liver tumor in a 57-years old Japanese in 1982. It usually grows in a 2D monolayers. Canonical grow medium is DMEM 5mM glucose supplemented with 10% FBS, L-glutamine 1% and Penicillin/Streptomycin 1%. To subculture: renew medium 2-3 times a week; ratio 1:4 - 1:7
- **MKN 28:** (kind gift from Dr. Marina De Bernard, Host-Pathogen interaction Lab.; Department of Biology, University of Padova) Human Gastric Cancer cell line; is an immortal cell line, adult human adenocarcinoma tubular; it derives from a stomach tumor of a 70-years old, Mongoloid female; canonical grow medium in RPMI 1640 supplemented with 10% of FBS and Penicillin/Streptomycin 1%. To subculture: renew medium 2-3 times a week; ratio 1:3 - 1:5
- **MKN 45:** (kind gift from Dr. Marina De Bernard, Host-Pathogen interaction Lab.; Department of Biology, University of Padova) Human Gastric Cancer cell line, semi-adherent cells; gastric adenocarcinoma, established from the poorly differentiated adenocarcinoma of the stomach (medullary type) of a 62-year-old woman; canonical grow medium in RPMI 1640 supplemented with 10% of FBS and Penicillin/Streptomycin 1%. To subculture: renew medium 2-3 times a week; ratio 1:4 - 1:8
- **PC12: (**ATCC® CRL-1721™) derived from a pheochromocytoma of the rat adrenal medulla; canonical growth medium: RPMI 1640 supplemented with 10% of horse serum; 5% of FBS, L-glutamine 1% and Penicillin/Streptomycin 1%. To subculture: renew medium 2-3 times a week; ratio 1:4 - 1:7
- **BJ** (ATCC® CRL-2522™): Human foreskin fibroblast cell line, adherent. The line was established from skin taken from normal foreskin-new born-male. Canonical grow

medium is DMEM 5mM glucose supplemented with 10% FBS and Penicillin/Streptomycin 1%. To subculture: renew every 2-3 days; ratio 1:2 - 1:9

3.2 METHODS

3.2.1 Cell culturing

Never allow culture to become completely confluent. Remove and discard culture medium, then rinse the cell layer with PBS 1x with Ca^{2+} and Mg^{2+} to remove all traces of serum that contains trypsin inhibitor. Add 2.0 to 3.0 mL of Trypsin-EDTA solution to flask, place it at 37°C to facilitate dispersal, and observe cells under microscope until cell layer is dispersed (usually within 5 to 15 minutes). Add 6.0 to 8.0 ml of complete growth medium and aspirate cells by gently pipetting. Add appropriate aliquots of the cell suspension to new culture vessels.

3.2.1 3T3-L1 Adipogenetic Differentiation

First of all, the 3T3 cells were initially plated and cultured in a proper number in canonical growth medium described above; then 24-hours post confluence (mature adipocytes do not undergo cell division and lose their ability to propagate) with the purpose of differentiate 3t3-L1 cells, DMEM medium has been added with:

- IBMX 0.5mM: It has the task to increase the turnover of cAMP through inhibition of the AMP cyclical phosphodiesterase enzyme of its degradation.
- DEXA 1µM: it's a gluocorticoid and activated the transcriptional factor C/EBPb.
- Insulin 2µM: (the most potent among the three inducers) induced the phosphokinase cascade
- Rosiglitazone 10µM: a potent agonist for PPARγ, working as an insulin sensitizer by binding to the PPARγ receptors in fat cells and making the cells more responsive to insulin.

After three days, this cocktail have been replace with fresh medium in which IBMX and rosiglitazone were excluded, whereas DEXA and insulin still added to the medium. This second cocktail refreshed twice time every three days, still maintain till 10^{th} -11^{th} day. Finally, the cocktail has been replaced with canonical growth medium to the 15^{th} day. As early as the third day, it is possible to detect firsts morphological changes that are accentuated gradually until reaching the phenotype fully differentiated.

To determine the effect of BSA or glycated BSA, methylglyoxal or several sugars on adipogenesis of 3T3-L1 cells, the compounds were either added to the growth medium.

Several sugars have been tested: glucose in three different concentrations (5mM-low glucose, 25mM-standard glucose and 100mM-very high glucose), fructose, lactose, sucrose (all three at 25mM); using as base medium the DMEM NO glucose.

Moreover, has been tested methylglyoxal (a dicarbonylic compound) and BSA in two forms: glycated or not, at different proportions of volume; using as base medium DMEM high glucose.

3.2.2 Oil-Red O staining and triglyceride quantification

Oil Red O is used to demonstrate the presence of fat or lipids in fresh, frozen tissue sections which have been in use since the first 1900s. Red Oil O can't form bonds with lipid components, it is a pigment that functions as an oil-soluble colorant, and the technique represents a physical method of staining. Briefly, gently rinse each well of the plate with 2 ml of sterile PBS 1x along the sides of each well of the adipogenic plate so as not to disturb the monolayer. Fix for 1 h in 10% formalin/PBS 1x at 4°C and rinse with distilled water. Stain with Oil-Red O solution in 40% isopropanol for 15 min at room temperature and rinse gently twice with water. View the plates on a phase contrast microscope. Lipids will appear red. Quantified the oil droplet contents by measuring the spectrophotometrically the absorbance of Oil-Red-O at 490 nm with Victor™, (PerkinElmer).

3.2.3 MTT cell viability assay

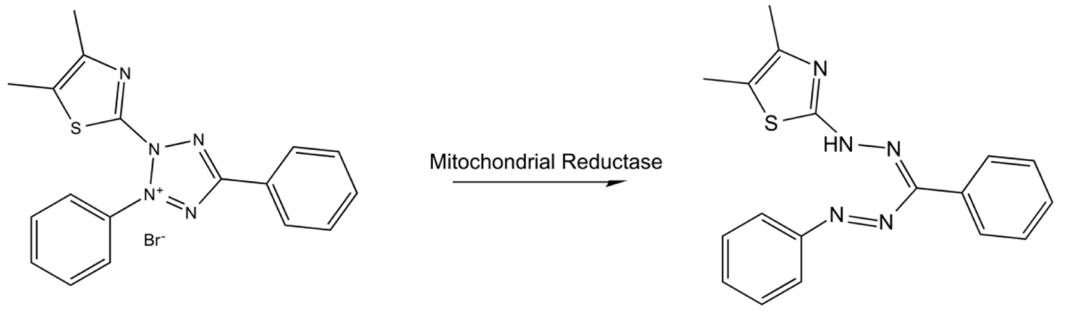

3-(4,5-dimethylthiazol-2-yl)-2,5-diphenyltetrazolium bromide **(MTT)**

(*E*,*Z*)-5-(4,5-dimethylthiazol-2-yl)-1,3-diphenylformazan **(Formazan)**

The MTT (3-[4,5-dimethylthiazol-2-yl]-2,5 diphenyl tetrazolium bromide) test is a colorimetric assay for assessing cell metabolic activity. It is based on the conversion of MTT into formazan crystals by living cells, which determines mitochondrial activity. Viable cells with active metabolism convert MTT into a purple colored formazan product with an absorbance maximum near 570 nm. When cells die, they lose the ability to convert MTT into formazan, thus color formation serves as a useful and convenient marker of only the viable cells. The quantity of formazan (presumably directly proportional to the number of viable cells) is measured by recording changes in absorbance at 570 nm using a plate reading spectrophotometer. A reference

wavelength of 630 nm is sometimes used.

Briefly: plate 10000cells/well in a 96-well plate, and 24h post adhesion, treat the culture with medium added with MGO, BSA-AGEs for 48h. Then, in the dark, add MTT at final concentration of 0.5mg/ml and incubate at 37°C for 3,5 hours until purple precipitate is visible. Eliminate supernatant and substitute with DMSO, then shaking in the dark, at room temperature for 35-45 minutes. Finally, record absorbance at 550-620 nm with Victor instrument (Victor^{TM}, PerkinElmer).

3.2.4 Mouse models

- *ob/ob (Lep ^{ob})* mice models*:* Mice homozygous for this mutation are hypometabolic and hypothermic, exhibit obesity, hyperphagia, hyperglycemia, glucose intolerance, elevated plasma insulin, subfertility, impaired wound healing and an increase in hormone production from both pituitary and adrenal glands. Their obesity is characterized by an increase in both adipocyte number and size. From genetic point of view: a nonsense spontaneous mutation in codon 105 resulting from a C to T point mutation. The 16 kDa leptin protein, expressed predominantly in adipose tissue of normal mice, is missing from homozygous mutant mice.
- *ob/+:* Relative control
- db/db (Lepr ^{db}) mice models: Homozygous mutant mice are polyphagic, polydipsic, and polyuric; become obese around three to four weeks of age, plasma insulin begins to elevate at 10 to 14 days of age and of blood sugar at four to eight weeks. From a genetic point of view: G-to-T transversion created a donor splice site that causes abnormal splicing and a 106 nt insertion in the transcript, leading to premature termination of the long cellular domain of the Ob-Rb splice form and loss of its signal transducing function.
- db/+: Relative control

During the experimental protocol, mice were housed six per cage and were provided their standard rodent food and water ad libitum. Changes in weight and the amount of food taken daily were carefully monitored throughout the experiment period. All experiments were approved by the ethics committee of our institution and were conducted respecting the Helsinki agreements for the humane treatment of laboratory animals.

3.2.5 Patients Selection

Informed consent was obtained from all patients. Patients were recruited at the outpatient clinic of the Metabolic Division, University Hospital of Padova. The Caucasian patients from which

originate the adipose tissue biopsies are chosen among the patients undergoing abdominal surgery for various reasons, including gastric banding, cholecystectomy, appendectomy, and weight-reduction surgery. Exclusion criteria were concomitant cancer or infective disease. Data like: age, sex, BMI, waist circumference, systolic and diastolic blood pressure, diabetes duration, HbA1c, lipid profile, concomitant risk factors, complications and medications were collected from the electronic outpatient clinic charts. Biopsies were immediately split into pieces. One pieces was processed; the others were frozen in liquid nitrogen before storage al -80°C until use.

3.2.6 ex vivo Adipose Tissue Processing

Ex vivo adipose tissue surgically removed from patient, is cut and fragmented under sterile conditions, taking care to remove the necrotic tissue, blood vessels and nerves. Adipose tissue fragments are digested with a solution of collagenase 1mg/ml diluted in DMEM F12 for 1h at 37°C. After the treatment, these fragments are centrifuged at 1300 rpm for 10 minutes, allowing the separation in: a fraction of mature adipocytes (MAF), and a stromal vascular fraction (hSVF). Once removed supernatant, the hSVF is suspended and filtered through a wide-mesh sieve in order to remove the coarser fibers. Whereupon, the red blood cells are eliminated with an osmotic shock with the Lysis Buffer. The cell suspension is filtered with Cell Strainer filters- 100 µm and centrifuged. Finally, the hSVF is suspended with an appropriate volume of DMEM F12 at the 10% FBS for perform cell counting and then plating.

3.2.7 hSVF Adipogenic Differentiation

First of all, plate cells in multi-well 24-well and culture them in a proper number in F12 medium supplemented with transferrin 10µg/ml; biotin 33µM; Pantothenate 17µM; FBS 10%, 1% L-glutamine and 1% penicillin-streptomycin. 24-hour post confluence add this grow medium with:

- IBMX: 0.25mM
- DEXA: 100nM
- Insulin: 66nM
- Rosiglitazone: 10µM
- 3,3', 5-Triiodo-L-thyronine (T3): 1nM

After three days replace this cocktail with fresh medium in which IBMX is excluded, whereas DEXA, T3 and insulin are still added to the medium. Refresh this second cocktail every three days, still maintain till 10th-11th day. Finally, substitute with canonical DMEM F12 growth medium to the 15th day. As early as the third day you can detect firsts morphological changes that are accentuated gradually until reaching the phenotype fully differentiated. (127)

3.2.8 RNA extraction

- *From CELLS*
  - Harvest cells according to standard cell culture procedures with trypsin to obtain a cell pellet if start from huge area of cells culture
  - To the cell pellet, or directly over cell culture, add an appropriate volume of Buffer RLT and transfer the mixture into a new tube.

- *From TISSUEs*
  - If necessary, crumble the frozen tissue using a mortar and pestle in liquid nitrogen. Then transfer the small pieces into a liquid-nitrogen–cooled appropriately sized tube and allow the liquid nitrogen to evaporate without allowing the sample to thaw.
  - Put over 30-90mg of frozen tissue 1ml of QIAzol® Lysis Reagent (is optimized for lysis of fatty tissues, while for fibrous tissue is better) and homogenize with Tissue Lyzer for 3min at 30Hz
  - Add chloroform, shake and separate aqueous and organic phases by centrifugation: 15min, 11000 g at 4°C. RNA partitions to the upper, aqueous phase while DNA partitions to the interphase and proteins to the lower, organic phase. Transfer the upper phase into a new tube.

At this point, both for cell culture and tissues extract RNA following the instructions of the kit *"RNeasy Mini" QIagen®,* briefly*:*

- Add an equal volume of ethanol at 70% for adipose and lipid tissues, at 50% for liver and fibrous tissues.
- Transfer up to 700µl of the sample to an RNeasy spin column placed in the collection tube, and centrifuge for 15 s at ≥8000 x g. Membrane of RNeasy spin column hold RNA, so discard the flow-through.
- Then wash with two different buffer of the kit, finally recoup RNA adding 30–50µl RNase-free water pre-heated at 37°C directly to the spin column membrane. Incubate 5min, and centrifuge for 1 min at ≥8000 x g to elute the RNA.
- Quantify with Nanodrop 2000 (Thermo Fisher Scientific ® Inc. Rockford, IL, USA), A260/A280 ratios were also calculated for each sample for calculated purity and evaluate quality with Agilent® 2100 Bioanalyzer (Agilent Technologies, USA).

Store RNA extracted at -80°C.

↳ *RNA Quality Evaluation*

The evaluation of the extracted RNA quality was carried out with the system Agilent 2100 Bioanalyzer (Agilent Technologies, Santa Clara, CA, USA). The system allows a comprehensive quantitative and qualitative analysis of RNA extracted in only 30 minutes. The electropherogram evaluates the integrity of the nucleic acid analyzing both the number of bands of the electrophoretic run and the distribution of peaks. A good quality RNA shows a spectrum characterized by two intense peaks fragments that correspond to 28S and 18S ribosomal RNA and the absence of smearing, fragmentation index.

3.2.9 DNAse Treatment

With the purpose to eliminate an eventual contamination of DNA, treat samples with DNAse using the kit Turbo DNA-free. For each sample, pick up 2µg of RNA, add 3µl of buffer and 1µl of enzyme, finally add water RNAse-free till 30µl and heat at 37°C for 30min. After that, add 3 µl of inactivating gel and keep at room temperature for 2 mins, finally centrifuge at 10˙000g for 90 seconds, collect the supernatant without touching the resin and transfer into a new tube kept on ice.

3.2.10 Retro-transcription

At the samples treated with DNAse, add 150ng of Random Primers and 5.5µl of H2O-free, incubate 5 min at 70°C and then decrease to 4°C. At this point, add to the mixture: 10µl di M-MLV RT Buffer, 0.5mmol/l di dNTPs, 200 U di M-MLV RT Enzyme; 20 U di RNAsin. Final volume of the reaction is 50µl. Put samples in a thermocycler keeping temperature at 37°C for an hour and then increased to 92° for 5minutes. Store cDNA as synthetized, at -20°C.

3.2.11 Real time PCR

The polymerase chain reaction (PCR) is one of the most powerful technologies in molecular biology. Through the use of PCR, specific sequences within a DNA or cDNA template can be copied, or “amplified” theoretically exponentially by doubling the number of target molecules with each amplification cycle using sequence specific oligonucleotides, heat stable DNA polymerase, and thermal cycling. In traditional or endpoint PCR, detection and quantification of the amplified sequence are performed at the end of the reaction after the last PCR cycle. In real-time quantitative PCR, product is measured at each cycle via fluorescent dyes that yield increasing fluorescent signal in direct proportion to the number of PCR product molecules (amplicons) generated. If a particular sequence is abundant in the sample, amplification is observed in earlier cycles; if the sequence is scarce, amplification is observed in later cycles. There are three major steps that make up each cycle in a real-time PCR reaction: denaturation, in which double strand

of DNA melt; annealing in which complementary sequences of primers hybridize and finally extension. Reactions are generally run for 40 cycles. Gene-specific primer pairs were designed using Primer-BLAST (NCBI) and were each validated prior to use by gradient PCR and gel analysis to test for optimal annealing temperature, reaction efficiency and specificity.

A measured difference in RNA expression level between two samples is the result of both true biological as well as experimentally induced (technical) variation. In a relative quantification study, the experimenter is usually interested in comparing the expression level of a particular gene among different samples. Reliable estimates can only be obtained by preventing or reducing technical variations between samples and measurements. The analysis of the data and the Ct value definition is performed using the "Method of Second Derivative", supplied algorithm provided by the software to the instrument. It was created a relative quantification of the expression of the gene in analysis on the basis of the comparison with serial 1:10 or 1:5 dilutions of a positive sample, which define a reference standard curve. The Ct comparison of an unknown concentration in the sample with the standard curve allows to define the initial amount of template in the unknown. Expression data were normalized to the mean of housekeeping gene and has been used a standard curve method of comparative quantification. Two blank real time PCR controls without template, a positive control with a template of known amplification and a negative control with known no amplification were included in each assay. The specificity of the PCR amplification was verified by a melt-curve analysis profiles (cooling the sample to 60° C and heating slowly to 95°C with measurement of fluorescence of the final products) and further verified by agarose-gel electrophoresis.

The primers used in this work to check the expression of different genes are presented in Table 1 for human tissues and primary cells hSVF and in Table 2 for mouse tissues and 3T3-L1 cell line.

H_Gene	Forward primer Sequence (5'->3')	Reverse primer Sequence (5'->3')	Primer ratio nM	Temp. C°	bp
AGER1/RAGE	TGCCAGGCAATGAACAGGAA	TTATTGGGAACACCAGCCGT	300/300	62	125
GLP1r	CAGGCTGGAGTTGTCCTTCT	CAGGCTGTTCGTGAATGT	300/300	60	125
DPP4	GGCACCTGGGAAGTCATCGGG	CCGGATTCAGCTCAACAACTGAGGC	300/300	57	158
PPARγ	ACCCAGAAAGCGATTCCTTCA	AGTGGTCTTCCATTACGGAGAGATC	900/900	60	68
PPIA	GCTGTTTGCAGACAAGGTCC	GAAGTCACCACCCTGACACA	300/300	60	133
GLUT4	AGCTCTTCTAAGACGAGATGC	AGCCACGTCTCATTGTAGC	300/300	57	200
LPL	GCACCTGCGGTATTTGTGAA	TGAAACACCCCAAACACTGG	300/300	60	160
LEPTIN	GTGCGGATTCTTGTGGCTTT	GGAATGAAGTCCAAACCGGTG	100/100	63	174
RPLP0	GCAGCATCTACAACCCTGAA	CAGACAGACACTGGGAACAT	300/300	60	95

Table 3.1: sequences of human primers: forward and reverse sequence, ratio primers, temperature and product length

M_Gene	Forward primer Sequence (5'->3')	Reverse primer Sequence (5'->3')	Primer ratio nM	Temp. C°	bp
Ager1/Rage	CACGAGGATGAGGGCACCTA	ACAGAGCCTTCAGCTGGCCC	100/100	65	122
Pparγ2	TTCGCTGATGCACTGCCTATGA	GAATGCGAGTGGTCTTCCATCA	100/100	60	128
Dpp4	GAGTTGCAATTTGGGGCTGG	ACAGGTGCCACAGCTATTCC	300/300	60	100
Glut4	TGTCGCTGGTTTCTCCAACTG	CCATACGATCCGCAACATACTG	300/300	60	73
Glo1	GAAGAAGCCTGATGACGGGA	GCCGCAGCATCTTGAATCAC	300/300	60	193
Lpl	TCAGAGCCAAGAGAAGCAGCAA	TGTGTTGCTTGCCATCCTCA	300/300	60	117
Cyclophilin	ACTGCCAAGACTGAATGGCT	TGCCATTCCTGGACCCAAAA	300/300	60	106
Glp1r	ACTTTCTTTCTCCGCCTTGGT	TCCTGGTGCAGTGCAAGTGT	100/100	56	71

Table 3.2: sequences of mouse primers, forward and reverse sequence, ratio primers, temperature and product length

cDNA was utilized to perform studies of gene expression for gene involved in adipogenesis, in metabolism of glucose or lipids and in detoxification. Experiment were done with StepOnePlus™ Real-Time PCR System – Thermo Fisher ®; GoTaq®qPCR Master Mix and CXR Reference Dye.

DNA gel electrophoresis

To verify specificity of real-time PCR amplification, a gel electrophoresis was done. All the 20µl of samples and blank control were mixed with 3µl of blue loading buffer and then was loaded in a 2% Agarose in TBE 1X gel, in which we added 5µl of Gel Red, a reagent that binds to DNA and allows its visualization when exposed to UV light. Gel electrophoresis run was done at 110V for 45/90 minutes.

3.2.12 [3H]-2-Deoxyglucose uptake

Before starting the experiments, leave cells overnight in culture with serum-free medium, while maintaining the glycation-inducing environment conditions where present. It is essential the time-period in serum free, not only for starvation, indeed and more important, serum is full of proteins with a broad spectrum of activity. It is awash with hormones (including insulin), paracrine, endocrine and autocrine growth factors which support cells.

Stimulate cells with 0-10-100-1000nM of insulin in incubator at 37°C for 30 minutes, after that wash twice with PBS 1X pre-warmed at 37°C. Begin glucose uptake by adding in the culture medium the 2-deossi-[3H]-D-glucose at a concentration of 1.5µCi/ml and glucose cold (not radioactive) to concentration 50µM. Incubate cells for 15 min at 37°C. Afterwards, stop the reaction putting cell-plates on ice and washing twice with PBS ice-cold. Finally, lysate cells with the addition of 0.5MNaOH solution. Measure the radioactivity by counting with the β-counter (Wallac-PerkinElmer, MA, U.S.A.). Measure glucose uptake in triplicate well (for three sets of experiments) and normalize with fold induction with respect to unstimulated cells.

The 2-deossi- [3H] D-glucose is a modified analogue of glucose, radioactively labeled with tritium; precisely, is a glucose molecule which has the 2-hydroxyl group replaced by hydrogen, so that it cannot undergo further glycolysis. After the stimulus insulin, the 2DG is carried within the cell, but it is not metabolized. Therefore, the accumulation of radioactive glucose is proportional to the insulin response of the cell.

3.2.13 Immunofluorescence Microscopy

Immunofluorescence can be used on tissue sections, cultured cell lines, or individual cells, and may be used to analyze the distribution of proteins, glycans, and small biological and non-biological molecules. This technique uses the specificity of antibodies to their antigen to target fluorescent dyes to specific biomolecule targets within a cell, and therefore allows visualization of the distribution of the target molecule through the sample. The unlabeled first (primary) antibody recognizes the target molecule (antigen) and binds specifically to the region, and the secondary antibody, which carries the fluorophore, recognizes the primary antibody and binds to it.

Huh7, Mkn28, Mkn45 and 3t3-L1 non-differentiated and differentiated ones in different glyco-oxidizing conditions were grown adhered on slides put in 24 multi-wells plate for each different glyco-oxidizing condition. After treatments of 48h or 15days by choice, were processed for immunofluorescence staining, first fixing for 15-20 min in paraformaldehyde 4% at room temperature, then rinsed twice with PBS 1X with Ca^{2+}/Mg^{2+} and conserved at +4°C.

Briefly: Culture cells making them adhere on sterile glass slides. Rinse cells on glass coverslip with PBS and (only for epitope intra-cellular) permeabilize them with Triton X-100 0.3% in PBS for 10 minutes at room temperature, in other cases proceeded straight away with blocking. In order to prevent the nonspecific binding of the antibodies all epitopes on the tissue sample should be blocked; thus, incubate in 1:50 donkey serum in PBS 1X with Ca^{2+}/Mg^{2+} for 40/60 min, then wash twice with PBS 1X with Ca^{2+}/Mg^{2+} to remove excess protein that may prevent detection of the target antigen. The blocking step is critical: inadequate sample blocking will result in excessive background staining, while excessive blocking may mask antibody-antigen interactions.
Proceeding, incubate slides with primary antibodies diluted in blocking buffer, in damp conditions, as described in table 3.

Anti-RAGE N-term	1:100	Overnight at +4°C
Anti-Glucagon-like Peptide 1 Receptor (extracellular)	1:100	Overnight at +4°C
Anti-GLUT4	1:200	1.5h at 37°C
Anti-AGEs	1:100	Overnight at +4°C

Table 3.3 Primary antibodies used and their dilutions, temperatures and incubation times

Wash for 2-5 mins thrice with PBS 1X with Ca^{2+}/Mg^{2+} at room temperature. Subsequently, slides were incubated with secondary antibodies Anti-Rabbit IgG Alexa Fluor 488 [green] or Anti-Rabbit IgG Alexa Fluor 594 [red] or Anti-Goat IgG Alexa Fluor 488 [green] (Molecular Probes, Invitrogen) diluted 1:200 in blocking for 45-60 mins at room temperature, kept in the dark, and then washed with PBS 1X with Ca^{2+}/Mg^{2+} trice again. Conclude counterstaining with DAPI or Hoechst 33342 trihydrochloride trihydrate with the purpose to color in blue the nuclei, and finally mounted on a clean glass slide with the cells faced down. Use slides so prepared, to analyze localization of fluorescence using a microscope (Leica Microsystems GmbH, Wentzler, Germany).

- *GLUT4 and AGEs co-staining*

The 3T3-L1 cells were cultured and differentiated making them adhere on sterile glass slides. Before to start the experiments, left cells overnight in culture with DMEM without serum, then stimulate for 30 minutes in sterility at 37°C with 1000nM of insulin. After stimulation, wash cells with 1x PBS with Ca^{2+}/Mg^{2+} and immediately fix in 4% paraformaldehyde in PBS 1X for 10/15 minutes at room temperature. Rinse twice again with PBS 1X with Ca^{2+}/Mg^{2+}. Saturate slides with PBS 1X with Donkey Serum 1:50 for one hour at room temperature and use to the following staining protocol: over-night at 4°C (in damp conditions) incubation with primary antibodies Rabbit Anti- AGEs ab23722 diluted 1:100 in blocking buffer and wash for 3/5 mins thrice with PBS 1X with Ca^{2+}/Mg^{2+} at room temperature. The slides are then incubated with the other primary antibody Goat anti-GLUT4 polyclonal (N-20) sc-1606 (Santa Cruz Biotechnology) diluted 1: 200 in 1X PBS for an hour at 37°C, then run two washes in PBS 1X with Ca^{2+}/Mg^{2+} for 3/5 minutes each. After that, incubate cells with a mix of the two secondary antibody Rabbit Anti-Goat IgG Alexa Fluor 488 [green] (Molecular Probes, Invitrogen) and Anti-Rabbit IgG Alexa Fluor 594 [red] (Molecular Probes, Invitrogen) diluted 1: 200 in 1X PBS for one hour each one. Finally, counterstaining with DAPI for color in blue the nuclei and mount slides on a clean glass slide with the cells faced down. Slides so prepared can be used to analyze localization of fluorescence using a microscope (Leica Microsystems GmbH, Wentzler, Germany)
The images were captured by selecting the most representative stack.

3.2.14 Protein extraction

- *Adherent cells*

For mass spectrometry: (10cm^2 petri) Retain medium for quantification of cellular consumption and secretion of metabolites, store at -80°C. Put petri on ice and wash cells twice with 3-4ml of ammonium bicarbonate NH_4HCO_3 100mM. For analysis with mass spectrometry, PBS must be

avoided because it would create a large phosphate peak during mass spectrometric analysis, masking metabolites and proteins. Then, keeping the plate on ice, lyse the cells with 1ml of 0,1% in H_2O of TFA solution containing protease and phosphatase inhibitors; scraping the *petri* with a cell scraper. Make sure that as few cells as possible remain attached to the plate through careful and thorough scraping. Transfer in a new tube, and store at -80°C, fur furtherer analysis.

For ELISA immunoassay: Rinse cell twice with PBS 1x. Then, scape cells with 150µl (for a well of a 24 well-plate) of fresh PBS 1X ice-cold containing protease and phosphatase inhibitors, and put the lysate in a new tube kept on ice. After, at least, two cycles of freeze/thaw, store at -80°C

↳ *Adipose Tissue*

For mass spectrometry: Cover the piece of frozen tissue with TFA 0.1% containing protease and phosphatase inhibitors and crumble tissues in a Tissue Lyser 3mins at 30Hz (important: pre-cooled plates to +4°C), verify by eye the successful lysis. Thereafter, put the tubes in a shaker or rotox pre-cooled at +4°C for 20-30min at 1400rpm, followed by 15min of centrifugation at 16,000g at +4°C. After centrifugation, the different phases are now separated: debris on the bottom, protein solution in the middle and the majority of lipids on the top. Carefully pull up with a syringe the central phase without touch neither the remains nor keep the fat-cake and transfer into a new tube. Store at -80°C.

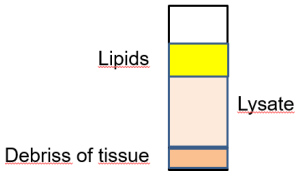

For ELISA immunoassay: Rinse 100mg of tissue with PBS 1x, homogenize in fresh PBS 1X with protease and phosphatase inhibitors. Then made at least two freeze-thaw cycles to break cell membranes and centrifuge 5 minutes at 5000g at +4°C. Carefully pull up with a syringe the central phase without touch neither the remains nor the fat-cake and transfer into a new tube. Store at -80°C.

3.2.15 Protein Quantification

To quantify proteins extracted has been used the Bio-Rad DC ® Protein Assay, a variant of the colorimetric method of Lowry. The method combines the reactions of copper ions with the peptide bonds under alkaline conditions (the Biuret test) with the oxidation of aromatic protein residues; the total protein concentration is exhibited by a color change of the sample solution in proportion to concentration, which can then be measured using colorimetric techniques. Briefly centrifuge the sample at 14000rpm for 10mins at +4°C; and prepare at least three dilutions (for example 1:5, 1:20, 1:100) in a proper buffer; prepare 6 dilutions of a standard protein (i.e. BSA) the standards should always be prepared in the same buffer as the sample and adding the specific

reagents following the protocol of the manufacturer, absorbance can be read at 750nm. Concentration of a protein is calculated with Lambert-Beer law:

$$Protein\ concentratios = \left({}^{OD280}/_{Extinction\ coeff.*\ Pathlenght}\right) * Sample\ Dilution$$

In this case, concentration was calculated with the program tool Microplate Manager® 6 Software.

3.2.16 E.L.I.S.A. assay

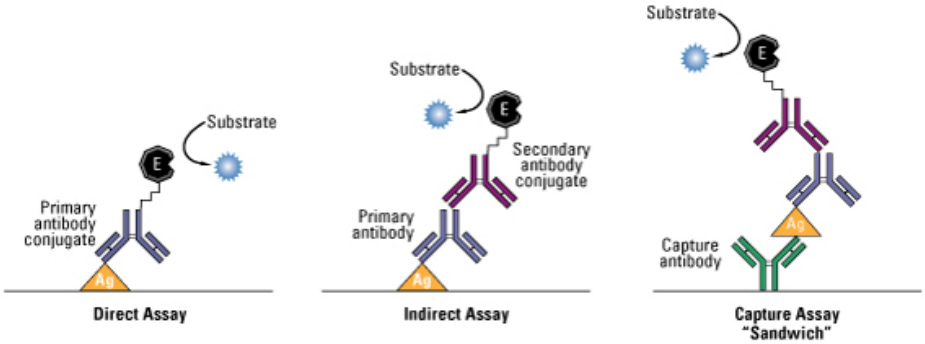

Figure 3.1: E.L.I.S.A. tests schematic representation

Enzyme-linked immunosorbent assay (E.L.I.S.A.) is a biochemical technique used mainly in immunology to detect the presence of an antibody or an antigen in a sample; it was developed in 1970s and it is still used nowadays in medical laboratories, manufacturers of *in vitro* diagnostic products, regulatory bodies, and external quality assessment and proficiency-testing organizations. (128, 129) The E.L.I.S.A. has been used as a diagnostic tool in medicine and plant pathology, as well as a quality-control check in various industries.

E.L.I.S.A. combine the specificity of antibodies with the sensitivity of simple enzyme assays, by using antibodies or antigens coupled to an easily-assayed enzyme. The assays can provide a useful measurement of antigen or antibody concentration. There are two main variations on this method: it can be used to detect the presence of antigens that are recognized by an antibody or it can be used to test for antibodies that recognize an antigen. There are four kind of E.L.I.S.A. tests: direct, indirect, competitive, sandwich. The last one, is a less common variant of E.L.I.S.A., but is highly efficient in sample antigen detection, the sandwich E.L.I.S.A. quantify antigens between two layers of antibodies, for this reason the antigen to be measured must contain at least two antigenic epitopes capable of binding to antibody, since at least two antibodies act in the sandwich.

In this work were used sandwich kind of E.L.I.S.A. assay: CSB-E09414m (CUSABIO® BioTech Co. LTD).

As recommended by the manufacturer, the supernatant was treated similarly to the serum, centrifuged for 15minutes ay 1000g; instead, tissue homogenates and cell lysates were

centrifuged again after thawing before the assay. Standard has been reconstitute as recommended by the manufacturer and used to produce a 2-fold dilution series with sample diluent; sample diluent alone served as zero standard. 100µl of standard or samples were added to each well, cover with adhesive strip and incubate for 2 hours at 37°C. The liquid was removed and without washing, were added 100ul of biotin 1x incubating at 37 ° C for one hour, then washed trice with the wash buffer. That wash procedure is critical, the complete removal of liquid at each step is essential to good performance; after the last wash by decanting or aspiration was removed any remaining drops. After that, were added 100ul of HRP-avidin 1x and incubated again at 37 ° C for one hour, then washed five times. In the dark, add 90µl of TMB substrate to each well and incubate at 37°C for 20 mins, controlling the reaction time, finally add 50µl of stop solution and read plates at 450nm within 5 minutes. Create a standard curve by reducing data using computer software capable of generating a four-parameter logistic (4-PL) curve fit. In this case, curve was calculated with the program tool Microplate Manager® 6 Software. The concentration read from the standard curve must be multiplied by the dilution factor.

3.2.17 Western Blot

RIPA 1X for 50ml of solution	
NP-40 -IGEPAL CA-630	500µl
Sodium deoxycholate	500mg
SDS	250µl (from a stock of 10%)
TRIS pH 6.8	2.5ml (from a stock of 0.5M)
NaCl	450mg
EDTA	50µl (from a stock of 1M)
Bring to volume	ddH_2O

Table 3.4: RIPA Buffer Composition

Transfer buffer 25X		**Transfer buffer 1X**	
SDS	1.86g	Buffer 25X	4ml
TRIS	29.1g	Methanol	20ml
Glycine	14.6g		
Bring to vol. ddH_2O	200ml	Bring to vol. ddH_2O	100ml

Table 3.5: Transfer buffer composition

TBS 10X		**TBS T 1X**	
NaCl	80.063g	TBS 10X	100ml
KCl	2.013g	Tween-20	1ml
TRIS base	60.57g		
Bring to pH 7.4 with HCl 37%			
Bring to vol. ddH_2O	1l	Bring to vol. ddH_2O	1l

Table 3.6: TBS buffer composition

↳ *SDS-Gel Electrophoresis, Reduced Samples*

To prepare samples: add NuPAGE ® Reducing agents (10X) and NuPAGE ®LDS Sample Buffer (4X) to 10µg of tissue lysates, then bring to volume to 22µl with RIPA 1X. Heat samples at 70˚C for 10 minutes. To prepare buffer: Add 25mL of 20X NuPAGE ® MOPS SDS Running Buffer to 475 mL of deionized water to prepare 1X SDS Running Buffer. To prepare the gel: The NuPAGE® Bis-Tris Gels is a precast polyacrylamide gels, in this work was used 10% Bis-Tris Gel. Remove white stripe on the bottom. Rinse the gel whit distilled water. Build the chamber in XCell SureLock® Mini-Cell gel

running tank, remove the comb and rinse wells three times using 1X Running. Fill the Upper Chamber and the Lower Chamber with the running buffer, then add 500µL of NuPAGE®. Antioxidant directly inside the Upper Buffer Chamber. Spun down and load samples into wells.

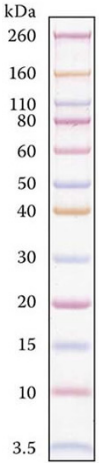

The Novex® Sharp Pre-Stained Protein Standard molecular weights marker (fig. 3.2) was loaded in each gel as reference.

The electrophoretic migration was carried out: 200V voltage constant for 50/55 minutes, until the dye front reached the end of the gel; it is advisable to check the run every 5-10 minutes.

Figure 3.2: Representation of Novex® Sharp Pre-Stained Protein Standard molecular weights marker in a 4-12% Bis-Tris acrylamide gel. The apparent molecular weights are shown.

Immunoblotting

The proteins separated in the electrophoresis gel were electrically transferred on a nitrocellulose membrane (0.45µm Protran®). Float nitrocellulose membrane, cut to the size of the gel in deionized water until completely wet, then soak and next equilibrate in transfer buffer 1X until use (at least 10 mins).

Semi-dry blotting with TRANS-BLOT® SD di Promega (Promega® Corporation, Madison, WI, USA) for 50 minutes at 200mA, constant ampere. To check for transfer of the samples onto the nitrocellulose stain in Ponceau Red for 2-5 min; rinse with ddH_2O to stain. To determine in the protein has eluted from the gel, stain gel with Coomassie Blue. Pay attention: Coomassie blue staining is NOT reversible, and it is not possible to re-blot proteins.

Block the membrane for 1h at room temperature using 5% nonfat dry milk in TBS-T 1X (blocking solution). Use the membrane for hybridization with the antibody Anti-AGEs 1:2000 in blocking solution at +4°C overnight. After that, wash the blot three times in TBS-T 1X for 5 min with fresh changes of wash buffer at room temperature. Dilute the appropriate biotinylated secondary antibody (goat anti rabbit, Novex ®) in blocking solution following the instructions provided by manufacturers; incubate the membrane in the diluted secondary antibody for 1h at room temperature on an orbital shaker. Wash the membrane three times in TBS-T 1X for 5 min with fresh changes of wash buffer at room temperature. Shield from intense light: mix an equal volume of detection solution 1 with detection solution 2 (Amersham ® ECL reagents) allowing sufficient total volume to cover the membrane. Drain the excess wash buffer from membrane and place it, with protein side up, on a clean surface; pipette the mixed solution on it. Incubate for 1-2min at room temperature and drain off the excess. Place the blot protein up in an x-ray film cassette. In

the dark: expose an autoradiography Hyperfilm ECL for 40seconds. The exposure of film to capture light emission, is estimated on the basis of appearance and can vary from 10 seconds to 1h.

3.3 *In vitro Glycation*

of Bovine Serum Albumin

In sterile conditions, using an ethanol washed spatula, dissolve either 2mg/ml or 10mg/ml of BSA in PBS buffer. Dissolve either glucose 1M, or fructose 1M, or lactose 1M or sucrose 1M or MGO 60mM. Filter the mixtures with Millipore™ Millex-GS 0.22µm for sterilization. Incubate the samples, in the dark, at constant temperature of 37 °C for 2/3 weeks. Thrice a week, mix the solutions by gently inverting the tubes. Use the same procedure, but without reducing sugar or MGO, to prepare the negative control protein. At the end of the incubation time period, aliquots and store at -20°C

of Human Leptin

In sterile conditions, dilute Recombinant Human Leptin protein ab51273 to 100µg/ml with ddH_2O, then add MGO 60mM. Make another dilution without MGO. Incubate the samples, without or with selected additives, in the dark, at a temperature of 37 °C for 2/3 weeks. Thrice a week, mix the solutions by gently inverting the tubes. At the end of the incubation period, aliquots and store at -20°C

3.4 *Mass Spectrometry*

In collaboration with "Servizio di Spettrometria di Massa" (CNR-IENI; Padova)

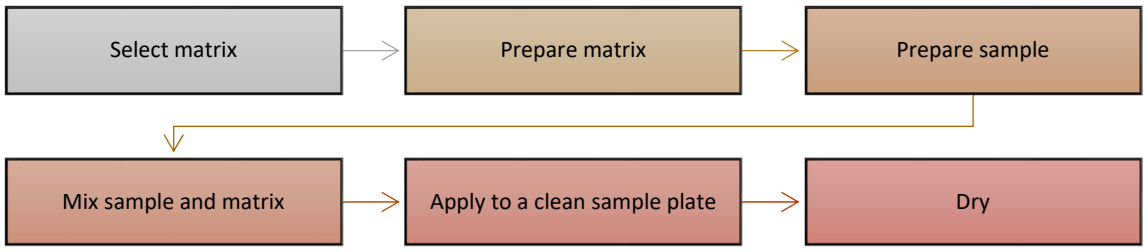

Figure 3.3: Scheme of procedural steps

3.4.1 Protein Precipitation with Acetone

Protein samples commonly contain substances that interfere with downstream applications. Several strategies exist for eliminating these contaminants, i.e. dialysis, precipitation or gel filtration (desalting columns). Precipitation has an advantage over dialysis or desalting methods in that it enables concentration of the protein sample as well as purification from undesirable substances, downside, proteins might denature, making the pellet difficult to re-solubilize. In this project, has been used the following protocol: Prepare a solution of acetone/milliQ water (4:1) and cool at -20°C; add 4 volumes of this chilled acetone to the sample's proteins extract and vortex very well. Place sample at -20° overnight. Spin at 13, 000 - 16,000g for 10 minutes at 4°C. Carefully pour off the supernatant. Wash pellet twice with 1ml of -20° acetone/water (4:1). During each washing, make sure the pellet is well broken up. Spin after each washing at 13,000 - 16,000g, at 0-4°C, for 10 minutes. Allow the acetone to evaporate from the uncapped tube at room temperature for 30 minutes. Do not over-dry pellet, or it may not dissolve properly. Add buffer appropriate for the downstream process and vortex thoroughly to dissolve protein pellet.

3.4.2 Lipids Extraction

Lipids were extracted from the adipose tissue simply by centrifugation (5 min, 12500 rpm), diluted 1:100 with methanol and analyzed by MALDI mass spectrometry using 2,5-dihydroxybenzoic acid as matrix. Identification has been done by searching in LipidMaps® database – Lipidomic Gateway.

3.4.3 MALDI lecture

MALDI-MS measurements were performed using an UltrafleXtreme MALDI-TOF instrument (Bruker Daltonics, Bremen, Germany), equipped with 1 kHz smart beam II laser (λ= 355 nm) operating in reflectron positive ion mode. The instrumental conditions were: IS1= 25.00 kV; IS2= 22.40 kV; lens= 8.00 kV, reflectron potential= 26.45 kV; delay time= 120 ns. The matrix was 2,5-dihydroxybenzoic acid (30 mg/mL in methanol, containing 0.1% TFA). 5µL of sample and 5µL of matrix solution were mixed and 1 µL of the resulting mixture was deposited on a stainless-steel sample holder and allowed to dry before introduction into the mass spectrometer. External mass calibration (Peptide Calibration Standard) was based on monoisotopic values of [M+H+] of Angiotensin II, Angiotensin I, Substance P, Bombesin, ACTH clip (1–17), ACTH clip (18–39), Somatostatin 28 at m/z 1046.5420, 1296.6853, 1347.7361, 1619.8230, 2093.0868, 2465.1990 and 3147.4714, respectively. MS/MS experiments were performed using the LIFT device in the following experimental conditions: IS1: 7.5 kV; IS2: 6.75 kV; Lift1: 19 kV; Lift2: 3.7 kV; Reflector1: 29.5 kV; delay time: 70 ns.

Software produces a graph with the absorbance intensity x 1,000 on the dependent axis, and

mass/charge *(m/z)* ratio on the independent axis.

The peaks were collected and analyzed by mass spectrometry in collaboration with Dr. Marco Roverso and Dr. Roberta Seraglia.

3.4.4 Enzymatic Digestion with Trypsin

1 mg of glycated BSA was dissolved in 1.3 ml of 50mM NH_4HCO_3 buffer solution (pH 8.3). After the addition of 15µl of a solution 45mM of Dithiothreitol (Fluka, St. Louis, MO), the mixture was heated at 50 °C for 15 min, then incubated with trypsin (Sigma) solution overnight at 37°C. The reaction was stopped with 80µl of 10% of TFA. Unglycated BSA was treated in the same manner.

3.4.5 Electrospray ionization - ESI

Electrospray ionization (ESI), was developed by Fenn and Whitehouse in the eighties of the last century. ESI is an ionization technique for small amounts of large and/or labile molecules such as peptides, proteins, organometallics, and polymers. A sample solution is sprayed from a small tube into a strong electric field in the presence of a flow of warm nitrogen to assist desolvation. The droplets formed evaporate in a region maintained at a vacuum of several torr causing the charge to increase on the droplets. The multiply charged ions then enter the analyzer. The most obvious feature of an ESI spectrum is that the ions can carry multiple charges, which reduces their mass-to-charge ratio compared to a singly charged species. This allows mass spectra to be obtained for large molecules. With this technique can form ions derived from the protonation of the analyte ($[M+H]^+$), multicharged ions ($[M+nH]^{n+}$) or by deprotonation of the analyte molecules ($[M+H]^-$). The electrospray ionization source can be coupled to mass analyzers of various types, such as the quadrupole.

3.5 STATISTICAL ANALYSIS

Statistical analysis was performed using the GraphPad Prism 7 software (GraphPad Software Inc., San Diego, CA). Values are reported as means ± SEM. * $p<0.05$ ** $p<0.01$ *** $p<0.001$

The D' Agostino and Pearson test (Normality tests) was used to check the Gaussian distribution of results in human gene expression.

Student t test was used for comparison between two groups: The Mann-Whitney test (non-parametric) was used for variables that were not normally distributed; Holm-Sidak (non-parametric) for survival and glucose uptake data analysis; in case of Gaussian distribution of population has been used a parametric test. 2-way-ANOVA Tukey's test for lipids analyses.

All the analyzes were performed at least in triplicate.

4. RESULTS

4.1 IN VITRO GLYCATION OF ALBUMIN

Albumin is the most abundant protein in plasma or serum, is involved both in many physiological processes and in maintaining the colloid osmotic pressure. It is normally present in serum at concentrations ranging from 30 to 50 g/L and accounts for approximately 60% of the total protein content. Protein glycation is a spontaneous post-translational modification (PTM) that occurs in biological systems. It involves the non-enzymatic addition of a reducing sugar or sugar derivative to specific residues, in particular for lysine and arginine, of proteins. Glycation, like others non-enzymatic reactions, is a process influenced by the concentration as well as the temperature. For this reason, albumin was proposed to have a strong proclivity to be glycated.

4.1.1 In silico Prediction of Albumin glycation

In order to estimate how many and which may be some potential glycation sites, it was used an appropriate bioinformatics software. The NetGlycate 1.0 server predicts glycation of ε amino groups of lysine in mammalian protein. It is important to note that the software, like other computational predictors, uses only the protein primary sequence and computer-generated functional knowledge.

In the table below, are reported the probability calculation results to glycation and a summary yes/no answer. The aim was to correlate the results with experimental reports of glycation and the glycation-prediction by NetGlycate 1.0.

Sequence 607 amino acids [bovin serum albumin]
#
netglycate-1.0 prediction results

Sequence	#	Score		Answer
Sequence	2	0,956	glycate	YES
Sequence	28	-0,846	glycate	.
Sequence	36	0,958	glycate	YES
Sequence	44	-0,89	glycate	.
Sequence	65	-0,89	glycate	.
Sequence	75	0,525	glycate	YES
Sequence	88	-0,871	glycate	.
Sequence	100	0,889	glycate	YES
Sequence	117	0,917	glycate	YES
Sequence	130	-0,768	glycate	.
Sequence	138	-0,942	glycate	.
Sequence	140	-0,819	glycate	.
Sequence	151	-0,908	glycate	.
Sequence	155	0,662	glycate	YES
Sequence	156	-0,916	glycate	.
Sequence	160	0,892	glycate	YES
Sequence	183	-0,932	glycate	.
Sequence	197	-0,845	glycate	.
Sequence	204	-0,914	glycate	.
Sequence	211	-0,938	glycate	.
Sequence	228	-0,915	glycate	.
Sequence	235	-0,925	glycate	.
Sequence	245	0,872	glycate	YES
Sequence	248	-0,792	glycate	.
Sequence	256	0,741	glycate	YES
Sequence	263	-0,677	glycate	.
Sequence	266	-0,71	glycate	.
Sequence	285	-0,919	glycate	.
Sequence	297	-0,855	glycate	.
Sequence	299	-0,951	glycate	.

Sequence	#	Score		Answer
Sequence	304	0,8	glycate	YES
Sequence	309	-0,934	glycate	.
Sequence	318	0,871	glycate	YES
Sequence	336	0,881	glycate	YES
Sequence	340	0,94	glycate	YES
Sequence	346	0,954	glycate	YES
Sequence	374	-0,721	glycate	.
Sequence	386	-0,77	glycate	.
Sequence	399	0,876	glycate	YES
Sequence	401	0,902	glycate	YES
Sequence	412	-0,918	glycate	.
Sequence	420	-0,938	glycate	.
Sequence	437	-0,876	glycate	.
Sequence	455	-0,767	glycate	.
Sequence	463	0,918	glycate	YES
Sequence	489	-0,89	glycate	.
Sequence	495	-0,941	glycate	.
Sequence	498	-0,9	glycate	.
Sequence	523	0,908	glycate	YES
Sequence	528	0,679	glycate	YES
Sequence	544	-0,936	glycate	.
Sequence	547	-0,934	glycate	.
Sequence	548	-0,875	glycate	.
Sequence	557	-0,907	glycate	.
Sequence	559	0,931	glycate	YES
Sequence	561	-0,846	glycate	.
Sequence	568	0,637	glycate	YES
Sequence	580	-0,858	glycate	.
Sequence	587	-0,888	glycate	.
Sequence	597	0,737	glycate	YES

```
    MKWVTFISLLLLFSSAYSRGVFRRDTHKSEIAHRFKDLGEEHFKGLVLIA   #     50
    FSQYLQQCPFDEHVKLVNELTEFAKTCVADESHAGCEKSLHTLFGDELCK   #    100
    VASLRETYGDMADCCEKQEPERNECFLSHKDDSPDLPKLKPDPNTLCDEF   #    150
    KADEKKFWGKYLYEIARRHPYFYAPELLYYANKYNGVFQECCQAEDKGAC   #    200
    LLPKIETMREKVLTSSARQRLRCASIQKFGERALKAWSVARLSQKFPKAE   #    250
    FVEVTKLVTDLTKVHKECCHGDLLECADDRADLAKYICDNQDTISSKLKE   #    300
    CCDKPLLEKSHCIAEVEKDAIPENLPPLTADFAEDKDVCKNYQEAKDAFL   #    350
    GSFLYEYSRRHPEYAVSVLLRLAKEYEATLEECCAKDDPHACYSTVFDKL   #    400
    KHLVDEPQNLIKQNCDQFEKLGEYGFQNALIVRYTRKVPQVSTPTLVEVS   #    450
    RSLGKVGTRCCTKPESERMPCTEDYLSLILNRLCVLHEKTPVSEKVTKCC   #    500
    TESLVNRRPCFSALTPDETYVPKAFDEKLFTFHADICTLPDTEKQIKKQT   #    550
    ALVELLKHKPKATEEQLKTVMENFVAFVDKCCAADDKEACFAVEGPKLVV   #    600
    STQTALA                                              #    650
%1  .G.............................G.............         #     50
%1  ........................G.....................G     #    100
%1  ................G.............................         #    150
%1  ....G....G.....................................         #    200
%1  ..............................................G.....   #    250
%1  .....G.........................................         #    300
%1  ...G.............G................G...G.....G....     #    350
%1  ...................................................G.   #    400
%1  G...............................................         #    450
%1  ............G...................................         #    500
%1  ......................G....G......................     #    550
%1  ........G........G.............................G...     #    600
%1  .......
```

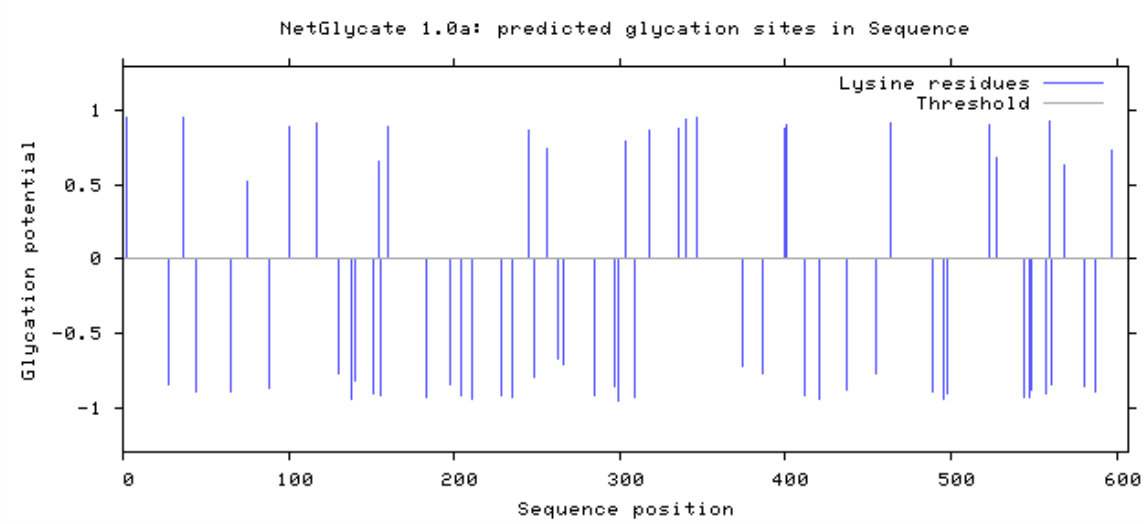

*Figure 4.1: Prediction of glycation sites for bovin serum albumin [serum albumin precursor of Bos Tauris: NCBI Reference Sequence: **NP_851335.1**] by using NetGlycate 1.0 software. For each input sequence, the length and the name of the sequence are stated followed by a table with the prediction results. There is a table row for each lysine residue in the sequence; the columns are: sequence name, residue position in the sequence (#); the score, a number between -1 and 1; when the score is above 0 the residue is a predicted glycation site; the answer: either the word "YES" or a dot ("."), reflecting the score. After the table, the whole sequence is printed alongside a summary of the predicted glycation sites and their positions. Finally, it displays a figure showing a plot of the score for each lysine residue against the sequence position of that residue. (**www.cbs.dtu.dk/services/NetGlycate 1.0**) (130, 131)*

The Bovin Serum Albumin (BSA), considering the sequence reported in NCBI Reference Sequence: NP_851335.1, has 60 lysines (K), and only 22 (36.67%) of them are predicted by NetGlycate 1.0 as potential glycation sites (indicated as “G” in dots line). BSA also has 26 arginines (R) that, along with the lysines and N-terminus, could potentially be prone to glycation.

4.1.2 Control BSA and glycated BSA

The production and the characterization of the glycated BSA have a fundamental importance for the simulation of the *in vivo* diabetic condition. The treatment of cells with these compounds, will provide an overview of the effects of a chronic exposure to a glycation-inducing environment on the adipogenetic process.

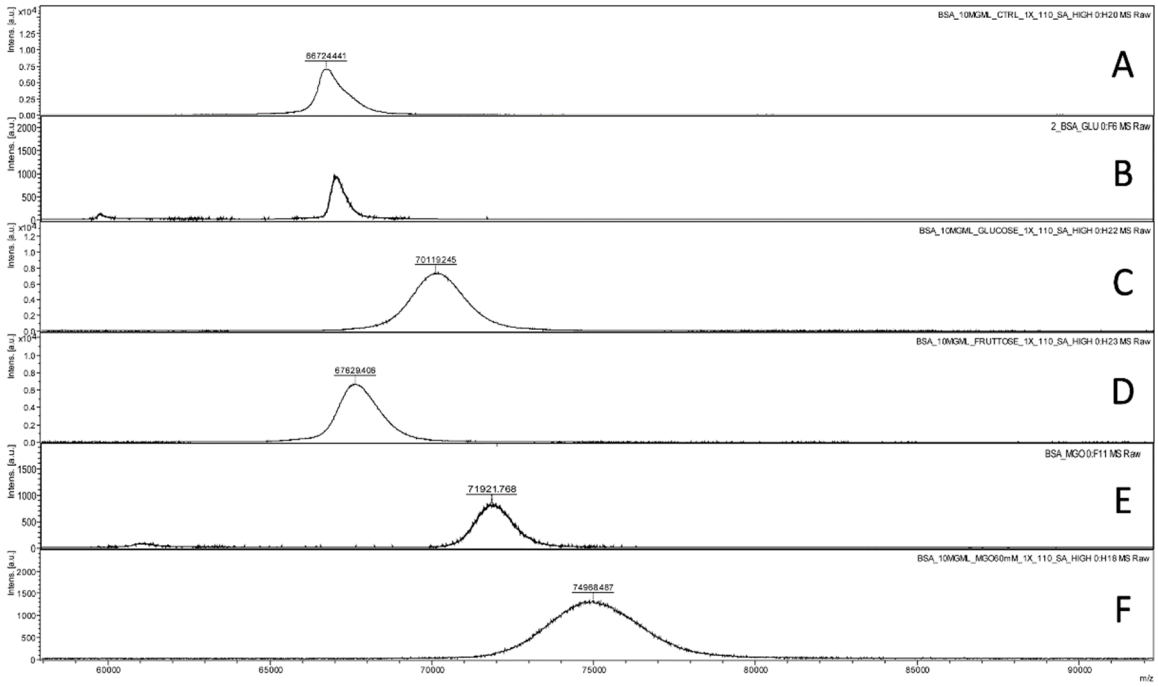

Figure 4.2: Comparison of mass spectra MALDI-TOF of BSA incubated in vitro for 3 weeks at 37°C with a reducing sugar or methylglyoxal (MGO): a) spectrum of 10mg/ml BSA diluted in PBS only; b) spectrum of 2mg/ml BSA diluted in PBS in presence of glucose 1M; c) spectrum of 10mg/ml BSA diluted in PBS in presence of glucose 1M; d) spectrum of 10mg/ml BSA diluted in PBS in presence of fructose 1M; e) spectrum of 2mg/ml BSA diluted in PBS in presence of MGO 60mM, e) spectrum of 10mg/ml BSA diluted in PBS in presence of MGO 60mM. The produced graph has the absorbance intensity on the dependent axis and mass/charge (m/z) ratio on the independent axis.

The molecular weight for each BSA-AGE preparation was determined using MALDI mass spectrometry. The figure n 4.2 shows the comparison between the MALDI-TOF spectra obtained by the analysis of samples of BSA 10mg/ml negative control (line A), BSA in two different concentrations: 2mg/ml and 10mg/ml treated with glucose 1M (lines B and C), BSA treated with fructose 1M (line D) and BSA in two different concentrations: 2mg/ml and 10mg/ml treated with MGO 60mM (lines E and F); as specified in Material and Methods. It may notice that for the treatment/incubation of BSA with fructose (line D), in the particular conditions used in this study, a significant increase of BSA molecular weight is not observed. The resulting peak, in fact, shows an *m/z* value comparable with the one obtained by analyzing the BSA control sample. For the treatment/incubation of BSA with glucose, is observed a small increase in molecular weight and a slightly broader shape of the peak with BSA 10mg/ml (line C); whereas no increase with BSA 2mg/ml is detected (line B). In order to evaluate their *in vitro* activities against the glycation

reaction other sugars, such as galactose, lactose and sucrose were tested. Similarly, as the fructose, a negligible mass increases were observed. (data not show) The molecular weight of BSA control did not change with incubation time.

Finally, considering the results obtained from the analysis of BSA sample treated with methylglyoxal (BSA-MGO) reported in lines E and F, there is a net mass increase (and therefore a shift to the right) of the signal when compared with the BSA of control sample (BSA-neg) in line A. The peaks coming from the BSA-MGO result to have a value of FWHM (Full Width at Half Height) greater than the peak resulting from the BSA-neg. The broader shape of the peak demonstrates that were formed a plethora of different kind of BSA-glycated proteins. The comparison between the two spectra of BSA-MGO displays that the glycated BSA samples are a mixture of proteins with different glycation levels, as proven by the broad shape of the peaks. For this reason, the mass value given above must be considered as the mean. The mass difference between the measured value for the sample of BSA-MGO and the value of the BSA-neg, divided by the mass of dehydrated MGO allows having an estimate of the number of linked MGOs. In this case, an average of 75 molecules of MGO has linked to BSA when it was diluted 2mg/ml and 114 molecules to BSA when it was diluted 10mg/ml. For the present project, this latter compound was chosen, because was wanted to test an extremely glycated form.

$$n = \Delta M / 72.06$$

On the basis of their chemical environment, statistically, some lysine or arginine, are located in a more favorable position to the glycation respect to the other; but this does not ensure that glycation happens nor if it was, that the glycation always happens in the same way, indeed, the process of glycation is random. For this reason, although the conditions are maintained unaltered, might form a little different composition of glycated proteins. Overall, may be considered that the mixture of compounds has a very similar average composition.

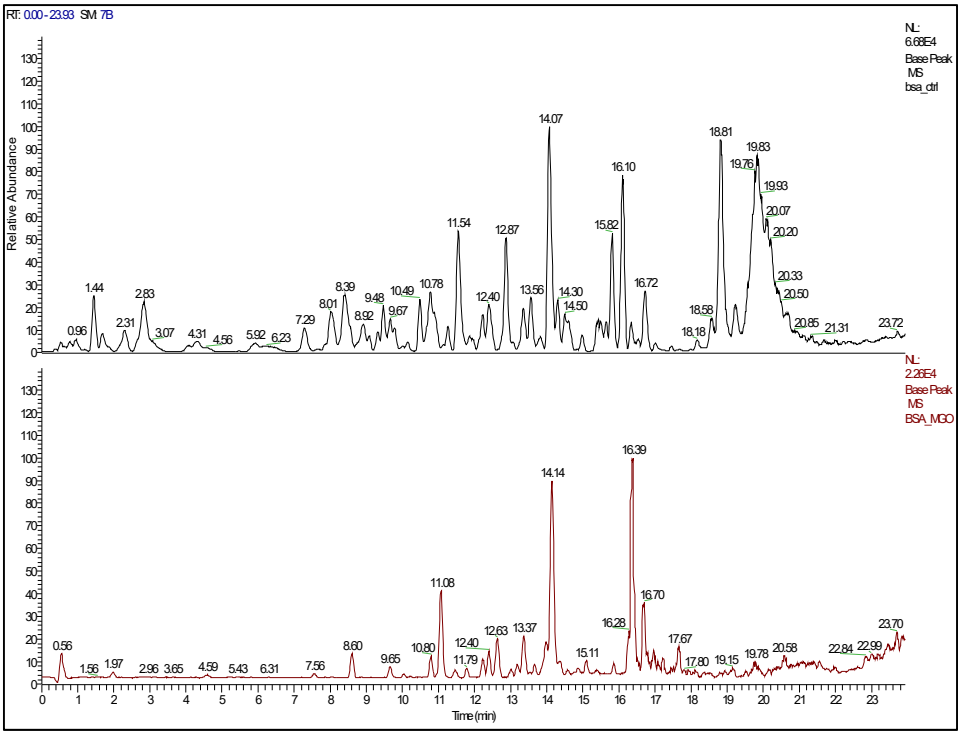

Figure 4.3: ESI chromatogram, analysis of the relative abundance of digestion products of BSA not glycated in the upper line (black), and BSA-MGO in the bottom (red).

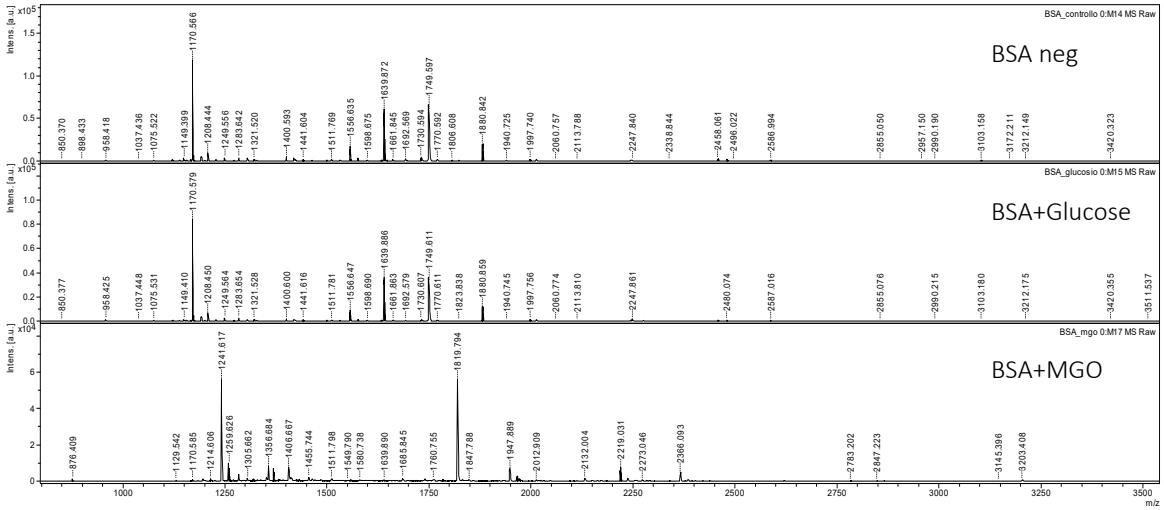

Figure 4.4: MALDI-TOF spectra of the digestion products obtained by the treatment of different BSA samples with trypsin: BSA control not glycated (BSA-neg); BSA incubated with glucose (BSA-glucose) and BSA incubated with methylglyoxal (BSA-MGO). (image at complete resolution in appendix)

In order to characterize the specific glycation sites and the peculiarly modified peptides, it was proceeded with tryptic digestion of BSA-neg and the treated ones.

In figure 4.3 are represent the ESI chromatograms of the digestion of the BSA-neg and the BSA-MGO. The comparison, clearly reveals differences between the two kinds of albumin. At first sight, focusing on the relative abundance of the peptides, the most evident result in the spectrum of BSA-MGO (bottom/red line) is the complete disappearance of several peptides and ionic species, but not a formation of a larger number of new different peaks. These results may appear

disappointing but indicate a strong resistance to being digested by trypsin of the glycated albumin. In figure 4.4 is represent MALDI-TOF spectra of the digestion products obtained by the treatment of three different BSA samples with trypsin. Comparing the specific peaks of the BSA-neg with the BSA-glucose and BSA-MGO is clear a substantial difference among the digestion products. The BSA-MGO shows fewer peaks and globally a net presence of heavier peaks (rightward shift of the spectrum), a clue of a probable protein glycation.

4.2 MURINE MODELS

4.2.1 3T3-L1 Cell Line

Viability Evaluation

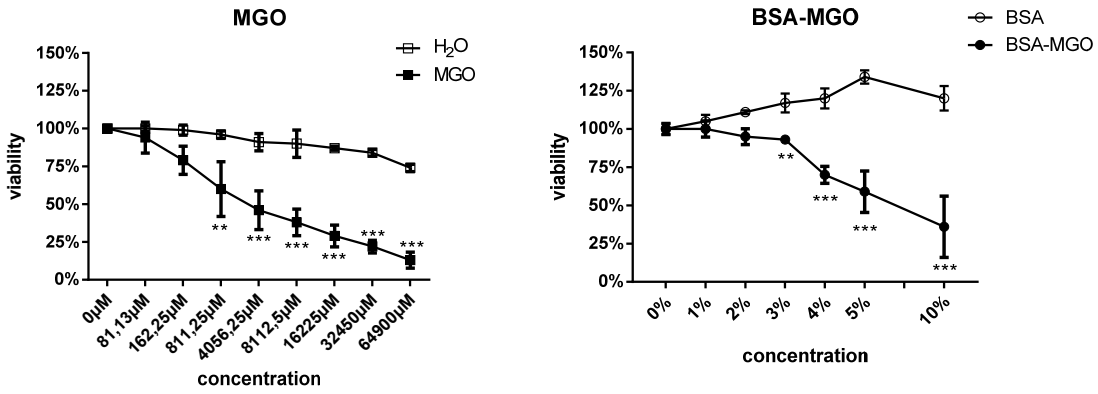

Figure 4.5: viability of fibroblast of 48h treatment with different concentrations of MGO and with BSA-neg/BSA-MGO. The H_2O quantity added in the control (white square) for MGO viability test is calculated as equivalent volume. Results are expressed in percentage of viability compared with the control kept in standard growth medium.
*Statistical significance determined using the Holm-Sidak method, without assuming a consistent SD. **p<0.01; ***p<0.001*

The 3T3-L1 cell line was selected because it is a well-known immortalized line of fibroblasts that can differentiate into adipocytes when subjected to appropriate stimuli. In literature, methylglyoxal has been shown to be toxic to cultured cells through the induction of ROS-mediated apoptosis. First of all, in our work, the biological effects of treatment with BSA-neg, BSA-MGO, and with MGO were studied *in vitro* on the 3T3-L1 cell line.

Before their use on the adipogenic protocols, MGO and BSA-MGO were tested on preadipocytes acutely for 48 hours with decreasing scalar concentrations. With the purpose to exclude potential confounding effects, the MGO was compared with the viability of a treatment with the equal total volume of water (the diluent of the compound); while the BSA-MGO was compared with the BSA-neg. By these analyses, was confirmed an important decreasing of vitality in 3T3-L1 cells proportional to the increasing of concentration of MGO in the medium. Water as well has mild

effects on cell survival, indeed, the viability falls to 75% when the total amount of water added to the growth medium is about 1% by volume. For the aim of this work was decided to use concentrations of MGO which would allow a survival of at least 70%.

The second compound for which was verified the cell viability, was the homemade BSA-MGO previously created *in vitro* (see Material and Methods) and consequently characterized in mass spectrometry as above specified. The survival to BSA-MGO was compared with its relative control, the BSA-neg. Cells treated with doses of BSA-MGO ranging from 2% to 10 %, show a rapid decline in viability, which varies from 95% ± 5% to 36% ± 20% when compared to the control kept in standard medium. For BSA-neg is also appreciable an effect, in particular, a slight increase of viability, with varies from to 111%±1% to 120%±8% with doses of BSA ranging from 3% to 10 % added to growth medium. It is not possible to substitute the serum with the BSA in the growth medium, because the serum contains essential growth factors, hormones and micronutrients, that are necessary for the survival. Since the two tested compounds affect the cell viability in the opposite way, the chosen concentration for the further studies was fixed to 2,5% a compromise between death and survival.

↳ *Morphological and Differentiation Evaluation*

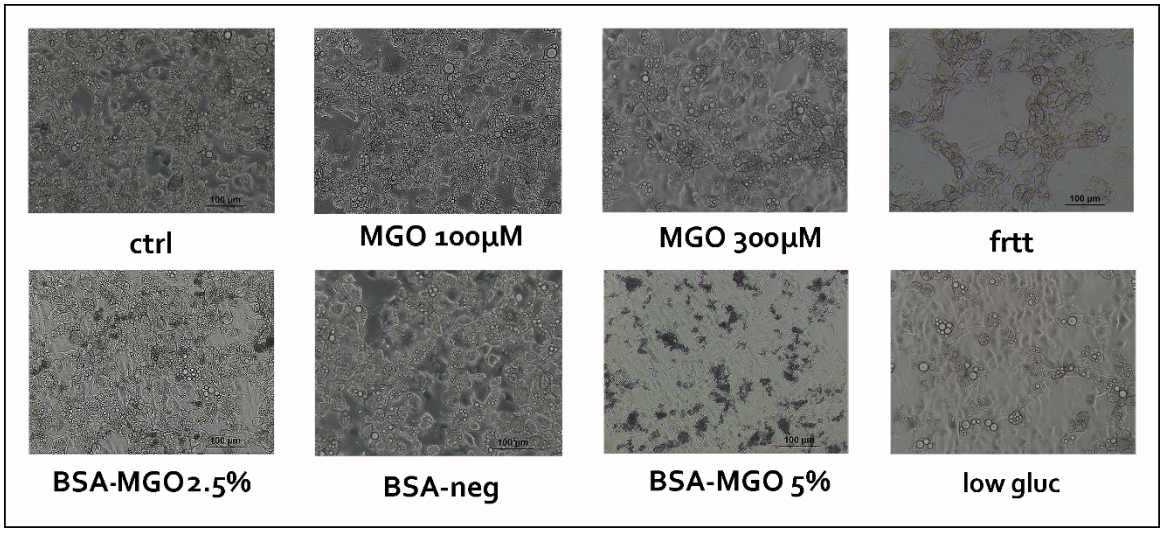

Figure 4.6: In the panels are represented the effects on 3T3-L1 cells at the end of adipocytes differentiation in the different glycating conditions. Images were taken on the fifteenth-day of differentiation. Ctrl: standard growth medium, 25mM of glucose; MGO: methylglyoxal at 100µM or 300µM; frtt: fructose 25mM; BSA-MGO and BSA-neg: BSA glycated or not; low glucose: glucose at 5.5mM.
Images were taken with optical microscope at 20x magnification. Scale bar: 100µm

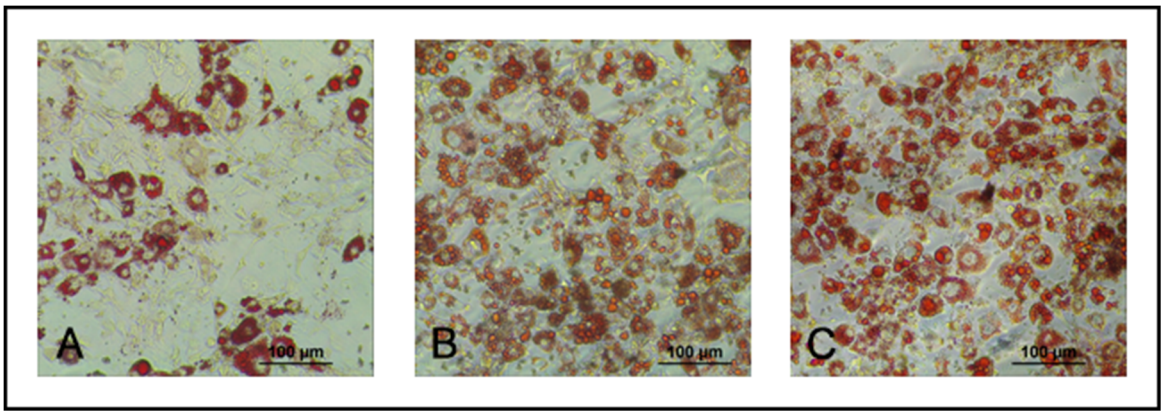

Figure 4.7: Oil Red O staining: A) mature adipocytes kept in low glucose (5mM); B) mature adipocytes grown in standard medium (25mM of glucose); C) mature adipocytes grown in MGO 100µM. Scale bar: 100µm

The effects of reducing sugars as glucose, fructose, lactose, sucrose and galactose, or compounds as MGO, BSA-MGO and BSA-neg, was evaluated. The sugars selected are supposed to have a causative role in the increasing rates of diabetes or diabetic-like changes (132-134). MGO is a well-known compound that can induces advanced glycation end product (AGEs) (135) First, the efficiencies of differentiation, the formation of lipid droplets and morphology of cells was taken into account. The adipogenic process is associated with a significant accumulation of lipid droplets. As example, in fig. 4.6 some images exemplifying of the final point of differentiation with eight tested conditions are reported. The sugars lactose, galactose and sucrose used in substitution of glucose have been forthwith excluded because of fibroblasts cannot differentiate into adipocytes. (data not show) BSA-MGO at the concentration of 5% in volume shows an important deleterious effect on cell morphology as cells appear wrinkled confirming the data of low survival. A good degree of adipogenesis was allowed by MGO at these specific concentrations. Finally, the low glucose (5.5mM) hasn't deleterious effects on morphology or viability, but was reject because of the very low capacity of preadipocytes to mature to adipocytes in that condition. Oil Red O staining test support these observations. (fig. 4.7).

↳ *Enzyme-linked immunosorbent assay (E.L.I.S.A.) for AGEs*

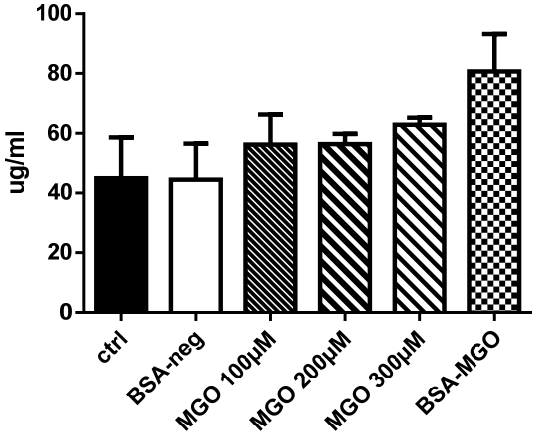

Figure 4.8: Quantity of advanced glycation end products contained in mature adipocytes exposed to: ctrl: control, BSA-neg: BSA of control not glycated, BSA-MGO: BSA glycated in vitro with methylglyoxal; MGO: methylglyoxal, measured by E.L.I.S.A. assay

In order to confirm and quantify the actual formation of AGEs, proteins extracted from cell lysates of mature adipocytes were analyzed in E.L.I.S.A. sandwich immunoassay technique. Even if the differences were not statistically significant, is assessed a potential positive effect on AGEs formation by culturing cells in a glycation-inducing environment, in particular for BSA-MGO. (fig. 4.8)

↳ *Real Time Quantifications*

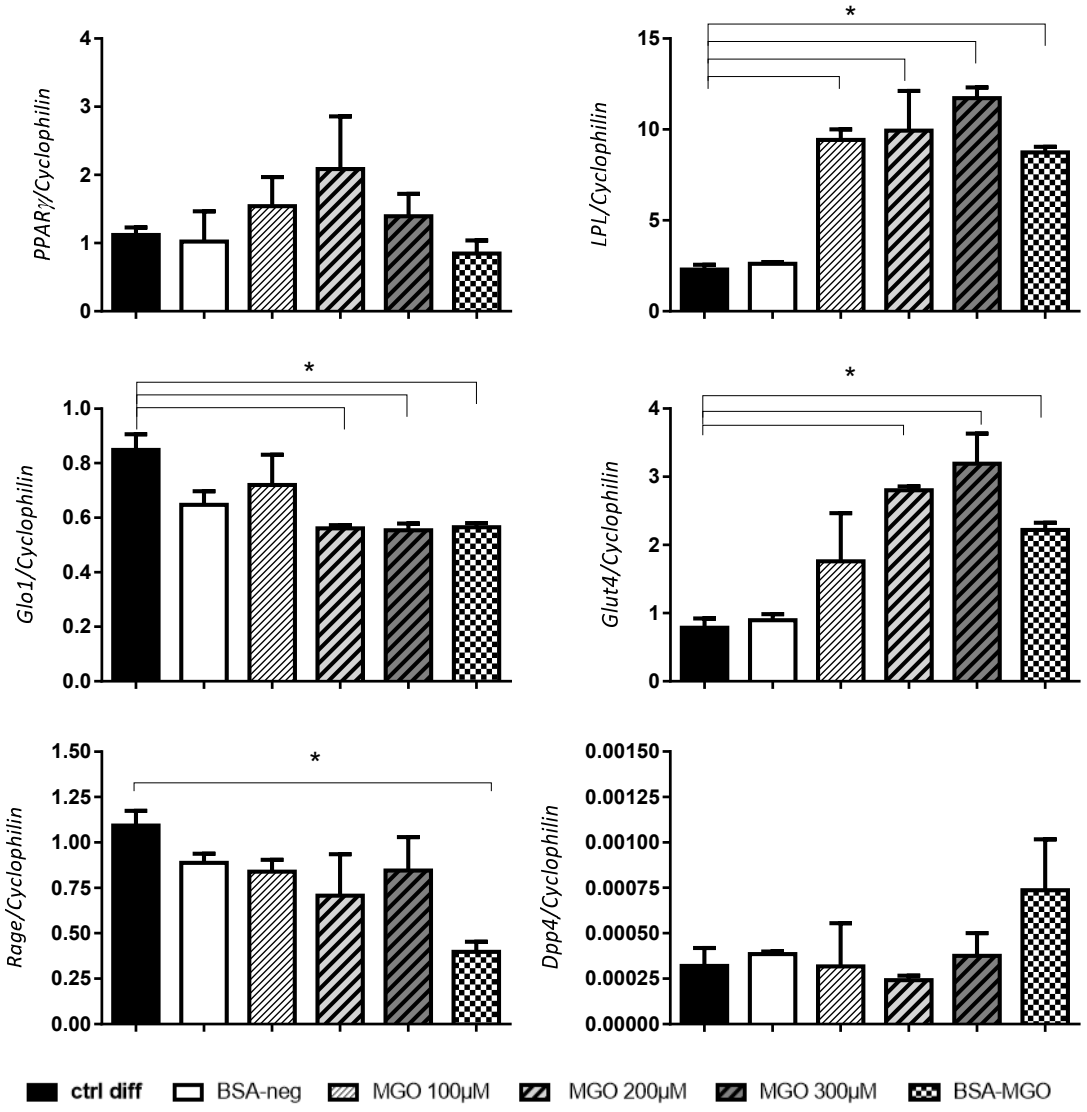

Figure 4.9: A panel of genes expression profile quantified by qPCR of 3T3-L1 mature adipocytes grown in different conditions: non-diff: fibroblast, pre-adipocytes; ctrl diff: adipocytes differentiated in the standard medium; BSA-neg: adipocytes differentiated in medium with the addition of 2.5% BSA not glycated in medium; MGO: methylglyoxal 100-200-300µM; BSA-MGO: adipocytes differentiated in medium with the addition of 2.5% BSA-MGO in medium.
*genes expression is reported as normalized with the expression of the house-keeping cyclophilin (peptidyl-prolyl cis-trans isomerase CYP1) Mann Whitney – nonparametric test *p<0.05*

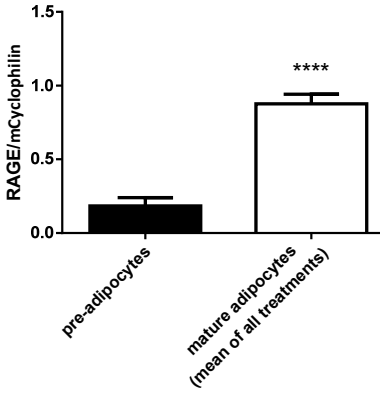

*Figure 4.10: Mean of expression of RAGE in mature adipocytes compared with pre-adipocytes. For simplicity, in the graph is represented the average of the expression of mature adipocytes of all conditions compared with expression of preadipocytes. Mann Whitney non-parametric test; P value **** p<0.0001*

In fig. 4.9 are summarized the expression analysis performed in adipocytes kept in different glycation-inducing environments: on one hand, the control standard medium (ctrl) and BSA-neg as second negative control; on the other hand, three different concentrations of MGO (100µM, 200µM and 300µM) and BSA-MGO that is supposed to be pro-glucotoxicity conditions.

The efficiency of the adipogenetic process, in addition to the visual estimation, was evaluated with the expression of Peroxisome Proliferator Activated Receptor Gamma (*Pparγ*), an important factor involved in adipogenesis, insulin sensitivity and dyslipidemia in AT. *Pparγ* expressions shows to be increased in each condition in comparison with the preadipocytes-fibroblasts, while significant differences among the differentiated adipocytes not emerged. (fig. 4.9) This means that all treatments have allowed the fibroblasts to achieve a good and comparable degree of maturation.

The expression of Lipoprotein lipase (*Lpl*), a member of the lipase gene family, shows a strong increase for all conditions when compared with the pre-adipocytes confirming that the adipogenetic process has taken place (data not show). Moreover, in all condition in which MGO or BSA-MGO were added into the medium compared with the standard control medium or the BSA-neg, *Lpl* is significantly more expressed. (fig. 4.9) This evidence suggests a potential induction of a higher metabolic activity for cells kept in a glycation-inducing environmental.

The Glyoxalase I (*Glo1*) is the key enzyme in anti-glycation defense, it is responsible for the catalysis and the formation of S-lactoyl-glutathione from methylglyoxal condensation and reduced glutathione. It is possible to appreciate a lesser expression of this enzyme for treatments with MGO 200µM, MGO 300µM and BSA-MGO compared to the control condition. (fig. 4.9) It is supposed that a glycation-inducing environmental might be a cause for decreased defense ability. Insulin-responsive glucose transporter 4 (*Glut4*) shows a significant greater expression in adipocytes treated with MGO 200µM, MGO 300µM or BSA-MGO in comparison with controls. (fig. 4.9)

Moreover, the increased expression seems to be proportional to the quantity of MGO added to the growth medium. The debatable results have to be considered very preliminaries.

The expression of AGEs receptor (*Rage*, also known as *Ager*), surprising shows a faint but significant decrease in BSA-MGO treated adipocytes compared with the control ones. (fig. 4.9) As aforementioned (see Introduction), the *Rage* receptor has numerous isoforms that are not yet be fully characterized. Moreover, these isoforms are present with different relative abundance expression levels throughout tissues but the main specific isoform for adipose tissue is still unknown. The primers mouse-specific used to generate the amplicon analyzed in expression were designed to be discriminating for the isoform 1, the most prevalent one. However, it is in no way possible to amplify only one specific variant from the more than 20 isoforms known, excluding all the others, due to their high similarity (see introduction). Globally analyzing the adipogenic process, it is appreciable a strong increase of the expression of *Rage* at the end of the differentiation compared to preadipocytes. (fig. 4.10)

Finally, *Dpp4* (dipeptidyl peptidase 4) shows a very low expression in 3T3-L1 mature adipocytes. *Dpp4* displays a faint increase for treatments with BSA-MGO, but both because of the high variability intra sample and due to the very low gene expression, such alterations are not statistically significant.

↳ *Immunofluorescence*

The protein translation process is very complex because of the many post-transcriptional controls, to this complexity must be added the post-translation controls and post-translational modifications. That's why, gene expression very often does not coincide with the protein expression. Hence, was decided to evaluate the question from another point of view, namely the proteins point of view.

To confirm the data of real-time expression and to evaluate if there is a different point of control, for example at translation instead of transcription; and how this can be reflected on the final protein expression, immunofluorescences (IF) of mature adipocytes for RAGE and GLP1R were done. For the *in vitro* characterization of receptors, cells were seeded making them adhere to sterile slides, were fixed in paraformaldehyde and then colored following the protocol reported in materials and methods.

The antibody used was described to be specific for the N-terminal portion of the full-length protein. On account of the characteristic hyper-variability of Rage isoforms, was been necessary validate the specificity of antigen-antibody before performing the IF on adipocytes.

For this purpose, two cell lines of human gastric carcinoma that are well known to be either positive or negative for the expression of RAGE (136), were used.

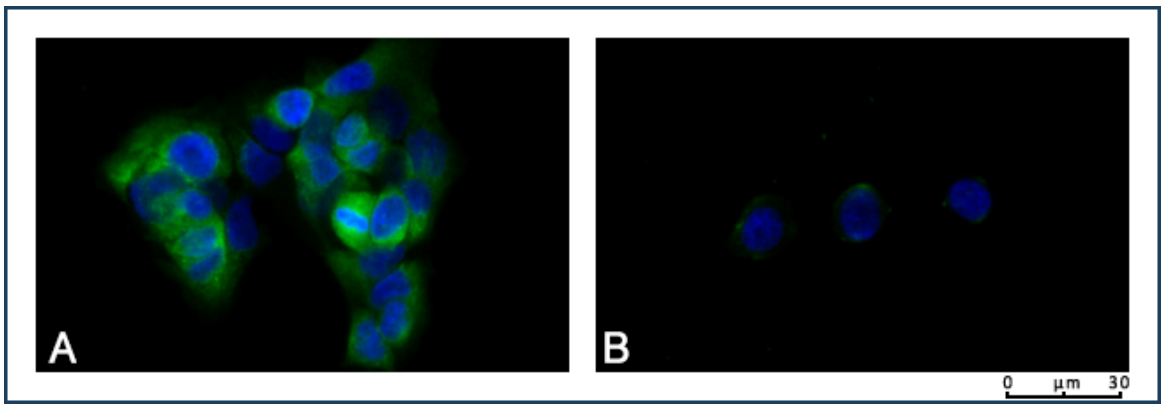

Figure 4.11: Panel of controls of RAGE receptor. A) MKN28 cells, positive control known in the literature; gastric cancer cell lines. B) MKN45 cell negative control know in literature, a non-RAGE-expressing gastric cancer cell lines. Green: Receptor for Advanced Glycation End products (RAGE); counterstaining of nuclei with DAPI (Blue) Magnification 20x. Scale bar= 30µm

These immunofluorescence analyses confirm a strong immunoreactivity and a constitutively high expression of the RAGE receptor for MNK28 cells. (fig. 4.11 A) In addition, the analyses of the MKN45 cell line show no marking, attesting in this way the lack of expression of RAGE in this cell line. These data certify the exclusion of possible non-specific recognitions by the antibody (fig. 4.11 B) allowing to proceed to adipocytes analysis.

Following are some representative IF images for RAGE in mature adipocytes grown either in standard/control medium, or with MGO 100µM or BSA-MGO.

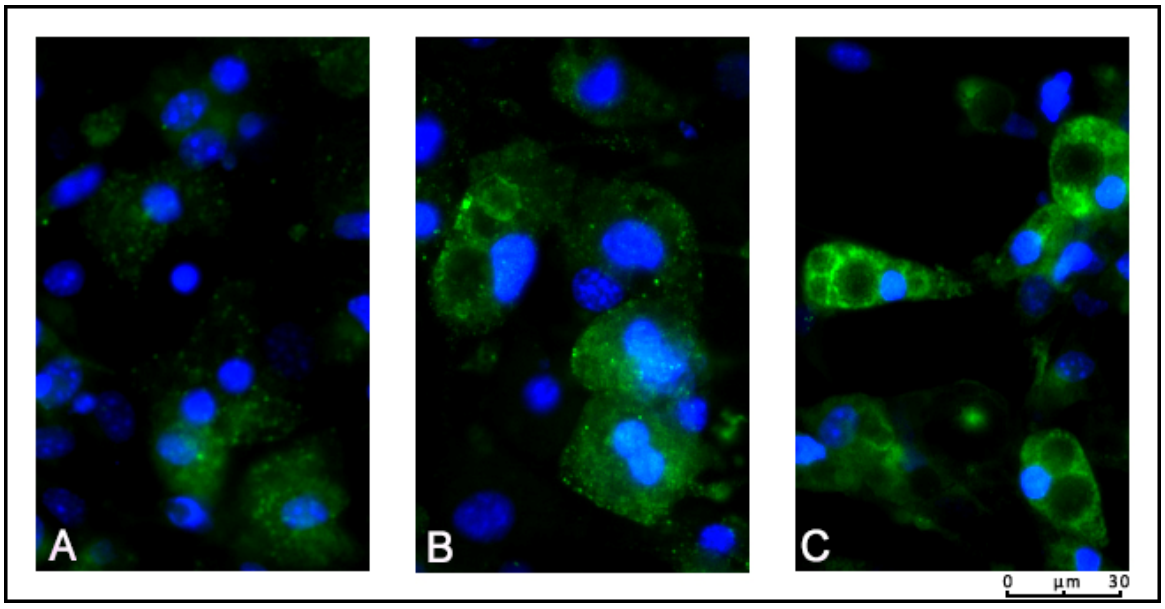

*Figure 4.12: RAGE IF panel, 3T3-L1 adipocytes differentiated in exposition to: A) standard/control DMEM 25mM glucose medium; B) DMEM with MGO 100µM in chronic treatment; C) DMEM with BSA-MGO 2,5% in volume in chronic treatment. Green: Receptor for Advanced Glycation End products (*RAGE*); counterstaining of nuclei with DAPI (Blue) Magnification 20x. Scale bar= 30µm*

Comparing the three photos of figure 4.12, it is possible to appreciate a sandy green staining dispersed in cytoplasm and a little labelling in the membrane for all conditions. The labelling appears more intense in cells chronically exposed to the BSA-MGO, leading to suppose an expression increased of the proteins, providing a result apparently contradictory to the gene expression data.

The second main objective of this work was to verify the presence of GLP1R in 3T3-L1 adipocytes and correlate its expression levels with the degree of glycation-inducing environment to which cells have been exposed. In the literature, the question relative to the presence or the absence and what could be the functionally active forms of GLP1r in AT finds controversial responses, furthermore, the molecular identity remains still unclear.

The gene expression analysis in the present experimental project, proved to be quite complex; in 3T3-L1 adipocytes *Glp1r* expression is very close to the limit of detection; for this reason, it was decided to support the real-time PCR analysis with those of IF. Analogously to RAGE, for GLP1r as well, it been necessary to validate the specificity of antigen-antibody recognition of the reagent in use before performing the IF. To resolve any possible doubt, in this case, two different types of cell lines renowned to express that receptor as positive control: the HuH7 (137) and the PC12 (138) were used.

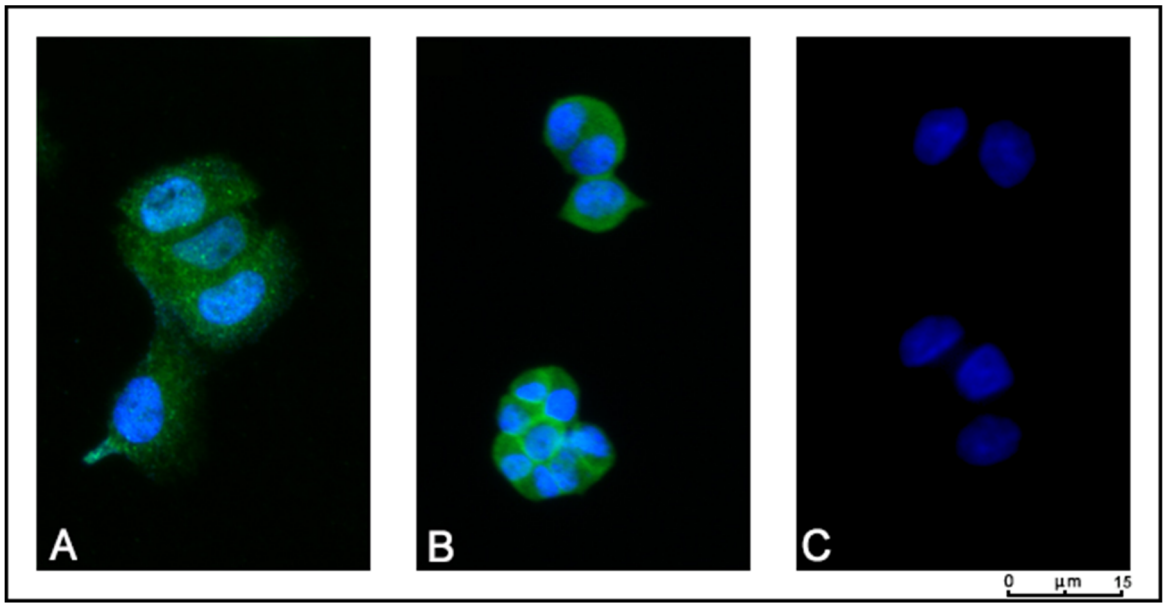

*Figure 4.13: Panel of controls for GLP1R. A) HuH7 cells, human cells as positive control; B) PC12 cells, rat cell as positive control C) negative control. Green: glucagon-like peptide 1 receptor (*GLP1R*); counterstaining of nuclei with DAPI (Blue). Magnification 40x. Scale bar= 15 µm*

Following are some representative IF images for GLP1R in mature adipocytes grown either in standard/control medium, or with MGO 100µM or with BSA-MGO.

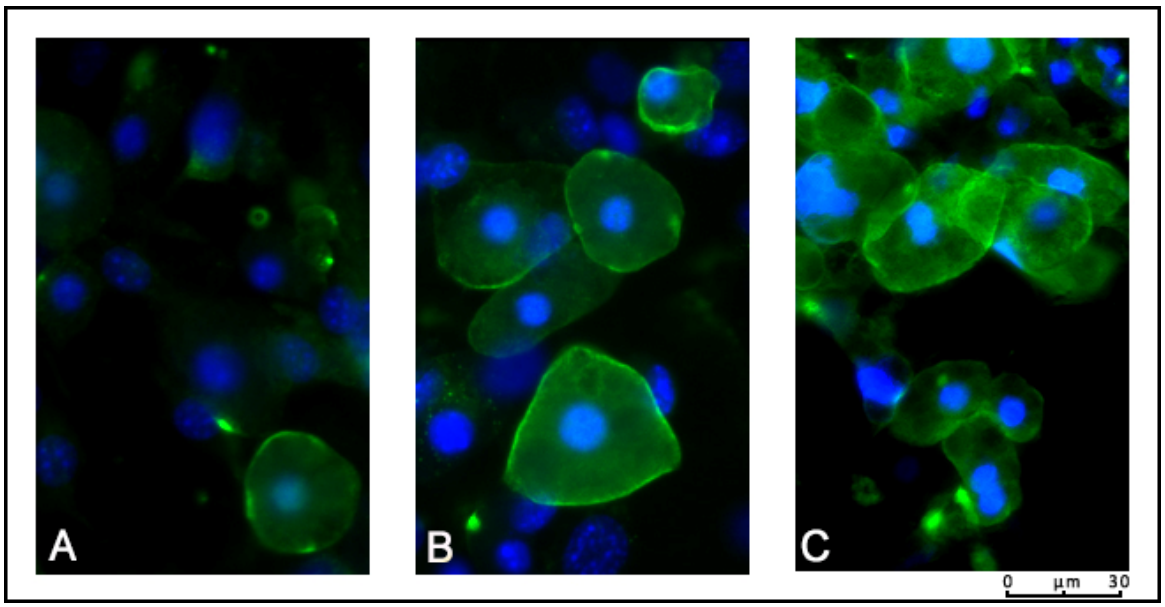

Figure 4.14: IF panel for GLP1R, 3T3-L1 adipocytes differentiated in exposition to: A) 3t3-L1 standard medium; B) 3t3-L1 treated with MGO100µM; C) BSA-MGO 2,5% in volume; Green: GLP1R labelling; Blue: counterstaining of nuclei with DAPI.
Magnification 20x. Scale bar= 30µm

Figure 4.14 shows three representative shoots of IF for the GLP1R in mature adipocytes, differentiated in exposure to three different conditions of glycation-inducing environment. It is possible to appreciate a uniform green labelling that, in particular, is localized on the plasma membrane, in all the conditions. Compared to control, the adipocytes chronically exposed to the BSA-MGO (frame C) show a more intense expression and the labeling is visible in a largest number of cells.

By the E.L.I.S.A. assay previous achieved, it was expected to found AGEs into the cells. In order to examine the presence, the formation and the peculiar pattern of intracellular products it was proceeded with immunofluorescence for those proteins.

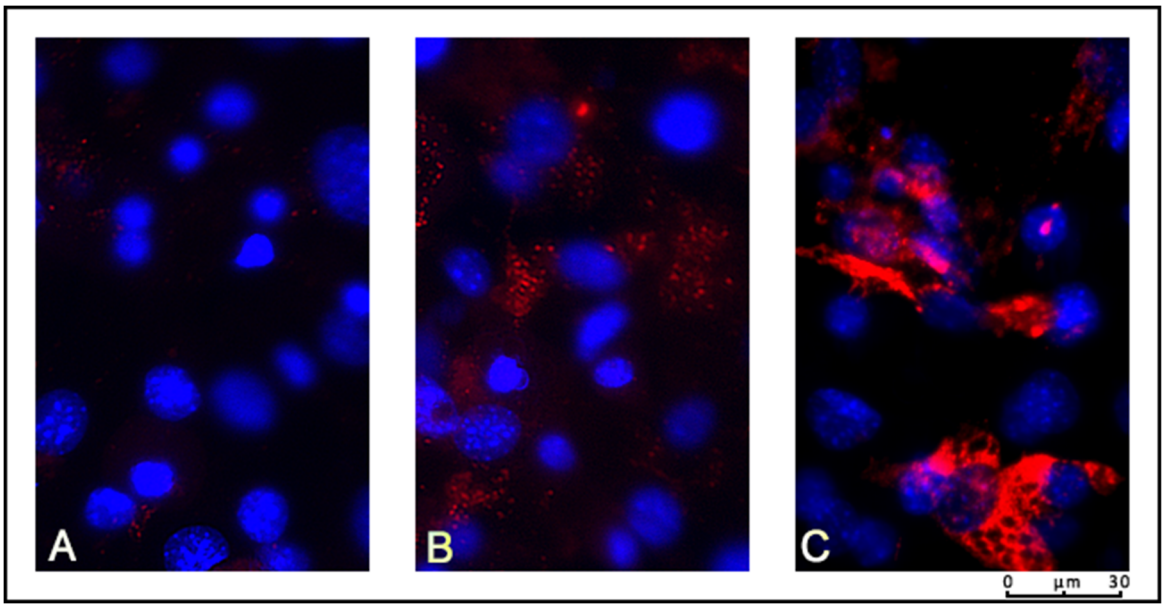

Figure 4.15: AGEs IF panel: 3T3-L1 adipocytes differentiated in exposition to: A) standard medium; B) MGO 100µM; C) BSA-MGO 2,5% in volume: AGEs products (Red labelling) counterstaining of nuclei with DAPI (blue labelling) Magnification 20x. Scale bar=30µm

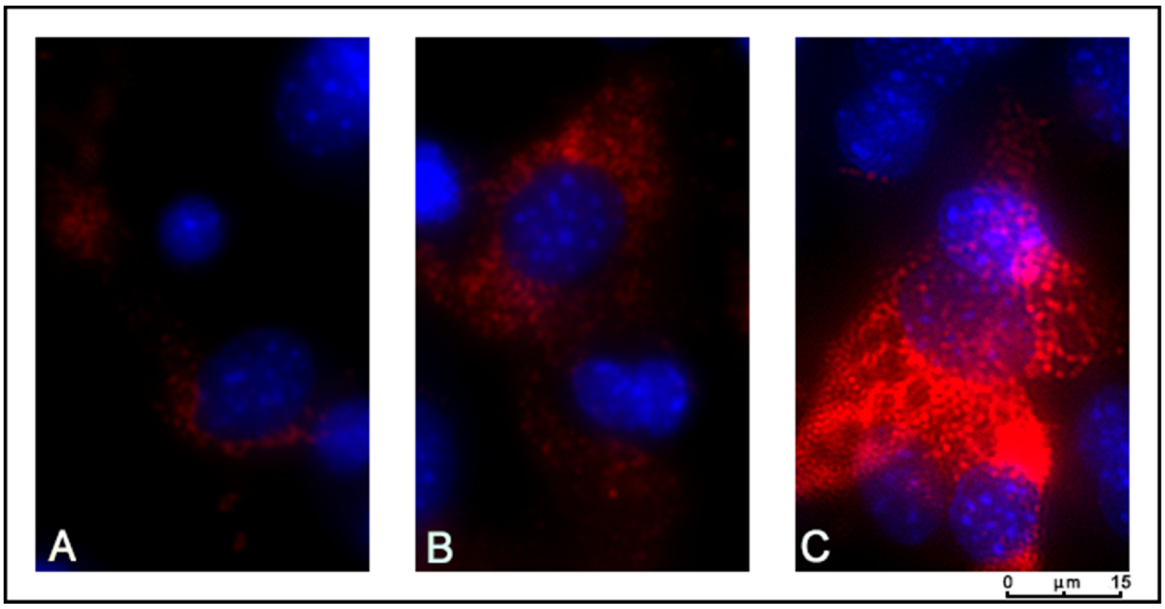

Figure 4.16: AGEs IF panel: zoomed particular of the upper panel; 3T3-L1 adipocytes differentiated in exposition to: A) standard medium; B) MGO 100µM; C) BSA-MGO 2,5% in volume: AGEs products (Red fluorescence) counterstaining of nuclei with DAPI (blue fluorescence). Magnification 40x. Scale bar=15µm

Figure 4.15 and 4.16 show three representative shoots of IF for AGEs products in mature adipocytes differentiated in the three different levels of glycation-inducing environment. Specifically, in 4.16 are represented images captured with higher zoom (40x). Cells show a red granulose fluorescence distributed in the cytoplasm. The pattern of labeling is very peculiar; it seems grainy but not draw any characteristic structure or patter. Comparing the conditions appears clear a direct correlation of red labelling and glycation-inducing environment, that seems to agree with E.L.I.S.A. assay. Moreover, the glycation phenomenon is ubiquitarian and it is present even in cells grown in standard/control and BSA-neg medium, even though it is very less intense.

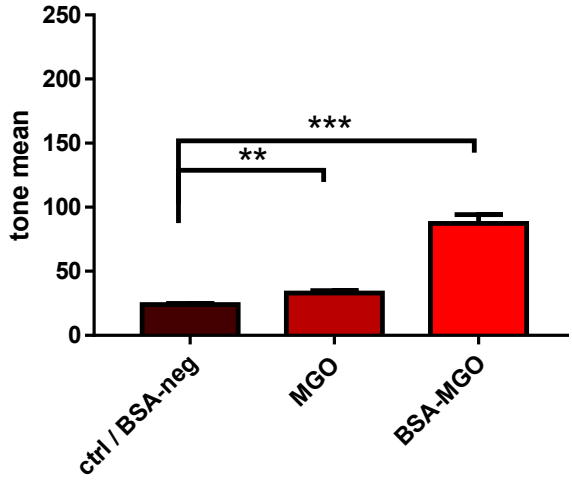

Figure 4.17: Quantification of red fluorescence with ImageJ ® software of 3T3-L1 cells differentiated with: ctrl, MGO or BSA-MGO. Were evaluate 8 shots for each condition, in each one was measured the average amount of red tone (range 0 to 255)

Both insulin and exercise can acutely stimulate the recruitment of GLUT4 to the cell surfaces in muscle and in adipose tissue, independently of transcription or translation. Insulin markedly stimulates GLUT4 exocytosis pathways and also significantly inhibiting its endocytosis from the plasma membrane, which together cause the overall redistribution of GLUT4 to the cell surface. Relatively recent studies on skeletal muscle cells (L6 or C2C12 cell line) point up that AGEs products can interfere with glucose transporter. In L6 myoblasts, after twenty-four-hour MGO treatment, an elevated GLUT4 presentation on the surface and an increased uptake of glucose even without insulin stimulation were detected. It was supposed that a prolonged treatment with MGO could augment GLUT4 level on the surface, at least in part through a higher translocation of GLUT4 from the intracellular compartment as well as a reduction of GLUT4 internalization. (139) (140) Their data could highlight a difference between a chronic exposition, that mimics a diabetic metabolism, and a short but intense exposure. The molecular mechanisms involved are still poorly understood.

In the light of our gene expression analyses for the *Glut4*, whom appears to be impaired in adipocytes grown by the presence of BSA-MGO in the growth medium, it was decided to focus attention on the protein performing a functional study.

In order to investigate whether and how the glycation-inducing treatment could alter the insulin sensitivity in mature adipocytes acting on the translocation of GLUT4, it was proceeded to perform

firstly a staining for GLUT4 and after that a colocalization for AGEs both in the presence and in the absence of insulin stimulation.

Following are some representative IF images for GLUT4 in mature adipocytes 3T3-L1 grown either in standard/control medium, or with MGO 100µM or with BSA-MGO.

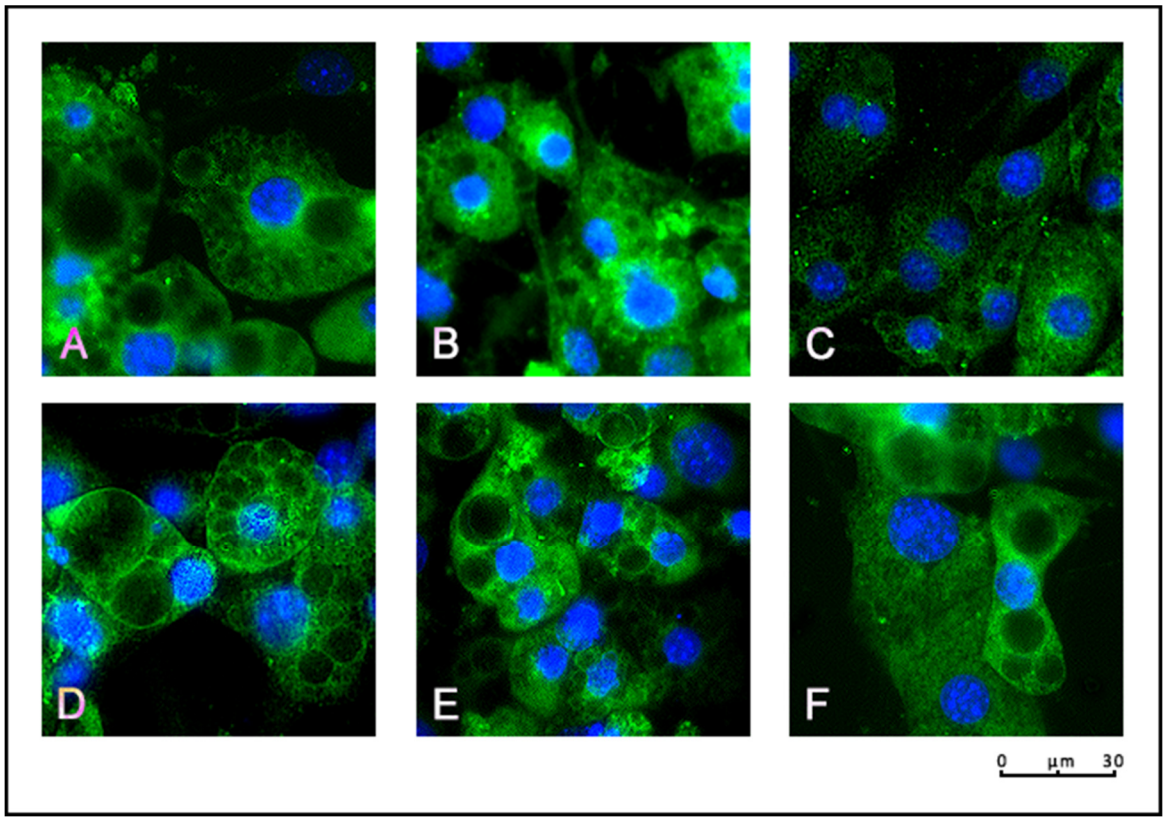

Figure 4.18: GLUT4 IF panel: 3T3-L1 adipocytes differentiated in exposition to: A and D) standard medium; B and E) MGO 100µM; C and F) BSA-MGO 2,5% in volume. Upper line (A-B-C): basal condition not stimulated by insulin; bottom line(D-E-F) after 30 minutes of 1000nM of insulin. GLUT4 protein (green fluorescence) counterstaining of nuclei with DAPI (blue fluorescence); Magnification 20x. Scale bar=30µm

In figure 4.18 are represented in A-B-C frames the basal conditions, in D-E-F frames the insulin stimulated condition. The GLUT4 immunofluorescence for 3T3-L1 cells was done for assess the localization the carrier both at the cytoplasmic level that on the cell membrane. Already in basal conditions, a decreased labelling of GLUT4 within the cells treated with BSA-MGO with respect to those not treated was observed (frame C). Following stimulation with 1000nM of insulin, cells treated with MGO (frame E), compared to control (frame D) shown an increased GLUT4 labelling in the cytosol near to the plasma membrane and in membrane itself. Cells treated with BSA-MGO globally show a less intense labelling (frame C and F) but the translocation of GLUT4 was observed, albeit, if compared to those of controls, seems to involve a less portion of the carrier. Comparing the staining for all the examined conditions, before and after insulin stimulus, globally the GLUT4 redistributes. Whit these only analyses, it is not clear if

and eventually how much, the treatment with a chronic glycation-inducing environment may to affect the translocation.

Following are some representative images of the co-staining for GLUT4 and AGEs products both in basal and in insulin stimulates condition.

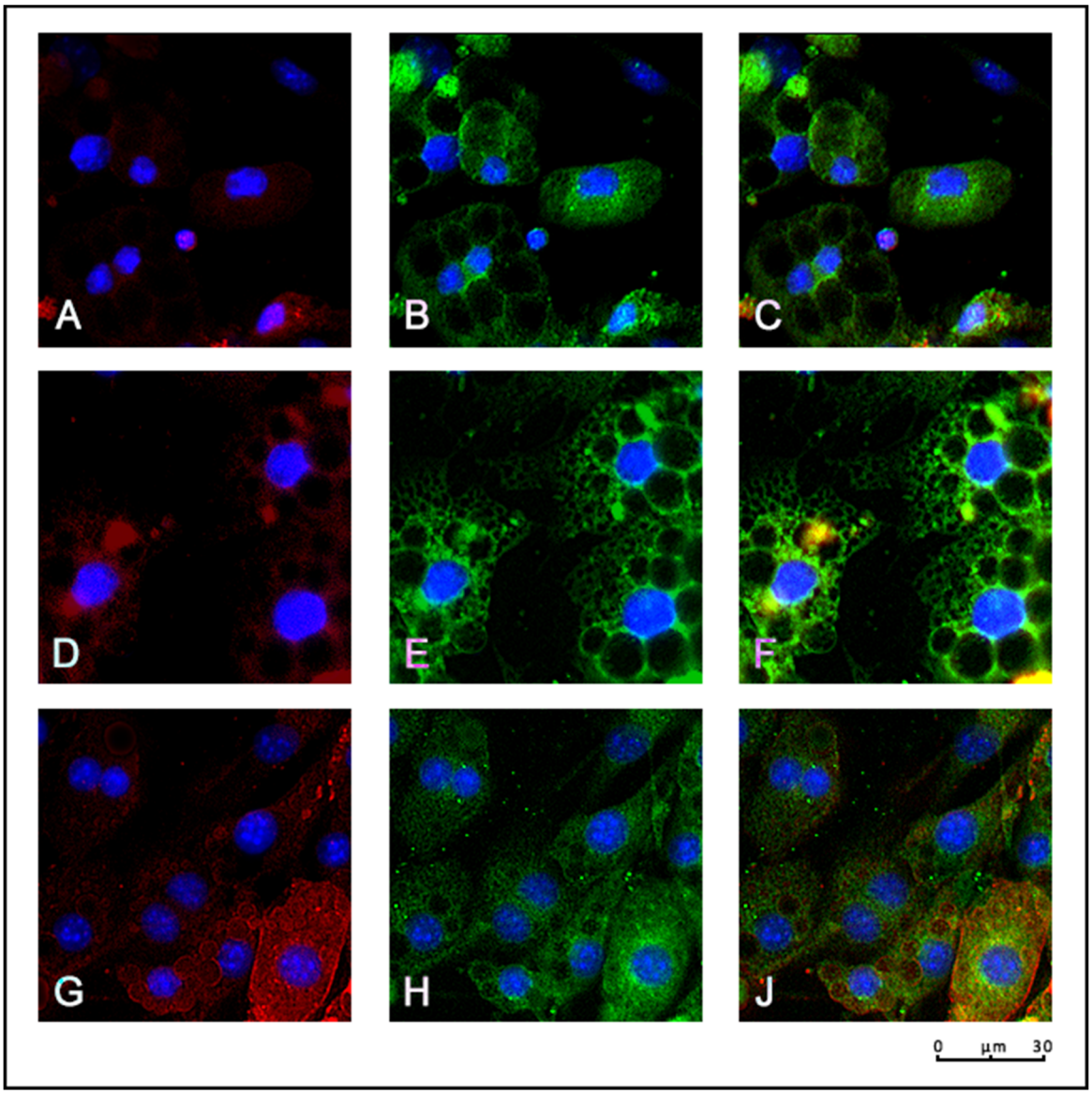

Figure 4.19: In the panel are represented images of staining for AGEs (red), GLUT4 (green) and nuclei counterstaining with DAPI (blue) with no insulin stimulus – basal conditions. The channels are overlapped in the images of the last column. A-B-C: 3T3-L1 cells differentiated in standard/canonical medium; D-E-F: 3T3-L1 cells differentiated in the medium in which was added MGO100µM; G-H-J: 3T3-L1 cells differentiated in the medium in which was added BSA-MGO. Magnification 20x. Scale bar=30µm

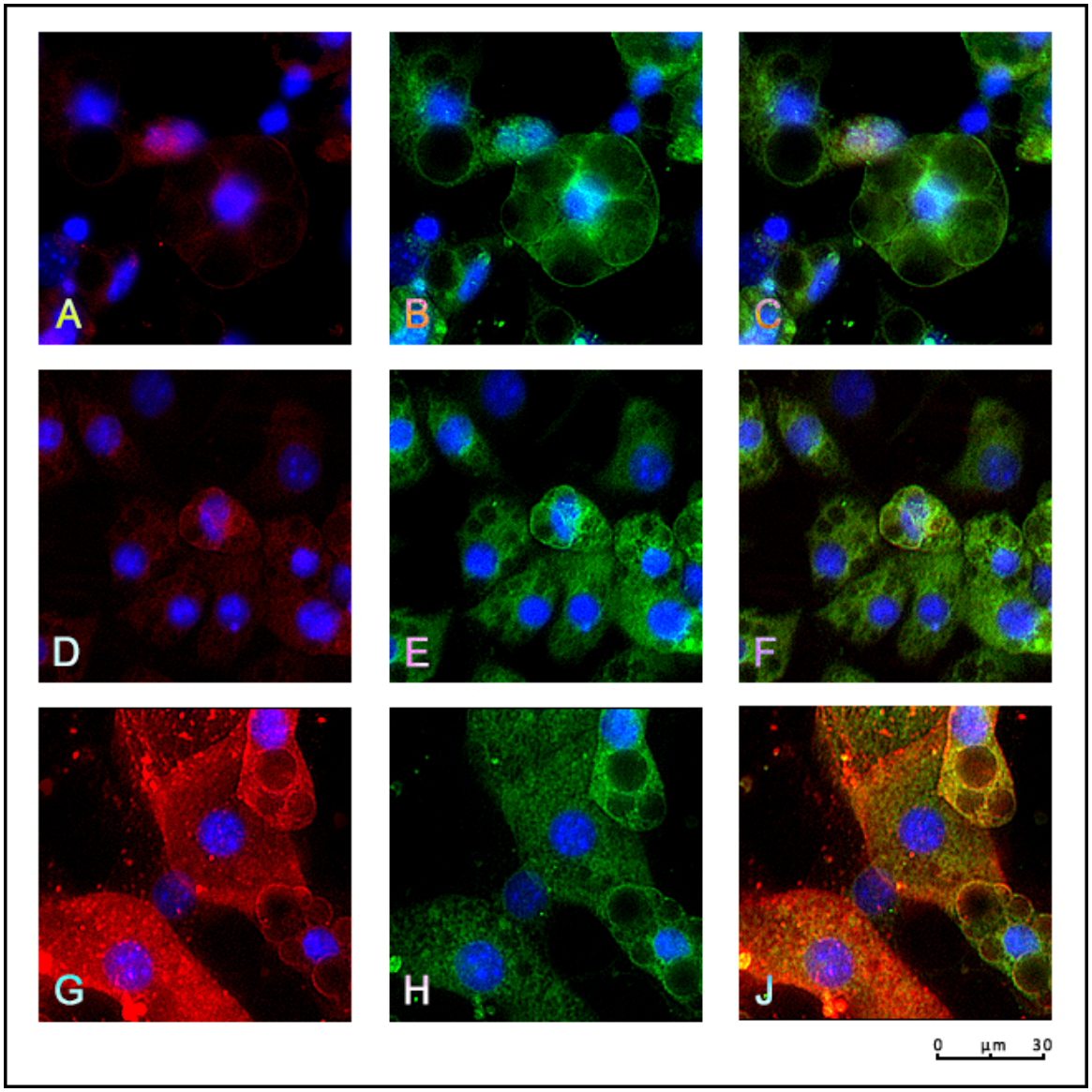

Figure 4.20: In the panel are represented images of staining for AGEs (red), GLUT4 (green) and nuclei (blue). The channels are overlapped in the images of the last column. A-B-C: 3T3-L1 cells differentiated in standard/canonical medium; D-E-F: 3T3-L1 cells differentiated in the medium in which was added MGO 100µM; G-H-J: 3T3-L1 cells differentiated in the medium in which was added BSA-MGO. 30 minutes of insulin stimulation had been done. Magnification 20x. Scale bar=30µm

In biomedical studies, the colocalization is commonly understood as the overlap between distinctive labeling in images, the bioimaging is a key for understanding the molecular orchestration of cellular processes and is generally achieved through the study of the spatial colocalization between the different populations of molecules.

In the basal condition, without insulin stimulation (fig. 4.19) the labelling of GLUT4, represented in green, has a fluorescence distributed in the cytoplasm and particularly intense in a region near the nucleus, but perinuclear. The red labelling specific for AGEs appears dispersed in the adipocytes for each condition without any specific pattern. This latter is more intense in the adipocytes grown in glycation-inducing conditions, confirming the quantification done with the

red-single labelling. (fig. 4.17) The C-F-J frames display the overlapping channels; the yellow dots are a sign of a probable co-localization in some points.

After 30 minutes of treatment with 1000nM of insulin, (fig. 4.20) the labeling of GLUT4 globally spreads quite uniformly in the cytoplasm for each condition and is possible to appreciate the trafficking to the membrane surface. Comparing the green fluorescence each other, it can be noted that it is more intense near to the plasmatic membrane both for MGO and control conditions, as like as staining for GLUT4 alone (frames B and E). Labelling for AGEs is dispersed in the cells without a specific pattern but is more intense in the adipocyte grown in MGO and even more in BSA-MGO 2,5% conditions (frames D and G), while is quite unnoticeable for standard/control medium (frame A). By these analyses we were able to confirm that the greater glycation-inducing condition (BSA-MGO) the greater is AGEs intracellular formation. Focusing on the overlapping channels (C-F-J frames) some yellow points are detectable; this leads to suppose that might exist a probable co-localization in some points. The phenomenon of glycation is random and therefore it is not uniform, that's why it is not possible to discover a similar co-labelling throughout the cells. These observations alone are not sufficient to confirm or deny the colocalization between GLUT4 and AGEs.

↳ *Glucose UP-TAKE*

Previous studies in the late years of 90's, have revealed that giving the GLP1 peptide to the fully differentiated 3T3-L1 adipocytes may increase insulin sensitivity by upregulating both GLUT1 and GLUT4 protein levels, without changes in gene expression. (103, 141). The mechanism of action of this process remains still unclear. In the case presented here, there is an increased expression for both the *Glut4* and the *Glp1r* that is supposed to be correlated with a glycation-inducing environment. To find out more, it is then thought to investigate with a functional assay. It is enquired if these alterations of gene expressions could have repercussions on insulin sensitivity and the related glucose intake.

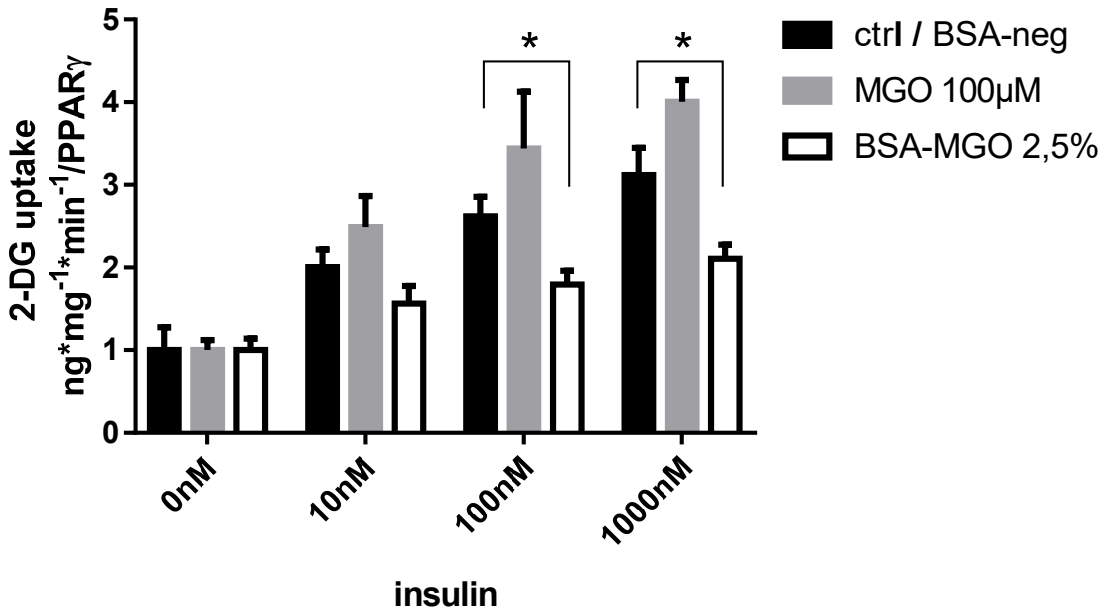

Figure 4.21: effects of glycation-inducing environment on insulin-stimulated glucose uptake in mature adipocyte. Results were normalized with the degree of differentiation using the expression of PPARγ, then put into graph as ratio considering the control as 1. Data are shown as the mean ±SD from independent experiments. Statistical significance determined using the Holm- Šídák method, without assuming a consistent SD calculated with alpha = 0.05.

The uptake of 2-deossi- [3H] D-glucose was measured both in basal conditions and after insulin stimulation, in fig. 4.21 are reported the results of the assay rationalized for PPARγ expression. The change of glucose uptake was calculate considering as 100% the value measured in the cells kept in the control/standard medium under basal conditions. It is noticeable a slight increasing in glucose up-taking insulin-stimulated in adipocytes grown in medium with chronic MGO 100µM compared to control. On the opposite, the ones grown with chronic BSA-MGO show a significant lower uptake of glucose. The evidences of the 2-deoxy [3H] D-glucose assay, lead to hypothesize that a chronic exposition to BSA-MGO might cause a decreased response to insulin.

↳ *Cell Lysates MALDI analyses*

In previous works, MALDI mass spectrometry was successfully employed in the field of diabetes, allowing the determination not only of the different proteins expressed in the presence of the pathology, but also to determine the number of glucose molecules condensed on a specific protein. (124, 142)

In the present study, which has to be considered as a preliminary step, cell lysate of mature 3T3-L1 adipocytes were directly analyzed in mass spectrometry.

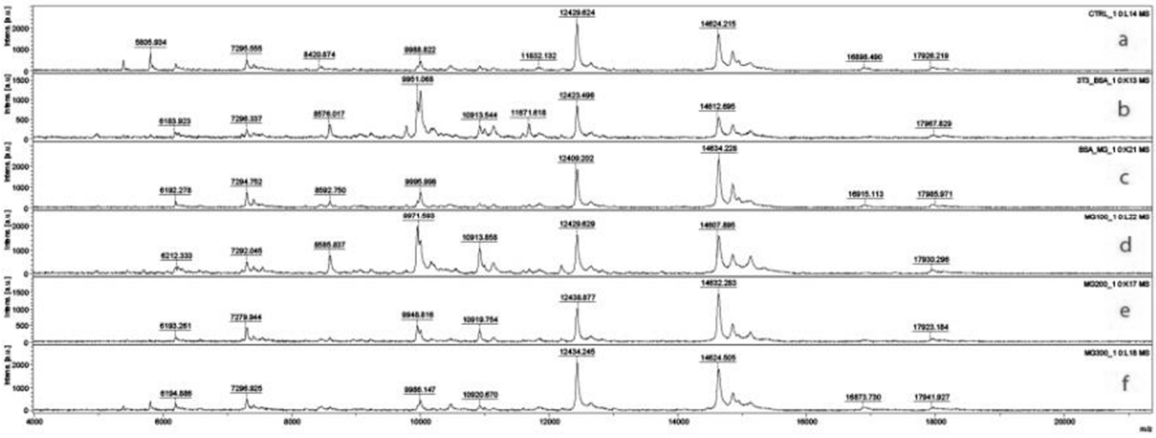

Figure 4.22: Summary panel of the spectra obtained by MALDI-TOF mass spectrometry of lysates obtained from adipocytes grown in different glycation inducing conditions object of the study, in order: a) lysate of adipocytes differentiated in control/standard medium, b) lysates of differentiated adipocytes in the presence of BSA-neg; c) lysate of adipocytes differentiated in the presence of BSA-MGO; d) lysate of adipocytes differentiated in the presence of MGO100μM; e) MGO200μM and f) MGO300μM (image at complete resolution in appendix)

The figure 4.22 shows a panel of the acquired MALDI-TOF spectra of lysates obtained for mature adipocytes grown in different conditions of glycation. Lysates were obtained by twice rinsing adipocytes with NH_4HCO_3 100mM, in order to remove all traces of growth medium and subsequently cells were lysed with a 0.1% TFA solution, maintaining the equipment in an ice-cold bath (see materials and methods section). Obtained mass spectra are characterized by a wide series of signals in the low mass region (*m/z* 5000-20000) of the spectrum, while for *m/z* higher than *m/z* 20000 no signals were measurable. Analyzing spikes individually, it is possible to observe that in the spectra of adipocyte grown in the presence of chronic either MGO 200μM or MGO 300μM (line E and F) the peak in the mass range of *m/z* 8500 is not detectable; whereas the pick around *m/z* 11600 is only present in the controls and BSA-neg (line A and B). Globally comparing the spectra of mature adipocytes, it is not appreciable any shift of the spectrum towards heavier molecular weights. It is known that the protein glycation causes qualitative alterations on the spectrum of the protein. It should be observed in the peak relative to the protein in the canonical mass flanked by a much smaller peak to the right of it due to the same protein glycated. However, on the spectra presented here, isn't possible to make such considerations. Therefore, it can be concluded that the glycation or has not taken place or that the amount of glycated protein produced is below the instrumental detection limits.

In order to evaluated the possible effects of glycation on adipogenetic process, it was also evaluated the spectrum of cells with another morphology and totally different functions, in this case, two different kind of fibroblasts.

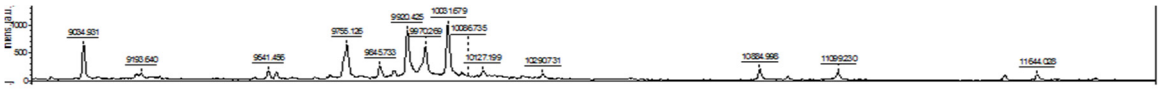

Figure 4.23: The spectra obtained by MALDI-TOF mass spectrometry of 3T3-L1 fibroblast cell lysates.

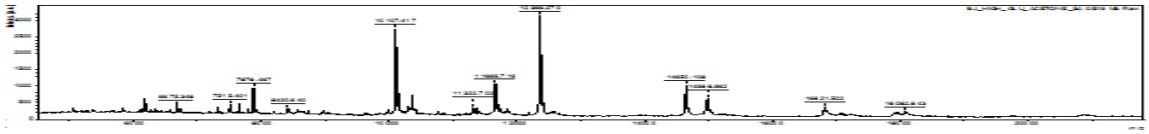

Figure 4.24: The spectra obtained by MALDI-TOF mass spectrometry of BJ fibroblast cell lysates

The spectra are reported in fig. 4.23 and fig. 4.24, as expected, display a completely different protein profile, but once again are not present alteration that allowing to demonstrate the possibility of a probable protein glycation.

4.2.2 Mice models

Following are summarized weights and the glycemic values of mice involved in the study.

	n°	weight (g)	glycaemia (mmol/l)
ob/ob	5	44.1±2.47	8.74±1.07
db/db	5	49.28±1.28	11.19±5.4
db/+	5	27.7±0.46	4.94±0.34
ob/+	5	28.8±3.81	7.79±1.03

Table 4.1: characteristics of mice models and relative controls used in this work.

- *ELISA Test*

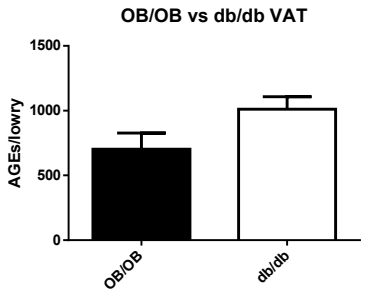

Figure 4.25: E.L.I.S.A. quantification of AGEs proteins of VAT tissue in ob/ob and db/db mice models normalized by the total amount of proteins.

In order to ascertain and to measure out the *in vivo* presence of endogenic glycation products in adipose tissues (AT) of mouse models for obesity and diabetes, VAT lysates of 5 *ob/ob* mice and 5 of *db/db* mice were analyzed in E.L.I.S.A. assay. Data were normalized with the absolute amount of proteins quantified with Lowry method (see Material and Methods). The AT of *db/db* mice, the obese diabetic model, show to contain a greater amount of AGEs when compared to the VAT of *ob/ob* mice, the obese normoglycaemic ones.

Gene expression analyses

For elucidate whether the gene expression of murine AT may be influenced by an environment supposed to be favoring the glycation, it was proceeded with the qPCR analysis of genes: *Rage, Dpp4 and Glp1r* in mice *ob/ob*, *db/db* and their relative non-obese/non-diabetic controls (*ob/+* and *db/+)* into the brown, subcutaneous and visceral adipose depots.

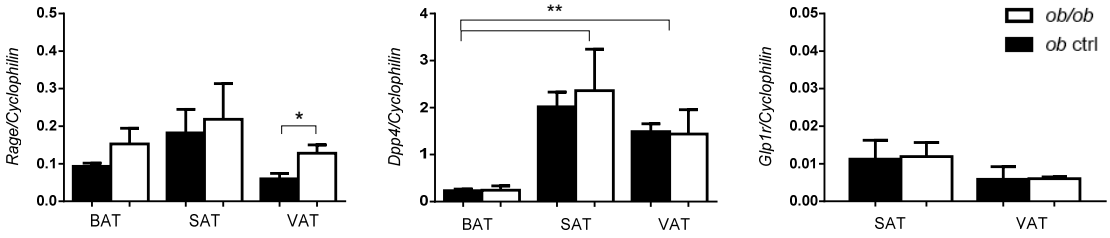

*Figure 4.26: Comparison of expression for Rage, Dpp4 and Glp1r in the three depots (BAT, SAT, VAT) of adipose tissue in the mice models ob/ob and relative controls. *p<0.05 *p<0.01*

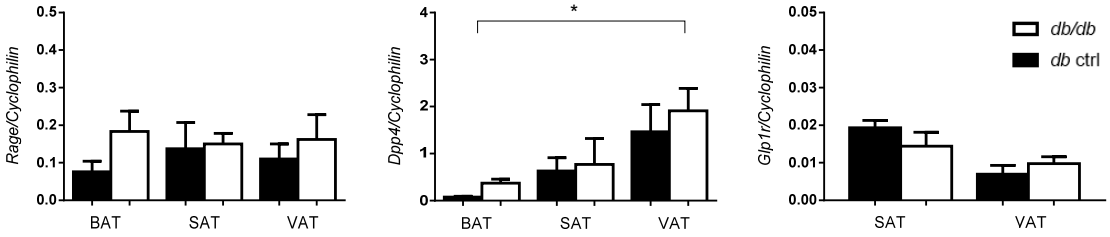

*Figure 4.27: Comparison of expression for Rage, Dpp4 and Glp1r in the three depots of adipose tissue (BAT, SAT, VAT) in the mice models db/db and relative controls. *p<0.05*

The expression of *Rage* in BAT, SAT and VAT mice tissues shows a slight increase in all three depots for both mice model compare with the relative control. In particular, in *ob/ob* mice for VAT tissue, the difference appears statistically significant (fig. 4.26).

Instead, expression of *Dpp4* does not show significant differences in between controls and models but, comparing each other the three diverse typologies of AT, appears an evident difference: expression in BAT is lower compared both with SAT and VAT tissues. These differences statistically significant, are found in both models, but are more noticeable in *ob/ob* mice and their relative controls.

The presence of *Glp1r* in the AT is still controversial. In the present work, the *Glp1r* expression was very low and no significant difference emerges between controls and models, while a slight difference between SAT and VAT was detected. Because of the high individual variability and the low sample size, this difference is not statistically significant.

4.3 HUMAN

In order to validate the results observed for the 3T3-L1 cells, the treatment conditions and analysis were replicated on stromal vascular fraction cells isolated from human adipose tissue (hSVF).

4.3.1 Human Adipocytes

From the subcutaneous AT of 5 patients who underwent into abdominoplasty in the III medical clinic, had been excised a small piece of AT for extract the hSVF according to the protocol given in materials and methods. Freshly isolated hSVF cells are a heterogeneous mixture of endothelial cells, smooth muscle cells, pericytes, fibroblasts, mast cells and pre-adipocytes. Culturing of these cells under standard conditions eventually results in the appearance of a relatively homogeneous population of mesodermal or mesenchymal cells. Once seeded, the hSVF cells were induced with appropriate adipogenic stimuli for 15 days leading to the formation of mature multi-locular adipocytes. The glycation conditions were chosen based on the results obtained with 3T3—L1 cells.

Morphological and Differentiation Evaluation

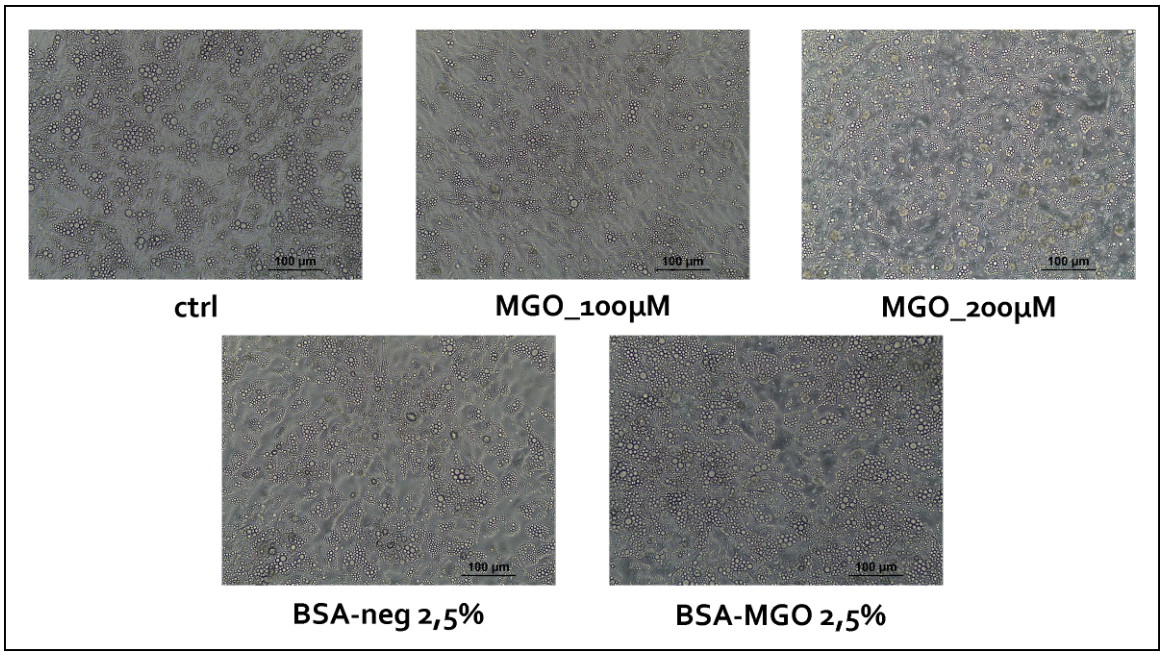

Figure 4.28: In the panels are represented the effects on human fully differentiated adipocytes in the different glycation-inducing environment. Ctrl: standard growth medium, 25mM of glucose; MGO: methylglyoxal at 100µM and 200µM; BSA-MGO and BSA-neg: BSA glycated or not glycated. Images were taken the fifteenth-day of differentiation with an optic microscope at 20x magnification. Scale bar: 100µm

In the first instance, analogously to the 3T3-L1 cells, the effects of the MGO, the BSA-MGO and the BSA-neg, were evaluated on the basis of the efficiencies of adipogenetic differentiation, the formation of lipid droplets and the morphology of cells.

Real Time quantifications: in acute and in chronic stimuli

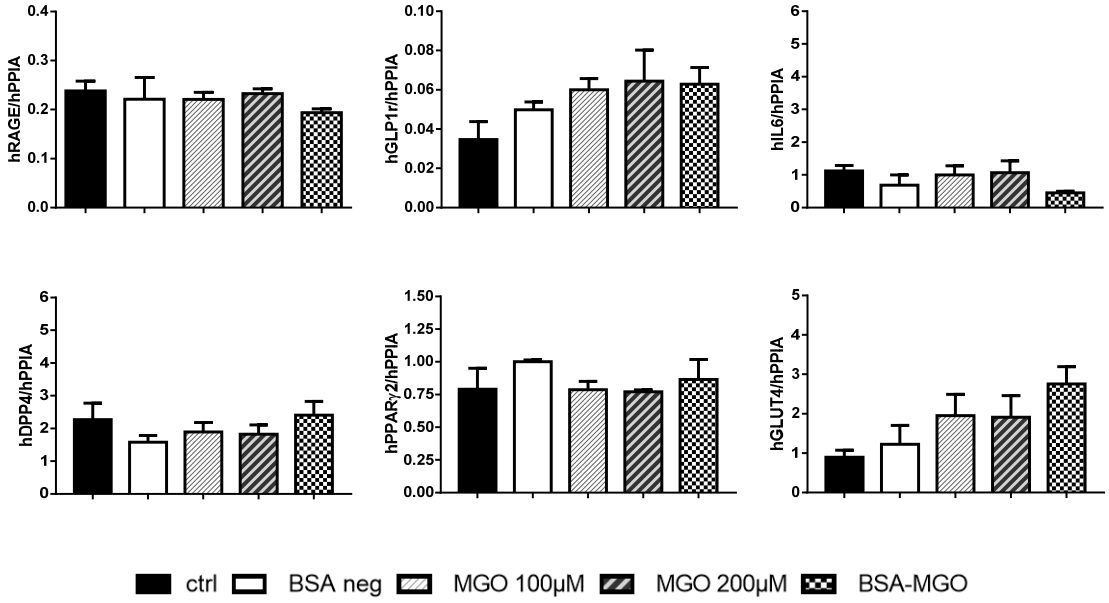

Figure 4.29: A panel of gene expression profile quantified by qPCR of human fully differentiated adipocytes in standard conditions and subjected at the 13th day to an acute stimulus (48h of treatments) with either MGO 100µM; MGO 200µM; BSA-neg or BSA-MGO added into medium in 2,5% in volume. The values are expressed as arbitrary units normalized for the content of the house-keeping gene: peptidylprolyl isomerase A (PPIA)

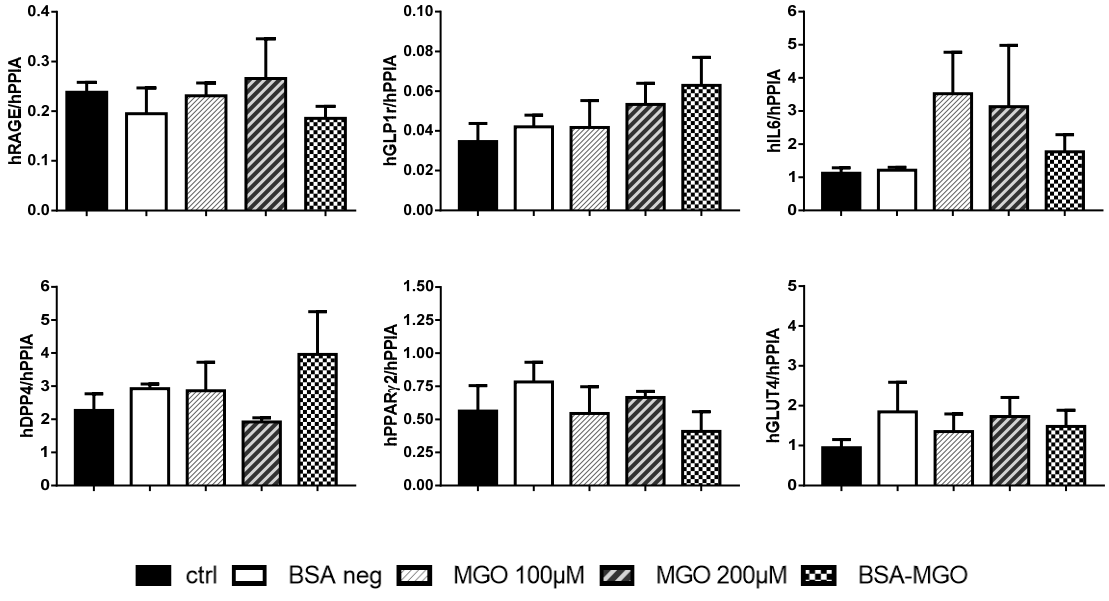

Figure 4.30: A panel of gene expression profile quantified by qPCR of human fully differentiated adipocytes cultured in chronic with either MGO 100µM; MGO 200µM; BSA-neg or BSA-MGO added into medium. The values are expressed as arbitrary units normalized for the content of the house-keeping gene: peptidylprolyl isomerase A (PPIA)

In fig. 4.29 and fig. 4.30 are summarized the expression analysis performed in human fully differentiated adipocytes kept in five different glycation-inducing conditions: control standard medium (ctrl), BSA non-glycated as second control (BSA-neg), two different concentrations of MGO (100µM and 200µM) and BSA-MGO. The cells were differentiated with two distinct

protocols: an acute stimulus (48h) and a chronic one.

No differences emerged in the expression of *PPARγ* at complete differentiation among the chronic glycation inducing treatments. This can confirm the morphological evaluations: all treatments have allowed the fibroblasts to achieve a good degree of differentiation.

The *GLP1r* in adipocytes is expressed at low grade. Preliminary results, even if not statistically significant, could suggest that may exist a possible effect due to a glycation-inducing environment on the *GLP1r* expression. Both in chronic and in acute stimulus is measured up a slightly increase in its expression for cells exposed either to MGO or BSA-MGO compared with the controls ones. In contrast, differences for *RAGE* or for *DPP4* expression among treatments both in acute and in chronic exposure cannot be appreciated.

Taking in account the expression for the *IL6* (interleukin 6), a net increased expression in adipocytes exposed either to MGO 100µM or MGO 200µM during the adipogenic process was found; conversely, in case of the acute treatments, these differences are flattened. Furthermore, comparing the effects of the acute stimulus to the chronic one, it is possible to postulate that MGO could have a long-term inflammatory effect.

A slight increase for the *GLUT4* expression was observed in the MGO and BSA-MGO acute stimuli, was observed. At the opposite, among all the chronic treatments these differences were flattened.

However, given the low sample size due to the difficulty of acquire the material, the results set forth herein are to be considered absolutely preliminaries.

↳ *Immunofluorescence*

Following are reported some representative IF images for RAGE, GLP1R and AGEs made on human fully differentiated adipocytes with three glycation protocols.

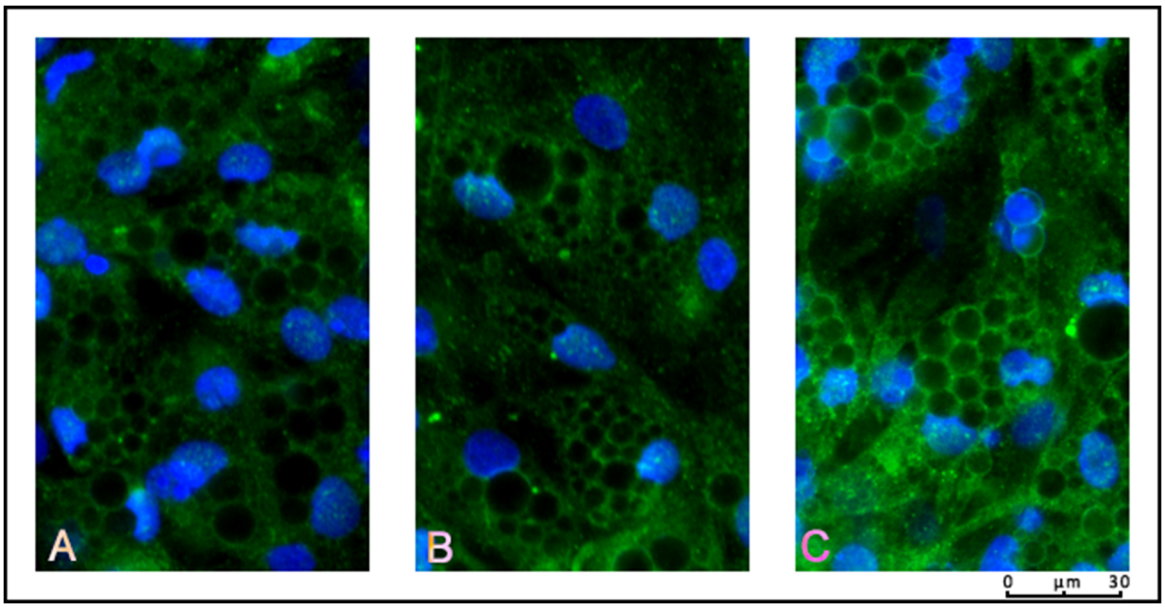

*Figure 4.31: RAGE IF panel, on human fully differentiated adipocytes in exposition to: A) standard/control DMEM F12 25mM glucose medium; B) DMEM F12 with MGO 100µM in chronic treatment; C) DMEM F12 with BSA-MGO 2,5% in volume in chronic treatment. Green: Receptor for Advanced Glycation End products (*RAGE*); counterstaining of nuclei with DAPI (Blue) Magnification 20x. Scale bar= 30µm*

In fig. 4.31 are reported shots of IF for RAGE in human adipocytes. The labelling looks dotted into the cytoplasm; no signal is appreciable nor into the nucleus nor into the lipid droplets. Comparing the staining, the labeling appears more intense for the cells chronically exposed to the glycation-inducing-condition BSA-MGO (C) that the control one (A). This could lead to suppose that might exist a potential auto sustained loop for RAGE/AGEs interaction and RAGE expression.

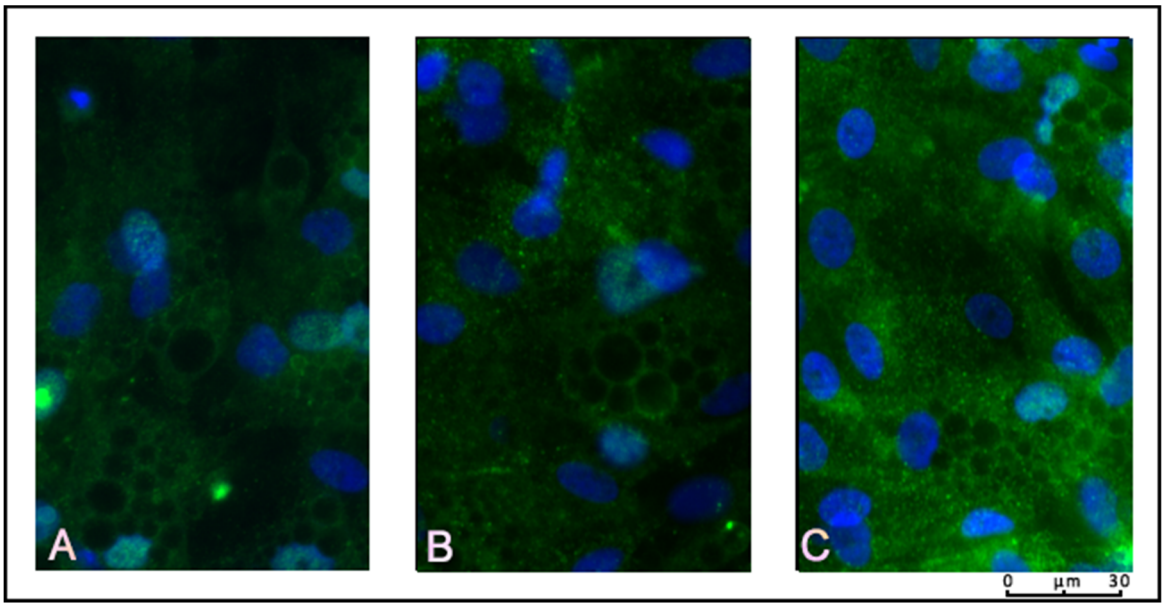

Figure 4.32: GLP1R IF panel, on human fully differentiated adipocytes in exposition to: A) standard/control DMEM F12 25mM glucose medium; B) DMEM F12 with MGO 100µM in chronic treatment; C) DMEM F12 with BSA-MGO 2,5% in volume in chronic treatment. Green: GLP1R; counterstaining of nuclei with DAPI (Blue) Magnification 20x. Scale bar= 30µm

Figure 4.32 reports three representative images of IF for the GLP1R in human adipocytes differentiated in exposure to three different levels of glycation-inducing environment. The staining appears sandy green dispersed into the cell. Compared to control, the ones grown in BSA-MGO-condition show a more intense labeling, supporting to both with the results of gene expression analysis and with IF for GLP1R in 3T3-L1.

It was expected that like for 3T3-L1 cells, a greater quantity of AGEs could be found in adipocytes grown in glycation-inducing environment. In order to examine the presence, the formation and the peculiar pattern of intracellular AGEs in fully differentiated human adipocytes was proceeded with immunofluorescence for those glycated proteins.

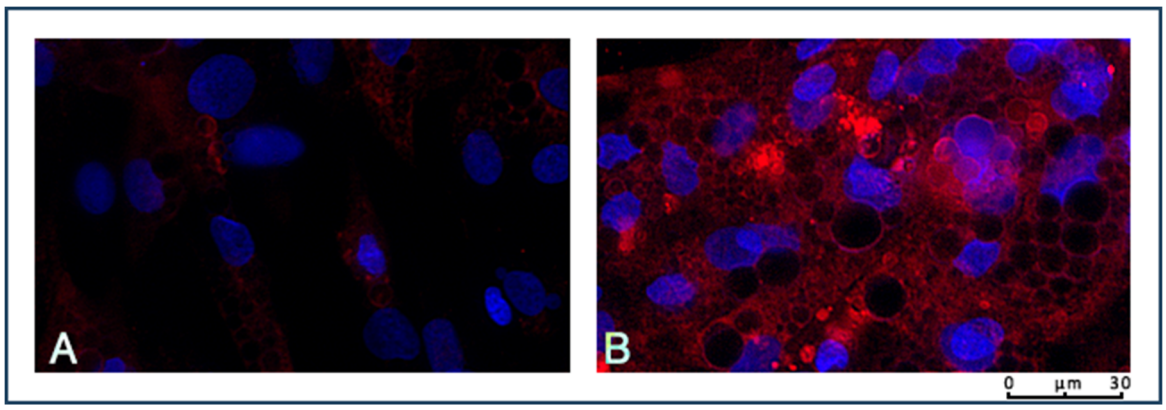

Figure 4.33: AGEs IF panel, on human fully differentiated adipocytes in exposition to: A) standard/control DMEM F12 25mM glucose medium; B) DMEM F12 with BSA-MGO 2,5% in volume in chronic treatment. Red: Advanced Glycation End products (AGEs); counterstaining of nuclei with DAPI (Blue)

Magnification 20x. Scale bar= 30µm

Figure 4.33 show representative shoots of IF for AGEs in human adipocytes in two different levels of a glycation-inducing environment. Cells show a red dotted fluorescence distributed into the cytoplasm. The pattern of labeling is very peculiar; it seems grainy but not draw any characteristic structure. These observations lead to assume that the adipogenic process in a glycation-inducing environment causes the formation of AGEs products intracellularly.

4.3.2 Human Tissues

Enrolled patients

10 subjects were recruited: 3 of them obese diabetic, 4 obese normoglycaemic and 3 post obese subjects undergone to abdominoplasty intervention.

	n°	F; M	age (years)	BMI (kg/m²)	glycaemia	HbA1c
obese diabetic	3	1; 2	55,5±6,5	42,49±6,45	13,23±5,31	84,3±33,6
obese normoglycaemics	4	2; 1	46,25±7	45,29±1,65	5,1±0,5	-
Post obese	3	3; 0	43,6±7,6	25,34±1	5,1±0,5	-

Table 4.2: anthropometric and clinical and biochemical characteristics of enrolled patients analyzed in mass spectrometry and in western blot

Western Blot analysis

In order to demonstrate the presence of AGEs products in the human AT, were done preliminary analyses in Western.

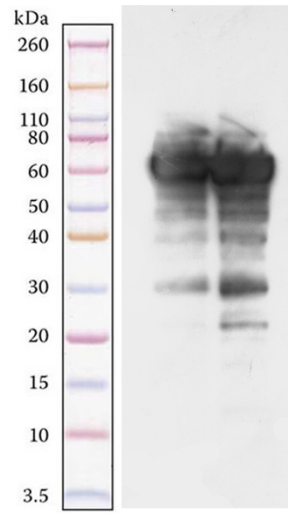

Figure 4.34: 1D western blotting images of AGEs modified adipose tissue proteins. In figure are represented the bands of AGEs proteins of two SAT adipose tissues from post obese patients.

Two samples of SAT lysate from post-obese subjects were loaded onto a pre-cast NuPAGE® 10% Bis-Tris 1.0 mm mini-gel until the dye front reached the end of the gel; then was immunoblotted on a nitrocellulose membrane. Next, AGEs modified proteins were detected using anti-AGEs antibody after transferring proteins to a nitrocellulose membrane, following the protocol presented in Materials and Methods. Representative image of the blotting is presented in figure 4.34, flanked by a set of molecular weight standards. Western blotting for AGEs modified proteins from 1D-SDS gels shows several bands, the major one at around 60 kDa, probably albumin, and many other are visible at lower weights. The results of the current preliminary test might demonstrate the presence of AGEs modified proteins in post obese adipose tissues.

↳ *Adipose Tissues MALDI analyses*

After that the presence of glycated proteins in AT have been confirmed by western blot, it was evaluated the use of MS to detect and eventually characterize the glycated proteins in AT. Following spectra of AT of normoglycemic obese, diabetic obese and post-obese.

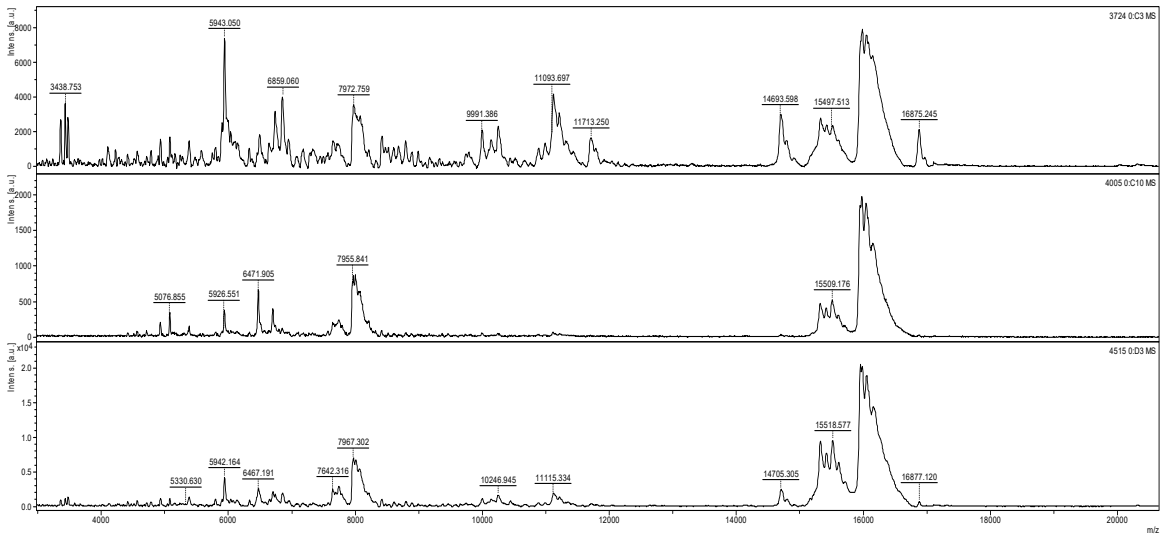

Figure 4.35: MALDI-TOF spectra of three VAT tissues of 3 diabetic obese patients. m/z 3000-20000

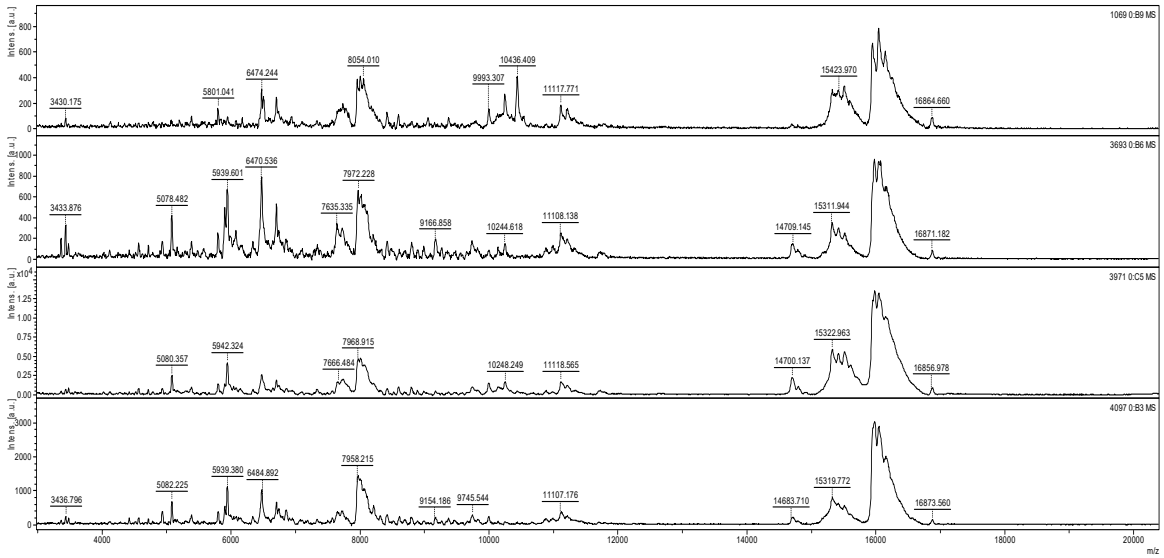

Figure 4.36: MALDI-TOF spectra of three VAT tissues of 4 obese patients. m/z 3000-20000

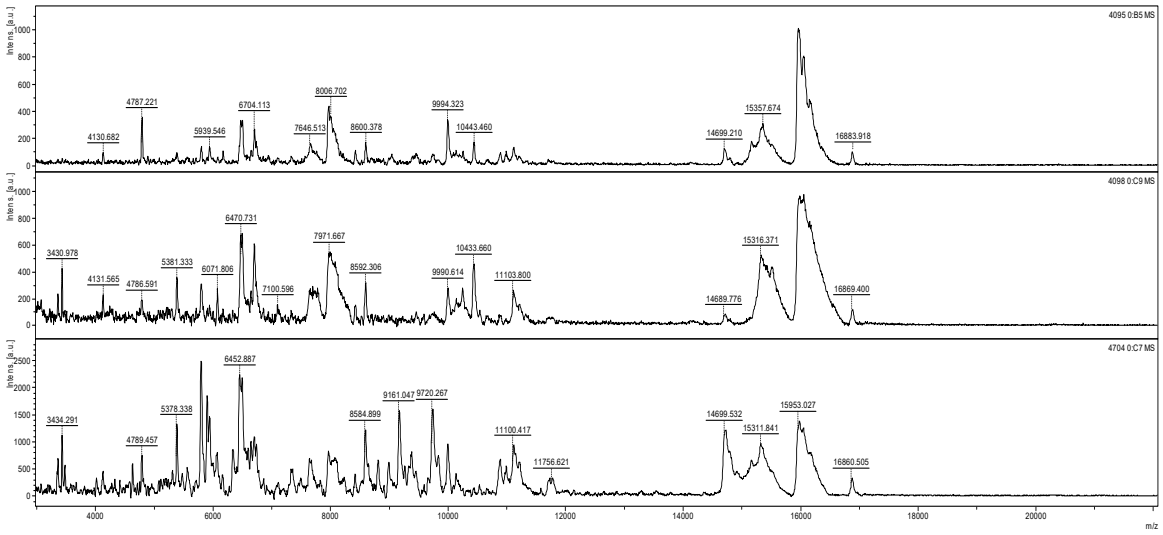

Figure 4.37: MALDI-TOF spectra of three abdominoplasty issues of three patients, post-obese. m/z 3000-20000

VAT samples were firstly lysed with urea and then, the proteins were precipitate with acetone (as explained in Materials and methods). The lysates were analyzed by MALDI-TOF mass spectrometry for the determination of the relative protein profile.

Although lysates of VAT have been cleansed from lipids and salts before MALDI analysis, obtained spectra, show a high background noise and are characterized by low resolved signals probably due to the presence of contaminants in the sample. Despite these difficulties, it was possible to perform some considerations. All the spectra are essentially characterized by the presence of some signals with high intensities, in the area from *m/z* 14000 to *m/z* 17000, attributable to the presence of haemoglobin residues. Furthermore, the haemoglobin (alpha chain and beta chain), generates the double-charged ions represented by the signals present in the low part of the spectrum (*m/z* 7500-8500). Its presence in AT lysates was also confirmed by MALDI-TOF/TOF analysis of the digestion products, obtained by treating the AT lysates with trypsin. Comparing the spectra for proteins profile of tissues of obese normoglycaemic subjects with those of obese diabetic only minor differences are displayed. These differences are appreciable in particular in *m/z* areas from 10000 to 12000 and in the *m/*z 6000 regions.

Instead, focusing attention on spectra of post-obese subjects, were found, as expected, more pronounced differences. In particular, the presence of a peak with *m/z* of about 8600 and a greater presence of spike to molecular weights lower than *m/z* 6000.

↳ *Lipids: Analysis of lipid mixtures*

Identifying the causative relationship between the lipids composition in AT and T2DM may fundamentally contribute to the understanding of the basic pathophysiological mechanisms of the disease.

To investigate whether specific lipid compositional changes occur in the AT in response to a diabetic/glycation-inducing condition, the lipid profile characteristic of the AT was analyzed for obese subjects with diabetes or with no diabetes and in weight loss/post-obese subjects.

71 lipids (belonging to different classes) in the mass range from *m/z* 311,322 to *m/z* 1077,794 were investigated. Of each of the 71 class of lipids, it has been calculated the percentage relative to the total amount of lipids. It is thought was interesting to verify if in the three different categories of patients, the species were present in the same proportions or not. From the analyses, it was possible to identify four specific lipids whose relative percentage differed between the three groups. The lipids were identified with searching in data base "Lipid Maps ®" and further confirmed by collisional mass experiment. *m/z* 347.282 that is presumably a derivate from arachidonic acid and *m/z* 501.05 who belongs to either the subclass of Diacylglycerophosphocholines or Monoacylglycerophospho-ethanolamines seem to be increased in weight loss/post-obese. Conversely *m/z* 577.527 decrease in the post-obese subjects. However, their mass is very low and for this reason their identification remains uncertain. The most intriguing variations is seen in *m/z* 881.781 lipid, presumably a triglyceride POO (C52:2), composed by two oleic acid (O) and one palmitic (P). The oleic acid has one unsaturation (i.e. presence of a double bond), whereas palmitic acid has two unsaturation. The *m/z* 881.781 is more present in diabetic obese, in comparison with both the other groups.

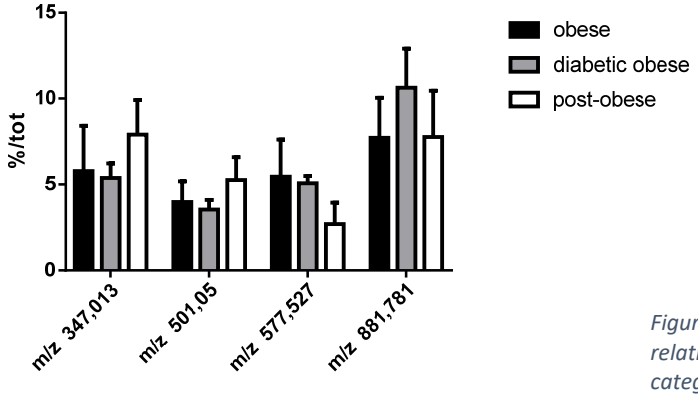

Figure 4.38: Histogram of the differences in the relative percentages of fatty acids for the three categories of subjects.

	m/z 347,013	*m/z* 501,05	*m/z* 577,527	*m/z* 881,781
obese vs post obese	**	ns	****	ns
diabetic obese vs post obese	***	ns	ns	****
obese vs diabetic obese	ns	*	**	****

Table 4.3: Summary of statistically significant results of 2-way ANOVA Tukey's statistic test.

Real Time quantifications

Enrolled patients

In order to elucidate whether the gene expression of human AT may be influenced by an environment supposed to be favoring to glycation, namely the diabetes, it was proceeded with the qPCR analysis of: *LEP* (Leptin), *RAGE*, *DPP4*, *GLP1r* in human subjects either with T2DM, with pre-diabetic condition or with a normal tolerance to glucose. Were recruited 64 obese subjects of which: 20 normoglycemic obese, 22 prediabetic obese and 22 diabetic obese. The diabetic ones are being treated with metformin.

In the following table (4.4) are summarized the clinical characteristics of the subjects enrolled in the study.

	n	**F; M**	**age (years)**	**BMI (kg/m^2)**	**HOMA (glyc*ins)/22,5**	**glycaemia (mmol/L)**	**Metformin treatment**
Normoglycaemic obese	20	18; 2	38,05±10,13	46,34±10,01	4,3 ± 2,7	5,07±0,37	no
pre-diabetic obese	22	18; 4	48,00±12,44	47,91±7,41	6,37±4,18	5,9± 0,68	no
Diabetic obese	22	11; 11	51,13±9,82	50,42±9,9	12,1±8,37	8,4±2,97	yes

Table 4.4: Anthropometric and clinical and biochemical characteristics of enrolled patients.

Expression profiling

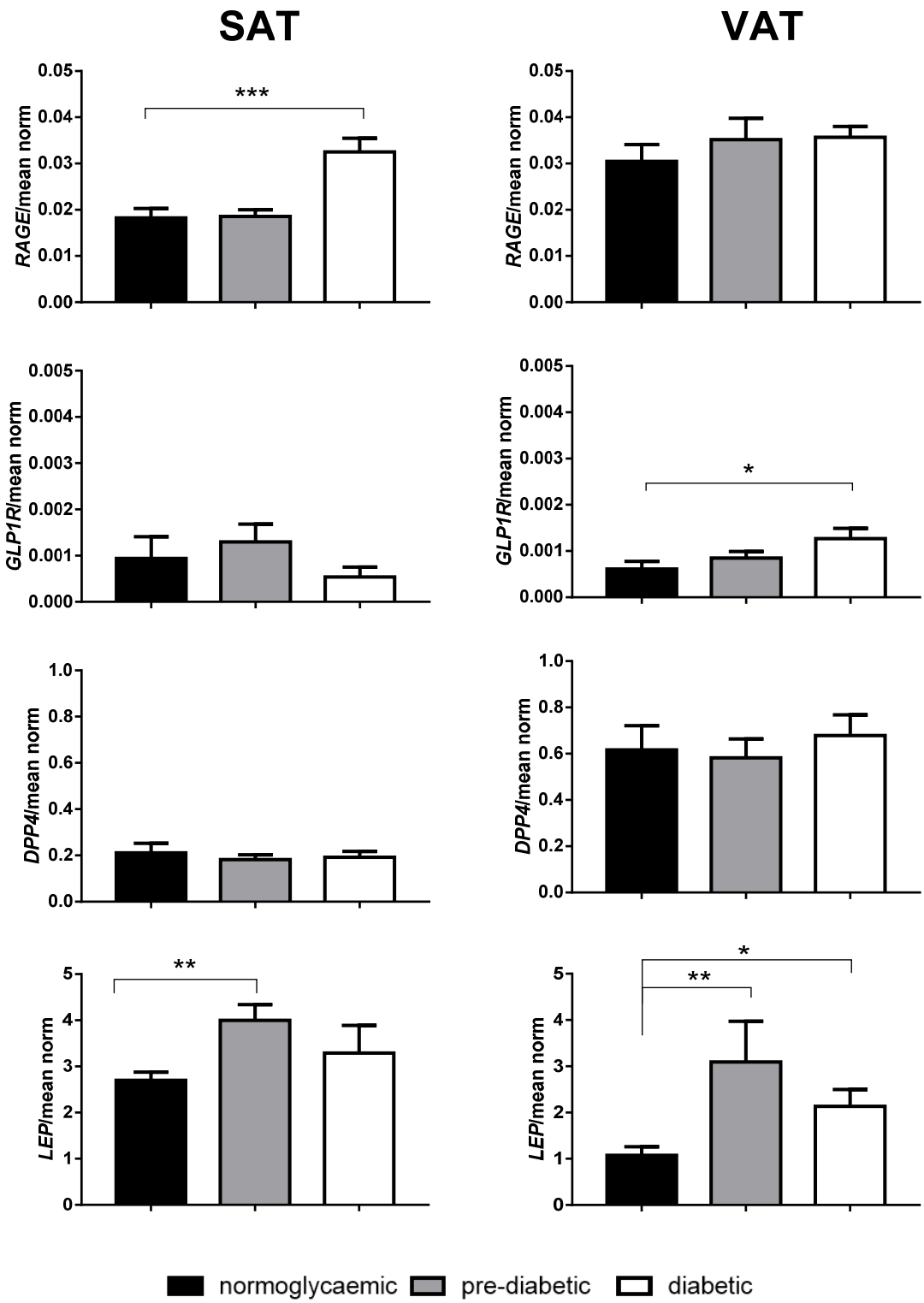

*Figure 4.39: Gene expression profile for: RAGE, GLP1 r, DPP4 and LEP for normoglycaemic, pre-diabetic and diabetic obese subjects. Normalized by the mean of RPLP0 and PPARγ. N=22 subjects for each group. Mann Whitney test. * p<0.05 **p<0.001 ***p< <0,0001. D'Agostino & Pearson normality test passed.*

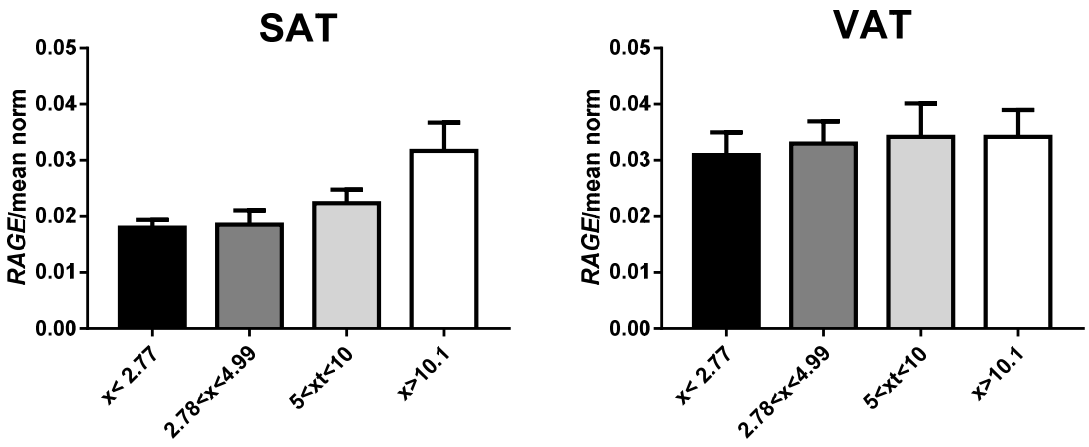

Figure 4.40: Gene expression profile for: RAGE subdivided by HOMA-IR categories

In SAT of diabetic subjects, the expression of *RAGE* displays (fig. 4.39) a significant increase that could be correlated with an altered glucose tolerance. On the contrary, in VAT the expression shows a quite flat trend, with only a slight increase in pre-diabetic and diabetic subjects. Reorganizing and re-processing data for the HOMA -IR index (fig. 4.40), in the subcutaneous tissue seems to appear an even more clear correlation of *RAGE* expression with insulin resistance. Nevertheless, in the visceral tissue the expression appears constant among the categories of subjects.

The expression for *GLP1R* in SAT proves to be lacking in a specific trend, with a slight increase in prediabetic and a decrease in the diabetic. On the opposite, in VAT it shows a little but significant increase in expression in diabetic VAT.

The expression of *DPP4* shows no quantitative differences among the three groups of subjects; on the other hand, a considerable difference between the SAT and VAT depots can be observed. In particular, VAT got nearly threefold of expression of SAT.

Finally, the trend of *LEP* suggests a possible link with the glycaemic state and metformin treatments. Pre-diabetic subjects show a significant increase of expression compared with the control group. Whereas, obese diabetic show a less substantial increase in expression.

4.3.3 Potential preparatory studies

For a long time, many investigators focused their attention on the role of leptin in the pathogenesis of obesity. Leptin is an “anti-obesity” hormone produced mainly by AT that is released into the circulatory system and plays a central role in regulation of metabolism, energetic balance, immune and inflammatory response, haematopoiesis, angiogenesis, bone formation, and wound healing.

Since the glycation can alter the functionality of the protein, the possibility that leptin could be glycated and thereby change its biologic activity, contributing to the leptin resistance mechanisms was investigated. Previous studies using ESI-MS in diabetic subject was successfully used to detect and characterize glycated insulin in plasma from patients with type 2 diabetes. AGEs precursors, i.e. MGO, can glycate insulin to form insulin-MGO adducts and in turn change the insulin structure, thereby abrogating its physiological function. (58) Taking in account that leptin is the most abundant protein in the obese, and on the basis of these evidence, it was decided to analyze its *in vitro* glycation.

In silico Prediction of Leptin glycation

In the table below, are reported the probability calculation result to glycation and a summary yes/no answer.

```
>Sequence       167 amino acids
#
# netglycate-1.0 prediction results
#
# Sequence                        #    Score            Answer
# ------------------------------------------------------------
# Sequence                       26   -0.927   glycate     .
# Sequence                       32   -0.957   glycate     .
# Sequence                       36    0.867   glycate    YES
# Sequence                       54    0.760   glycate    YES
# Sequence                       56    0.926   glycate    YES
# Sequence                       74    0.792   glycate    YES
# Sequence                      115   -0.885   glycate     .
#
    MHWGTLCGFLWLWPYLFYVQAVPIQKVQDDTKTLIKTIVTRINDISHTQS   #     50
    VSSKQKVTGLDFIPGLHPILTLSKMDQTLAVYQQILTSMPSRNVIQISND   #    100
    LENLRDLLHVLAFSKSCHLPWASGLETLDSLGGVLEASGYSTEVVALSRL   #    150
    QGSLQDMLWQLDLSPGC                                    #    200
%1  .....................................G.............   #     50
%1  ...G.G..................G............................   #    100
%1  ...................................................   #    150
%1  .................
```

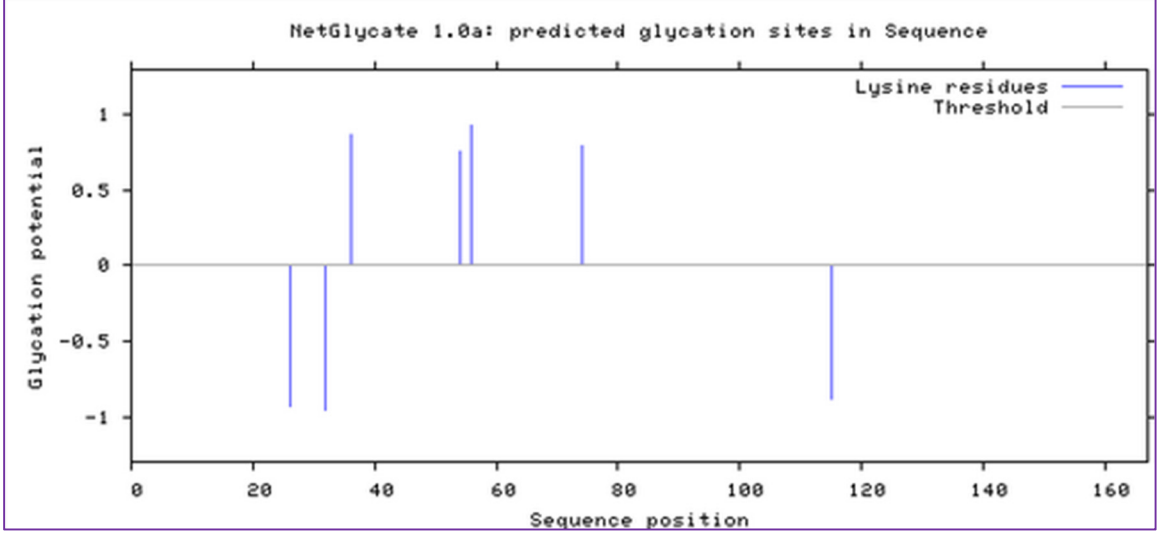

*Figure 4.41: Prediction of glycation sites of leptin [leptin Homo sapiens, NCBI Reference Sequence: **NP_000221.1**] by using NetGlycate 1.0 software. For each input sequence the length and the name of the sequence are stated followed by a table with the prediction results. There is a table row for each lysine residue in the sequence; the columns are: sequence name, residue position in the sequence (#); the score, a number between -1 and 1; when the score is above 0 the residue is a predicted glycation site; the answer: either the word "YES" or a dot ("."), reflecting the score. After the table, the whole sequence is printed alongside a summary of the predicted glycation sites and their positions. Finally, it displays a figure showing a plot of the score for each lysine residue against the sequence position of that residue. (**www.cbs.dtu.dk/services/NetGlycate 1.0**) (130, 131)*

It was aimed to correlate the experimental results with report of glycation and glycation-prediction by NetGlycate 1.0. The human leptin [NP_000221.1] has 7 lysine (K), and 4 (57,17%) of them are predicted by NetGlycate 1.0 as potential glycation sites (indicated as “G” in dots line).

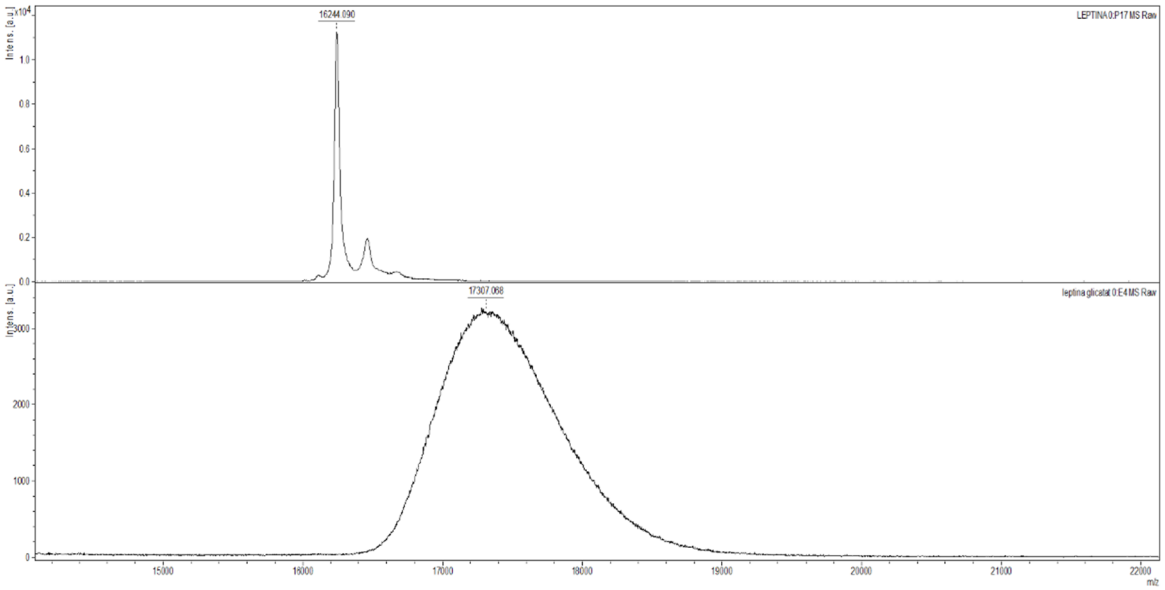

Figure 4.42: In the upper part of the figure is represent the spectra of full length protein leptin not glycated; in the bottom is represent the spectra of leptin glycated (leptin-MGO).

Considering the results obtained from the analysis of *in vitro* MGO-treated leptin, there is a net shift to the right (and therefore an increase in mass) of the signal when compared with the control sample; moreover, the peak coming from leptin-MGO results to have a value of FWHM greater than the peak resulting from the non-glycated leptin and the broader shape of the peak demonstrates that have formed a plethora of glycated proteins. The comparison between the two spectra showed that the glycated leptin is a mixture of proteins with different glycation levels, as proven by the broad shape of the peak; the mass value given above must be considered as the mean. The mass difference between the measured value for the control leptin and the value of leptin-MGO divided by the mass of methylglyoxal dehydrated, indicate that an average of 15 molecules of methylglyoxal linked to leptin.

5. DISCUSSION & CONCLUSION

The cascade of pathological events triggered by advanced glycation end products could play a crucial role in the hyperglycemia-independent complications of diabetes. The main focus of our research was to study the effect of hyperglycemia on adipose tissue pathophysiology.
Little is known about effects of AGEs in adipose tissue and their role on adipogenesis and fat cell functionality, this work aimed to create an *in vitro* model able to recapitulate all the possible conditions that could be detected *in vivo* in obese diabetic subjects; namely, adipocytes deeply exposed to a glycation-inducing environment.

There are only a few data available in the literature studying the effects induced by glyco-oxidation either on preadipocytes or on adipocytes and describing their impact on the differentiation and proliferation. (143) In the vast majority of the cases, the glycating insult is supplied only for a short time window (e.g. 30min - 24/48h) which hardly can mimic the long-lasting in vivo exposure of adipose tissue cellular components to AGEs. Moreover, only one study made a comprehensive analysis of the effects on adipocytes exposed to a glucose concentration ranging from 0mM to 30mM.(144). The strength of our experimental protocol lies in the time period of exposure to the glycation-inducing environment during all the adipogenic process.

In order to investigate the effects due to or mimicking chronic hyperglycaemia, the following substances were tested: sugars, (as glucose, fructose, lactose, galactose and sucrose); the di-carbonyl organic compound MGO and a homemade BSA-MGO.
The sugars selected are supposed to have a causative role in the increasing rates of diabetes or diabetic-like changes, were tested to evaluate theirs *in vitro* activities against the glycation. (132-134) MGO was selected to be used in our experiments because of its elevation in the plasma of diabetic patients. (145, 146), (147).
Finally, albumin was selected because is the most abundant protein in the plasma (35-50 g/l) and has a quite long half-life which implies its high susceptibility for glycation. (148-153) Moreover, previous studies with [(125)I] AGEs-BSA showed that adipocytes have the ability to endocytose the BSA-AGE via CD36. (154) In addition, albumin's tertiary dimensional structure allows it to bind and transport quite diverse small size metabolites such as metal ions, fatty acids, bilirubin and small molecules. Because of these particular features albumin is involved in the pharmacokinetics of many drugs and a significant correlation exists between glycation-mediated changes in its biochemical and pharmacological properties and the variability in the drug response of diabetic patients (155) (151).

Glycation is a spontaneous process which induces several structural modifications, including an increase in total molecular weight, thus bringing to a significant impact on the physical and functional properties of proteins. The chemical kinetics of a glycating reaction depends on various factors: reagents concentration, temperature, physical states and surface areas of reactants, solvent and catalyst properties. Other authors tried to create *in vitro* AGEs using albumin, collagen, elastin, keratin and proteoglycan with fructose, glucose, ribose or other reducing sugars. (156) In the literature, there are conflicting reports concerning the protocols used for the preparation of BSA-AGEs and the mechanisms of glycation itself, leads to a great inconsistency in the characterization of the produced adducts. (120, 123, 148, 156-158).
In this work, several compounds of BSA-sugars and BSA-MGO were produced and subsequently checked in MS, before their use in cell culture. The relative spectra show that the most important effects are obtained with MGO, while in the same conditions fructose and glucose, produce a smaller effect on albumin glycation. Moreover, it is possible to argue that the kinetic of reaction depends on the concentration of the protein. In presence of an equal amount of sugar the greater the concentration of protein the greater is the glycation obtained. (fig. 4.2)
The BSA-MGO thus produced and then characterized was used in cell culture for mimic the *in vivo* diabetic condition.

Leptin, "the satiety hormone", is a mediator of long-term regulation of energy balance, suppressing the food intake and thereby inducing weight loss. Consider that in the diabetic subjects, the process of protein glycation is largely favored and that this process can modify the characteristic of proteins, we investigated the possibility that leptin could be glycated and thereby changing its biologic activity, contributing to the leptin resistance mechanisms.

Interesting, we were able to demonstrate that in the presence of MGO, leptin shows a mass shift (fig. 4.42) suggesting a probable glycation. We reached this results using the most favorable glycation condition, the same utilized to obtain glycated BSA (incubation with MGO 60mM for 3 weeks). The present study confirms the possibility that leptin is prone to undergo a non-enzymatic glycation. By contrast, leptin displays a short half-life and this reduces the possibility of its *in vivo* glycation, even if other proteins with a short half-life such as insulin, are prone to glycation. (58)

MS is an analytic technique with high specificity and widely used in highly qualified laboratories. In the clinical laboratory, its use has resulted in significant advancements in clinical pathology. The monitoring of HbA1c is usually employed for the assessment of the glycation levels present in a subject and provide valid information on the “glycation stress”. (123, 124). In order to detect possible new diagnostic biomarkers linked to the glucotoxicity, spectra of human AT were

analyzed in MS. The use of this high sensitive method has, in the downside, several disadvantages and technical challenges. Complexes that differ only marginally are extremely difficult to analyze in MS, because of overlapping charge states of the individual species. Moreover, many PTMs, both enzymatic or non-enzymatic, may be present simultaneously on the same protein; thus, the total mass increase of a modified protein will reflect the sum of all modifications. Moreover, AT entails some more technical difficulties, being very rich in lipids. In a complex mixture, it is impossible to recognize if the peak displacement is due to glycation or another PTM and to identify if a specific peak is due to a particular protein. For this reason, it could be required a multi-step analysis dividing the spectrum into small parts, in which specific range of protein dimension will be examined.

On the other hand, the use of E.L.I.S.A. immunoassay apparently demonstrates to be a better tool for quantifying the presence of AGEs in a whole lysate. Albeit, there are many doubts both about the specificity of the antibodies used due to the multiple and complex characteristic of AGEs used in the protocol of animal immunization. Furthermore, these composts might either lead to a generation or to an unmasking of epitopes. The highly immunogenic compound could be recognized as heterologous molecule inducing autoantibodies in diabetic patients. These autoantibodies can also react with the antibodies used in the immunoassay test resulting in a false negative result. (151)

5.1 Cell Culture

The quantification of several genes expressed in 3T3-L1 and human adipocytes grow-up in different condition was then performed. In 3T3-L1, no significant differences were observed in *Pparγ* expression; whereas slight significant change for *Lpl*, *Glut4* and *Glo1* were detected.
Chen et al. in 2012 (143) demonstrates a double-sided feature of AGEs-RAGE axis in 3T3-L1 senescent cells (specifically, passage 15th). AGEs-RAGE could modulate the effects of senescence-induced by p53 in adipocytes, restoring the impaired adipogenic potential of the aged AT. In this project, 3T3-L1 cells were used always after the 15th culture cycle, but no problems with the adipogenic differentiation, nor in the control condition nor in the BSA-MGO treatment emerged. However, it is possible to note in gene expression analyses, that the exposure either to MGO or to BSA-MGO seems to increase the expression of the *Lpl* leading to assume a possible improvement of the adipogenic potential. (fig. 4.9) A decreased expression and activity of GLO1 both in endothelial and neuronal cells, implying the inhibition of the cellular defenses, has been associated with the activation of AGEs-RAGE axis. (69, 94) (54, 76, 93, 159, 160). Our results, agree

with this evidences, suggesting that the activation of AGEs-RAGE axis probably could impair the anti-oxidative protections also in AT. The increased expression of *IL6* observed in human adipocytes chronically exposed to MGO, partially confirm these suggestions.
In contrast, in short-term (48h) treated cells there we did not find any increase in the gene expression. (fig. 4.29; fig. 4.30)

Several studies have evaluated the effects of GLP1 or GLP1 analogs on adipocytes aiming to use them for therapeutic purposes. GLP1 treatment of 3T3-L1, resulted in the increase in lipid accumulation, as assessed by measuring the size and the number of droplets, and the expression of adipocyte-specific markers. (105, 106, 109) Nevertheless, in literature, there is not so clear evidence for the presence or the absence of GLP1 receptor in adipocytes.

This issue was examined, firstly by setting up a reliable qPCR and to look at the specific localization of the expressed gene in a specific cell compartment which is: the fully differentiated fat cells of the stromal-vascular fraction of human AT and in adipocyte cell lines. The *Glp1r* gene expression results negligible in the 3T3-L1 adipocytes; while, in the human fully differentiated adipocytes, albeit present at very low levels, it displays a slight even if not statistically significant increase when the cells were exposed to a glycation-inducing environment (fig. 4.29; 4.30). All these results lead to suggest that the presence of a functioning GLP1R in AT still remains to be fully ascertained, they lead also to suppose that the gene could be up-regulated only in condition in which a dysfunctional AT arise as a result of the chronic exposure to hyperglycaemia inducing fat cell insulin resistance.

Despite the weakness of any conclusion based on the results obtained with qPCR, protein detection by IF analysis in 3T3-L1 (fig. 4.14) clearly showed the presence of GLP1R in this cell line. Comparison of the immunostaining of adipocytes exposed during differentiation to different conditions allowed to observe a more intense fluorescence in adipocytes exposed to BSA-MGO. These still preliminary results are the proof of concept for a more detailed investigation on the presence and the role of GLP1R in adipocytes.
Another controversial aspect is the presence of RAGE and conflicting results have been obtained by IF and gene expression. The quantification of *RAGE* expression is quite challenging because of the presence of more than 20 different isoforms (fig. 1.10) (82). In particular, our primers were directed for the *RAGE Tv.1* (Transcript variant 1) the full-length and most abundant isoform. Conversely, the antibodies (ab135513) were specific for the N-terminal extracellular region of the receptor characterized by many splicing isoforms. For this reason, it is possible to hypothesize that a glycation-inducing environment could change the relative abundance of the different isoforms.

Our particular glycation-inducing conditions were able to induce an increased *Glut4* expression in murine adipocytes. BSA-MGO treated adipocytes shown also a decreased insulin sensitivity. On the other hand, adipocytes chronically kept in MGO gave a result comparable to the controls.

Previous studies on L6 myoblasts have demonstrated that an incubation with MGO could affect GLUT4 trafficking, resulting in a higher translocation of the transporter from the intracellular compartment to the plasmatic membrane, as well a reduction of its internalization. (139, 161, 162), (163) In fully differentiated 3T3-L1 adipocytes the greater the MGO concentration the greater the *Glut4* gene expression. Glucose uptake in adipocytes chronically exposed to MGO was slightly increased in comparison to controls. On the contrary, adipocytes chronically exposed to BSA-MGO show a significantly lower uptake, revealing that the glycation-inducing environment could induce an insulin resistance state. Subsequently, to localize GLUT4 both in basal condition and after insulin stimulus IF staining was performed, focusing on the possible alterations of the trafficking of the glucose transporter. Furthermore, to investigate if AGEs may directly interfere with the trafficking of GLUT4, a co-staining for AGEs and GLUT4 were performed in order to verify the hypothesis that glycation of GLUT4 could result in a functional impairment, because of the well-known effect of glycation on both structure and protein function. Despite a co-localization of the two proteins have been found, further investigations with co-immunoprecipitation and cell membranes fractionating are mandatory to confirm these interesting suggestions.

5.2 HUMAN TISSUES

Lipidome analysis revealed an obesity-related specific signature in both subcutaneous and visceral adipose tissue depots. (164) The expansion of AT in response to a positive energy balance is challenging for adipocytes in the maintenance of membrane integrity and functionality. The growth and the enlargement of adipocytes requires that more phospholipids have to be incorporated into cell membranes. The lipid metabolism and the immune response are highly integrated; indeed, the accumulation of harmful lipids may interfere with the immune regulation in multiple tissues, causing a vicious cycle of immune-metabolic dysregulation. The tight correlation between glucose metabolism, inflammation, FFA and metabolic syndrome is well known. (165, 166)(167)(31, 168)(169) A selective enrichment of specific triglycerides, glycerol-phospholipids, and sphingolipids in the AT of obese subjects were observed. In the particular case of acquired obesity, an increased proportion of palmitoleic and arachidonic acids in AT was discovered. (164, 170) Thus, the relative proportion of 71 lipid species ranging from 300Da to

1100Da was enquired, focusing the attention on the difference between obese normoglycaemic and obese diabetic. The most intriguing lipid is the *m/z* 881.781, seemingly a triglyceride POO (C52:2), that seems increased in AT of obese diabetic subjects. At present, we do not know whether and how, the lipids composition might be influenced by a glycation-inducing environment. Moreover what could be the functional aspects of these modified in cell lipids remains to be discovered.

It was thought that among the pathological alterations present in the AT of obese subjects with T2DM those related to chronic exposure to a glycation-inducing environment could be a great importance in the development of the so-called adiposophaty. In order to investigate these aspects, the expression of *GLP1, RAGE, DPP4* and *LEP* in SAT and VAT of 64 patients were collected. Obese diabetic subjects were all treated with metformin, a well-known first line anti-hyperglycaemic agent mostly acting on hepatic glucose production and increasing glucose utilization. Metformin activates AMP-activated protein kinase which is a major cellular regulator of lipid and glucose metabolism. Moreover, metformin induces GLP1 release from intestinal L cells, and also GLP-1R expression on pancreatic β-cells, is associated with amelioration of low-grade tissue inflammation in the adipose tissue of obese animals. (171) In addition, previous studies indicate that it could dose-dependently inhibit the AGEs-induced apoptosis and the inflammatory and fibrotic reactions in tubular cells probably by reducing ROS generation via down-regulation of *RAGE* expression through AMP-activated protein kinase activation. (172-174) Metformin could also reduce leptin level in morbidly obese individuals and this fact has been proven in several studies, suggesting that the, even small, anorectic effects of metformin could be potentially mediated via an increase in the central sensitivity to leptin. (175, 176) At the contrary, others studies have shown opposite results. (177)
Our results (fig. 4.39) lead to hypothesize that a glycation-inducing environment, in particular in VAT, could result in a stimulation of leptin gene expression. This effect could be observed very early in the progression from obesity to diabetes and starting from the condition of prediabetes. In metformin-treated obese diabetic patients, the effect of glycation on leptin could be dampened by the pharmacological action of the drug. The increased expression of leptin, a common feature in obesity, could be further increased through a glycation-inducing environment thereby prompting the already present leptin resistance.

Using the western blot analysis (fig. 4.34) we were able to confirm the presence of AGEs whiting AT. These products can crosslink with both intracellular and extracellular proteins inducing dysfunction. Moreover, binding to their receptor can prompt the expression of *RAGE* itself. (76, 80, 178). On the basis of our experimental evidence, it is possible to suggest that although the

slight increase of *RAGE* expression begins in VAT starting from the pre-diabetic condition and that, metformin could limit this upward trend. SAT, on the other hand, shows a great increase only in the obese diabetic patients (fig. 4.39) leading to suggest that this depot could be less susceptible than VAT to the glycation-inducing environmental. This is the reason why the rising of *RAGE* expression is delayed.

In literature, has also been reported that metformin can increase the *GLP-1R* expression on islet cells (171), but so far no data are available about the effects of metformin on *GLP1R* expression in AT. In VAT of treated-obese patients, a significant increased *GLP1R* expression was detected. (fig. 4.39) Our experimental conditions do not allow to distinguish if VAT *GLP1R* expression is due to the glycation-inducing environment or to metformin therapy. However, our data performed on 3T3-L1 (fig. 4.14) strongly suggest that the glycation-inducing environmental could be the cause of the increased *GLP1R* expression. Further studies are needed to clarify this open question.

DPP4 is an enzyme that inactivates GLP1. The levels of GLP1 can be enhanced for their beneficial effects by inhibiting the action of DPP4 through a DPP4 inhibitor, resulting in enhanced levels of endogenous secretion of GLP1. Previous studies (179, 180) revealed that serum levels of DPP4 are independently associated with various metabolic parameters and that AGEs could up-regulate its expression. On the contrary, in our analyses, the expression of *DPP4* does not seem to be impaired either by glycation-inducing-environment nor by treatment with metformin. However, a considerable difference between the SAT and VAT depots can be observed, confirming that VAT consistently displays a higher expression than SAT. (181)

6. BIBLIOGRAPHY

1. Rosen ED, Spiegelman BM. What we talk about when we talk about fat. Cell. 2014;156(1-2):20-44.
2. Giralt M, Villarroya F. White, brown, beige/brite: different adipose cells for different functions? Endocrinology. 2013;154(9):2992-3000.
3. Kwok KH, Lam KS, Xu A. Heterogeneity of white adipose tissue: molecular basis and clinical implications. Experimental & molecular medicine. 2016;48:e215.
4. Ibrahim MM. Subcutaneous and visceral adipose tissue: structural and functional differences. Obesity reviews : an official journal of the International Association for the Study of Obesity. 2010;11(1):11-8.
5. Bjorndal B, Burri L, Staalesen V, Skorve J, Berge RK. Different adipose depots: their role in the development of metabolic syndrome and mitochondrial response to hypolipidemic agents. Journal of obesity. 2011;2011:490650.
6. Nedergaard J, Bengtsson T, Cannon B. Unexpected evidence for active brown adipose tissue in adult humans. American journal of physiology Endocrinology and metabolism. 2007;293(2):E444-52.
7. Cousin B, Cinti S, Morroni M, Raimbault S, Ricquier D, Penicaud L, et al. Occurrence of brown adipocytes in rat white adipose tissue: molecular and morphological characterization. Journal of cell science. 1992;103 (Pt 4):931-42.
8. Wu J, Bostrom P, Sparks LM, Ye L, Choi JH, Giang AH, et al. Beige adipocytes are a distinct type of thermogenic fat cell in mouse and human. Cell. 2012;150(2):366-76.
9. Giordano A, Smorlesi A, Frontini A, Barbatelli G, Cinti S. White, brown and pink adipocytes: the extraordinary plasticity of the adipose organ. European journal of endocrinology / European Federation of Endocrine Societies. 2014;170(5):R159-71.
10. International Diabetes Federation. IDF Diabetes Atlas Update Poster, 6th ed.; International Diabetes Federation: Brussels, Belgium, 2014.2014.
11. Catoi AF, Parvu A, Muresan A, Busetto L. Metabolic Mechanisms in Obesity and Type 2 Diabetes: Insights from Bariatric/Metabolic Surgery. Obesity facts. 2015;8(6):350-63.
12. Ligibel JA, Alfano CM, Courneya KS, Demark-Wahnefried W, Burger RA, Chlebowski RT, et al. American Society of Clinical Oncology position statement on obesity and cancer. Journal of clinical oncology : official journal of the American Society of Clinical Oncology. 2014;32(31):3568-74.
13. Furukawa S, Fujita T, Shimabukuro M, Iwaki M, Yamada Y, Nakajima Y, et al. Increased oxidative stress in obesity and its impact on metabolic syndrome. The Journal of clinical investigation. 2004;114(12):1752-61.
14. Xu H, Barnes GT, Yang Q, Tan G, Yang D, Chou CJ, et al. Chronic inflammation in fat plays a crucial role in the development of obesity-related insulin resistance. The Journal of clinical investigation. 2003;112(12):1821-30.
15. Fuentes E, Fuentes F, Vilahur G, Badimon L, Palomo I. Mechanisms of chronic state of inflammation as mediators that link obese adipose tissue and metabolic syndrome. Mediators of inflammation. 2013;2013:136584.
16. Perseghin G, Petersen K, Shulman GI. Cellular mechanism of insulin resistance: potential links with inflammation. International journal of obesity and related metabolic disorders : journal of the International Association for the Study of Obesity. 2003;27 Suppl 3:S6-11.
17. Ceolotto G, De Kreutzenberg SV, Cattelan A, Fabricio AS, Squarcina E, Gion M, et al. Sirtuin 1 stabilization by HuR represses TNF-alpha- and glucose-induced E-selectin release and endothelial cell adhesiveness in vitro: relevance to human metabolic syndrome. Clinical science (London, England : 1979). 2014;127(7):449-61.

18. Aguiari P, Leo S, Zavan B, Vindigni V, Rimessi A, Bianchi K, et al. High glucose induces adipogenic differentiation of muscle-derived stem cells. Proceedings of the National Academy of Sciences of the United States of America. 2008;105(4):1226-31.
19. Negre-Salvayre A, Salvayre R, Auge N, Pamplona R, Portero-Otin M. Hyperglycemia and glycation in diabetic complications. Antioxidants & redox signaling. 2009;11(12):3071-109.
20. Korsgren O, Jansson L, Sandler S, Andersson A. Hyperglycemia-induced B cell toxicity. The fate of pancreatic islets transplanted into diabetic mice is dependent on their genetic background. The Journal of clinical investigation. 1990;86(6):2161-8.
21. Jin Y, Wang G, Han SS, He MY, Cheng X, Ma ZL, et al. Effects of oxidative stress on hyperglycaemia-induced brain malformations in a diabetes mouse model. Experimental cell research. 2016;347(1):201-11.
22. Lang J. Molecular mechanisms and regulation of insulin exocytosis as a paradigm of endocrine secretion. European journal of biochemistry / FEBS. 1999;259(1-2):3-17.
23. Takahashi A, Nagashima K, Hamasaki A, Kuwamura N, Kawasaki Y, Ikeda H, et al. Sulfonylurea and glinide reduce insulin content, functional expression of K(ATP) channels, and accelerate apoptotic beta-cell death in the chronic phase. Diabetes research and clinical practice. 2007;77(3):343-50.
24. De Beer K, Michael S, Thacker M, Wynne E, Pattni C, Gomm M, et al. Diabetic ketoacidosis and hyperglycaemic hyperosmolar syndrome - clinical guidelines. Nursing in critical care. 2008;13(1):5-11.
25. Polonsky KS. The past 200 years in diabetes. The New England journal of medicine. 2012;367(14):1332-40.
26. Accardi G, Caruso C, Colonna-Romano G, Camarda C, Monastero R, Candore G. Can Alzheimer disease be a form of type 3 diabetes? Rejuvenation research. 2012;15(2):217-21.
27. Amutha A, Mohan V. Diabetes complications in childhood and adolescent onset type 2 diabetes-a review. Journal of diabetes and its complications. 2016;30(5):951-7.
28. Sivitz WI. Lipotoxicity and glucotoxicity in type 2 diabetes. Postgraduate medicine. 2015;109(4):55-64.
29. Zheng H, Wu J, Jin Z, Yan LJ. Protein Modifications as Manifestations of Hyperglycemic Glucotoxicity in Diabetes and Its Complications. Biochem Insights. 2016;9:1-9.
30. Luo X, Li R, Yan LJ. Roles of Pyruvate, NADH, and Mitochondrial Complex I in Redox Balance and Imbalance in beta Cell Function and Dysfunction. Journal of diabetes research. 2015;2015:512618.
31. Erikci Ertunc M, Hotamisligil GS. Lipid signaling and lipotoxicity in metabolic inflammation: indications for metabolic disease pathogenesis and treatment. Journal of lipid research. 2016.
32. van de Weijer T, Schrauwen-Hinderling VB, Schrauwen P. Lipotoxicity in type 2 diabetic cardiomyopathy. Cardiovascular research. 2011;92(1):10-8.
33. Kuo M, Zilberfarb V, Gangneux N, Christeff N, Issad T. O-GlcNAc modification of FoxO1 increases its transcriptional activity: a role in the glucotoxicity phenomenon? Biochimie. 2008;90(5):679-85.
34. Prasad K, Dhar I, Caspar-Bell G. Role of Advanced Glycation End Products and Its Receptors in the Pathogenesis of Cigarette Smoke-Induced Cardiovascular Disease. The International journal of angiology : official publication of the International College of Angiology, Inc. 2015;24(2):75-80.
35. R. Singh AB, T. Mori, L. Beilin. Advanced glycation end-products: a review. Diabetologia. 2001;44:129-46.
36. Sharma C, Kaur A, Thind SS, Singh B, Raina S. Advanced glycation End-products (AGEs): an emerging concern for processed food industries. Journal of food science and technology. 2015;52(12):7561-76.
37. Uribarri J, Woodruff S, Goodman S, Cai W, Chen X, Pyzik R, et al. Advanced glycation end products in foods and a practical guide to their reduction in the diet. Journal of the American Dietetic Association. 2010;110(6):911-16.e12.

38. Uribarri J, Del Castillo MD, de la Maza MP, Filip R, Gugliucci A, Luevano-Contreras C, et al. Dietary Advanced Glycation End Products and Their Role in Health and Disease. Advances in nutrition (Bethesda, Md). 2015;6(4):461-73.
39. Vlassara H, Striker GE. Advanced glycation endproducts in diabetes and diabetic complications. Endocrinology and metabolism clinics of North America. 2013;42(4):697-719.
40. Thornalley PJ. Pharmacology of methylglyoxal: formation, modification of proteins and nucleic acids, and enzymatic detoxification--a role in pathogenesis and antiproliferative chemotherapy. General pharmacology. 1996;27(4):565-73.
41. Sampath C, Zhu Y, Sang S, Ahmedna M. Bioactive compounds isolated from apple, tea, and ginger protect against dicarbonyl induced stress in cultured human retinal epithelial cells. Phytomedicine : international journal of phytotherapy and phytopharmacology. 2016;23(2):200-13.
42. Yuan LJ, Qin Y, Wang L, Zeng Y, Chang H, Wang J, et al. Capsaicin-containing chili improved postprandial hyperglycemia, hyperinsulinemia, and fasting lipid disorders in women with gestational diabetes mellitus and lowered the incidence of large-for-gestational-age newborns. Clinical nutrition (Edinburgh, Scotland). 2016;35(2):388-93.
43. Lopez-Moreno J, Quintana-Navarro GM, Delgado-Lista J, Garcia-Rios A, Delgado-Casado N, Camargo A, et al. Mediterranean Diet Reduces Serum Advanced Glycation End Products and Increases Antioxidant Defenses in Elderly Adults: A Randomized Controlled Trial. Journal of the American Geriatrics Society. 2016;64(4):901-4.
44. Zhang Q, Ames JM, Smith RD, Baynes JW, Metz TO. A perspective on the Maillard reaction and the analysis of protein glycation by mass spectrometry: probing the pathogenesis of chronic disease. Journal of proteome research. 2009;8(2):754-69.
45. Munch G, Schicktanz D, Behme A, Gerlach M, Riederer P, Palm D, et al. Amino acid specificity of glycation and protein-AGE crosslinking reactivities determined with a dipeptide SPOT library. Nature biotechnology. 1999;17(10):1006-10.
46. Rabbani N, Thornalley PJ. Glycation research in amino acids: a place to call home. Amino acids. 2012;42(4):1087-96.
47. Buetler TM, Leclerc E, Baumeyer A, Latado H, Newell J, Adolfsson O, et al. N(epsilon)-carboxymethyllysine-modified proteins are unable to bind to RAGE and activate an inflammatory response. Molecular nutrition & food research. 2008;52(3):370-8.
48. Takahashi K. Further studies on the reactions of phenylglyoxal and related reagents with proteins. Journal of biochemistry. 1977;81(2):403-14.
49. Semchyshyn HM. Reactive carbonyl species in vivo: generation and dual biological effects. TheScientificWorldJournal. 2014;2014:417842.
50. Thornalley PJ, Rabbani N. Detection of oxidized and glycated proteins in clinical samples using mass spectrometry--a user's perspective. Biochimica et biophysica acta. 2014;1840(2):818-29.
51. Gregersen PBaN. Protein misfolding and disease: Principles and protocols. Protein Science, Human Press. 2004;13(6):1704-5.
52. Ceriello A. The emerging challenge in diabetes: the "metabolic memory". Vascular pharmacology. 2012;57(5-6):133-8.
53. Chilelli NC, Burlina S, Lapolla A. AGEs, rather than hyperglycemia, are responsible for microvascular complications in diabetes: a "glycoxidation-centric" point of view. Nutrition, metabolism, and cardiovascular diseases : NMCD. 2013;23(10):913-9.
54. Ramasamy R, Yan SF, Schmidt AM. Receptor for AGE (RAGE): signaling mechanisms in the pathogenesis of diabetes and its complications. Annals of the New York Academy of Sciences. 2011;1243:88-102.
55. Wendt T, Tanji N, Guo J, Hudson BI, Bierhaus A, Ramasamy R, et al. Glucose, glycation, and RAGE: implications for amplification of cellular dysfunction in diabetic nephropathy. Journal of the American Society of Nephrology : JASN. 2003;14(5):1383-95.

56. Yamagishi S. Role of advanced glycation end products (AGEs) and receptor for AGEs (RAGE) in vascular damage in diabetes. Experimental gerontology. 2011;46(4):217-24.
57. Yamagishi S, Nakamura N, Suematsu M, Kaseda K, Matsui T. Advanced Glycation End Products: A Molecular Target for Vascular Complications in Diabetes. Molecular medicine (Cambridge, Mass). 2015;21 Suppl 1:S32-40.
58. Hunter SJ, Boyd AC, O'Harte FP, McKillop AM, Wiggam MI, Mooney MH, et al. Demonstration of glycated insulin in human diabetic plasma and decreased biological activity assessed by euglycemic-hyperinsulinemic clamp technique in humans. Diabetes. 2003;52(2):492-8.
59. Chikazawa M, Otaki N, Shibata T, Miyashita H, Kawai Y, Maruyama S, et al. Multispecificity of immunoglobulin M antibodies raised against advanced glycation end products: involvement of electronegative potential of antigens. The Journal of biological chemistry. 2013;288(19):13204-14.
60. Li XH, Du LL, Cheng XS, Jiang X, Zhang Y, Lv BL, et al. Glycation exacerbates the neuronal toxicity of beta-amyloid. Cell death & disease. 2013;4:e673.
61. Cai W, Uribarri J, Zhu L, Chen X, Swamy S, Zhao Z, et al. Oral glycotoxins are a modifiable cause of dementia and the metabolic syndrome in mice and humans. Proceedings of the National Academy of Sciences of the United States of America. 2014;111(13):4940-5.
62. Juranek J, Ray R, Banach M, Rai V. Receptor for advanced glycation end-products in neurodegenerative diseases. Reviews in the neurosciences. 2015.
63. Pugliese G. Do advanced glycation end products contribute to the development of long-term diabetic complications? Nutrition, metabolism, and cardiovascular diseases : NMCD. 2008;18(7):457-60.
64. Dion Foster LS, Katherine R. Walter, Lourdes M. Nogueira, Hleb Fedarovich, Ryan Y. Turner,, Mahtabuddin Ahmed JDS, Marvella E. Ford, Victoria J. Findlay, and David P. Turner. AGE Metabolites: A Biomarker Linked to Cancer Disparity? Cancer epidemiology, biomarkers & prevention : a publication of the American Association for Cancer Research, cosponsored by the American Society of Preventive Oncology. 2014;23(10):7.
65. Maritim AC, Sanders RA, Watkins JB, 3rd. Diabetes, oxidative stress, and antioxidants: a review. Journal of biochemical and molecular toxicology. 2003;17(1):24-38.
66. Stig B, Hajdu N. [Endproducts and receptors of advanced glycation and lipoxidation (AGE, ALE, RAGE) and chronic diseases from the perspective of food and nutrition]. Orvosi hetilap. 2008;149(17):771-8.
67. Reddy MA, Zhang E, Natarajan R. Epigenetic mechanisms in diabetic complications and metabolic memory. Diabetologia. 2015;58(3):443-55.
68. Falone S, D'Alessandro A, Mirabilio A, Petruccelli G, Cacchio M, Di Ilio C, et al. Long term running biphasically improves methylglyoxal-related metabolism, redox homeostasis and neurotrophic support within adult mouse brain cortex. PloS one. 2012;7(2):e31401.
69. Gaens KH, Stehouwer CD, Schalkwijk CG. Advanced glycation endproducts and its receptor for advanced glycation endproducts in obesity. Current opinion in lipidology. 2013;24(1):4-11.
70. Nowotny K, Jung T, Hohn A, Weber D, Grune T. Advanced glycation end products and oxidative stress in type 2 diabetes mellitus. Biomolecules. 2015;5(1):194-222.
71. Nogueiras R, Habegger KM, Chaudhary N, Finan B, Banks AS, Dietrich MO, et al. Sirtuin 1 and sirtuin 3: physiological modulators of metabolism. Physiological reviews. 2012;92(3):1479-514.
72. Rajan S, Shankar K, Beg M, Varshney S, Gupta A, Srivastava A, et al. Chronic hyperinsulinemia reduces insulin sensitivity and metabolic functions of brown adipocyte. The Journal of endocrinology. 2016;230(3):275-90.
73. Yao D, Brownlee M. Hyperglycemia-induced reactive oxygen species increase expression of the receptor for advanced glycation end products (RAGE) and RAGE ligands. Diabetes. 2010;59(1):249-55.
74. Talukdar D, Chaudhuri BS, Ray M, Ray S. Critical evaluation of toxic versus beneficial effects of methylglyoxal. Biochemistry Biokhimiia. 2009;74(10):1059-69.

75. Gawlowski T, Stratmann B, Stirban AO, Negrean M, Tschoepe D. AGEs and methylglyoxal induce apoptosis and expression of Mac-1 on neutrophils resulting in platelet-neutrophil aggregation. Thrombosis research. 2007;121(1):117-26.
76. Ott C, Jacobs K, Haucke E, Navarrete Santos A, Grune T, Simm A. Role of advanced glycation end products in cellular signaling. Redox biology. 2014;2:411-29.
77. Li YM, Tan AX, Vlassara H. Antibacterial activity of lysozyme and lactoferrin is inhibited by binding of advanced glycation-modified proteins to a conserved motif. Nature medicine. 1995;1(10):1057-61.
78. Neeper M, Schmidt AM, Brett J, Yan SD, Wang F, Pan YC, et al. Cloning and expression of a cell surface receptor for advanced glycosylation end products of proteins. The Journal of biological chemistry. 1992;267(21):14998-5004.
79. Lizotte PP, Hanford LE, Enghild JJ, Nozik-Grayck E, Giles BL, Oury TD. Developmental expression of the receptor for advanced glycation end-products (RAGE) and its response to hyperoxia in the neonatal rat lung. BMC developmental biology. 2007;7:15.
80. Kierdorf K, Fritz G. RAGE regulation and signaling in inflammation and beyond. Journal of leukocyte biology. 2013;94(1):55-68.
81. Chen Y, Akirav EM, Chen W, Henegariu O, Moser B, Desai D, et al. RAGE ligation affects T cell activation and controls T cell differentiation. Journal of immunology (Baltimore, Md : 1950). 2008;181(6):4272-8.
82. Lopez-Diez R, Rastrojo A, Villate O, Aguado B. Complex tissue-specific patterns and distribution of multiple RAGE splice variants in different mammals. Genome biology and evolution. 2013;5(12):2420-35.
83. Hudson BI, Carter AM, Harja E, Kalea AZ, Arriero M, Yang H, et al. Identification, classification, and expression of RAGE gene splice variants. FASEB journal : official publication of the Federation of American Societies for Experimental Biology. 2008;22(5):1572-80.
84. Kalea AZ, Schmidt AM, Hudson BI. Alternative splicing of RAGE: roles in biology and disease. Frontiers in bioscience (Landmark edition). 2011;16:2756-70.
85. Koch M, Chitayat S, Dattilo BM, Schiefner A, Diez J, Chazin WJ, et al. Structural basis for ligand recognition and activation of RAGE. Structure (London, England : 1993). 2010;18(10):1342-52.
86. Goldin A, Beckman JA, Schmidt AM, Creager MA. Advanced glycation end products: sparking the development of diabetic vascular injury. Circulation. 2006;114(6):597-605.
87. Riehl A, Nemeth J, Angel P, Hess J. The receptor RAGE: Bridging inflammation and cancer. Cell communication and signaling : CCS. 2009;7:12.
88. Fritz G. RAGE: a single receptor fits multiple ligands. Trends in biochemical sciences. 2011;36(12):625-32.
89. Park H, Adsit FG, Boyington JC. The 1.5 A crystal structure of human receptor for advanced glycation endproducts (RAGE) ectodomains reveals unique features determining ligand binding. The Journal of biological chemistry. 2010;285(52):40762-70.
90. Ishibashi T, Kawaguchi M, Sugimoto K, Uekita H, Sakamoto N, Yokoyama K, et al. Advanced glycation end product-mediated matrix metallo-proteinase-9 and apoptosis via renin-angiotensin system in type 2 diabetes. Journal of atherosclerosis and thrombosis. 2010;17(6):578-89.
91. Fukami K, Taguchi K, Yamagishi S, Okuda S. Receptor for advanced glycation endproducts and progressive kidney disease. Current opinion in nephrology and hypertension. 2015;24(1):54-60.
92. Soro-Paavonen A, Watson AM, Li J, Paavonen K, Koitka A, Calkin AC, et al. Receptor for advanced glycation end products (RAGE) deficiency attenuates the development of atherosclerosis in diabetes. Diabetes. 2008;57(9):2461-9.
93. Ramasamy R, Vannucci SJ, Yan SS, Herold K, Yan SF, Schmidt AM. Advanced glycation end products and RAGE: a common thread in aging, diabetes, neurodegeneration, and inflammation. Glycobiology. 2005;15(7):16r-28r.

94. Bierhaus A, Nawroth PP. Multiple levels of regulation determine the role of the receptor for AGE (RAGE) as common soil in inflammation, immune responses and diabetes mellitus and its complications. Diabetologia. 2009;52(11):2251-63.
95. Kislinger T, Tanji N, Wendt T, Qu W, Lu Y, Ferran LJ, Jr., et al. Receptor for advanced glycation end products mediates inflammation and enhanced expression of tissue factor in vasculature of diabetic apolipoprotein E-null mice. Arteriosclerosis, thrombosis, and vascular biology. 2001;21(6):905-10.
96. Song F, Hurtado del Pozo C, Rosario R, Zou YS, Ananthakrishnan R, Xu X, et al. RAGE regulates the metabolic and inflammatory response to high-fat feeding in mice. Diabetes. 2014;63(6):1948-65.
97. Piperi C, Goumenos A, Adamopoulos C, Papavassiliou AG. AGE/RAGE signalling regulation by miRNAs: Associations with diabetic complications and therapeutic potential. The international journal of biochemistry & cell biology. 2015;60c:197-201.
98. Rohrborn D, Wronkowitz N, Eckel J. DPP4 in Diabetes. Frontiers in immunology. 2015;6:386.
99. Baggio LL, Drucker DJ. Biology of incretins: GLP-1 and GIP. Gastroenterology. 2007;132(6):2131-57.
100. Drucker DJ. The biology of incretin hormones. Cell metabolism. 2006;3(3):153-65.
101. Gromada J, Ding WG, Barg S, Renstrom E, Rorsman P. Multisite regulation of insulin secretion by cAMP-increasing agonists: evidence that glucagon-like peptide 1 and glucagon act via distinct receptors. Pflugers Archiv : European journal of physiology. 1997;434(5):515-24.
102. Perfetti R, Merkel P. Glucagon-like peptide-1: a major regulator of pancreatic beta-cell function. European journal of endocrinology / European Federation of Endocrine Societies. 2000;143(6):717-25.
103. Wang Y, Kole HK, Montrose-Rafizadeh C, Perfetti R, Bernier M, Egan JM. Regulation of glucose transporters and hexose uptake in 3T3-L1 adipocytes: glucagon-like peptide-1 and insulin interactions. Journal of molecular endocrinology. 1997;19(3):241-8.
104. Joao AL, Reis F, Fernandes R. The incretin system ABCs in obesity and diabetes - novel therapeutic strategies for weight loss and beyond. Obesity reviews : an official journal of the International Association for the Study of Obesity. 2016;17(7):553-72.
105. Yang J, Ren J, Song J, Liu F, Wu C, Wang X, et al. Glucagon-like peptide 1 regulates adipogenesis in 3T3-L1 preadipocytes. International journal of molecular medicine. 2013;31(6):1429-35.
106. Challa TD, Beaton N, Arnold M, Rudofsky G, Langhans W, Wolfrum C. Regulation of adipocyte formation by GLP-1/GLP-1R signaling. The Journal of biological chemistry. 2012;287(9):6421-30.
107. Vendrell J, El Bekay R, Peral B, Garcia-Fuentes E, Megia A, Macias-Gonzalez M, et al. Study of the potential association of adipose tissue GLP-1 receptor with obesity and insulin resistance. Endocrinology. 2011;152(11):4072-9.
108. Yamagishi S, Fukami K, Matsui T. Crosstalk between advanced glycation end products (AGEs)-receptor RAGE axis and dipeptidyl peptidase-4-incretin system in diabetic vascular complications. Cardiovascular diabetology. 2015;14:2.
109. Donnelly D. The structure and function of the glucagon-like peptide-1 receptor and its ligands. British journal of pharmacology. 2012;166(1):27-41.
110. Gupta V. Glucagon-like peptide-1 analogues: An overview. Indian journal of endocrinology and metabolism. 2013;17(3):413-21.
111. Hansen L, Deacon CF, Orskov C, Holst JJ. Glucagon-like peptide-1-(7-36)amide is transformed to glucagon-like peptide-1-(9-36)amide by dipeptidyl peptidase IV in the capillaries supplying the L cells of the porcine intestine. Endocrinology. 1999;140(11):5356-63.
112. Das SS, Hayashi H, Sato T, Yamada R, Hiratsuka M, Hirasawa N. Regulation of dipeptidyl peptidase 4 production in adipocytes by glucose. Diabetes, metabolic syndrome and obesity : targets and therapy. 2014;7:185-94.

113. Zillessen P, Celner J, Kretschmann A, Pfeifer A, Racke K, Mayer P. Metabolic role of dipeptidyl peptidase 4 (DPP4) in primary human (pre)adipocytes. Scientific reports. 2016;6:23074.
114. Tomkin GH. Treatment of type 2 diabetes, lifestyle, GLP1 agonists and DPP4 inhibitors. World journal of diabetes. 2014;5(5):636-50.
115. Ishibashi Y, Matsui T, Maeda S, Higashimoto Y, Yamagishi S. Advanced glycation end products evoke endothelial cell damage by stimulating soluble dipeptidyl peptidase-4 production and its interaction with mannose 6-phosphate/insulin-like growth factor II receptor. Cardiovascular diabetology. 2013;12:125.
116. Edmond de Hoffmann VS. Mass Spectrometry: Principles and Applications: Wiley; 2007. 1-485 p.
117. Hoffmann ESV. <Mass Spectrometry, principles and application_De Hoffman.pdf>. 2007.
118. Kislinger T, Humeny A, Pischetsrieder M. Analysis of protein glycation products by matrix-assisted laser desorption ionization time-of-flight mass spectrometry. Current medicinal chemistry. 2004;11(16):2185-93.
119. Stoeckli M, Chaurand P, Hallahan DE, Caprioli RM. Imaging mass spectrometry: a new technology for the analysis of protein expression in mammalian tissues. Nature medicine. 2001;7(4):493-6.
120. Wa C, Cerny RL, Clarke WA, Hage DS. Characterization of glycation adducts on human serum albumin by matrix-assisted laser desorption/ionization time-of-flight mass spectrometry. Clinica chimica acta; international journal of clinical chemistry. 2007;385(1-2):48-60.
121. van Duijn E. Current limitations in native mass spectrometry based structural biology. J Am Soc Mass Spectrom. 2010;21(6):971-8.
122. Rabbani N, Ashour A, Thornalley PJ. Mass spectrometric determination of early and advanced glycation in biology. Glycoconjugate journal. 2016;33(4):553-68.
123. Lapolla A, Fedele D, Reitano R, Arico NC, Seraglia R, Traldi P, et al. Enzymatic digestion and mass spectrometry in the study of advanced glycation end products/peptides. J Am Soc Mass Spectrom. 2004;15(4):496-509.
124. Lapolla A, Molin L, Traldi P. Protein glycation in diabetes as determined by mass spectrometry. International journal of endocrinology. 2013;2013:412103.
125. Roverso M, Lapolla A, Cosma C, Seraglia R, Galvan E, Visentin S, et al. Some preliminary matrix-assisted laser desorption/ionization imaging experiments on maternal and fetal sides of human placenta. Eur J Mass Spectrom (Chichester, Eng). 2014;20(3):261-9.
126. Hattan SJ, Parker KC, Vestal ML, Yang JY, Herold DA, Duncan MW. Analysis and Quantitation of Glycated Hemoglobin by Matrix Assisted Laser Desorption/Ionization Time of Flight Mass Spectrometry. J Am Soc Mass Spectrom. 2016;27(3):532-41.
127. Zimmerlin L, Donnenberg VS, Pfeifer ME, Meyer EM, Peault B, Rubin JP, et al. Stromal vascular progenitors in adult human adipose tissue. Cytometry Part A : the journal of the International Society for Analytical Cytology. 2010;77(1):22-30.
128. Lequin RM. Enzyme immunoassay (EIA)/enzyme-linked immunosorbent assay (ELISA). Clinical chemistry. 2005;51(12):2415-8.
129. Schuurs AH, van Weemen BK. Enzyme-immunoassay: a powerful analytical tool. Journal of immunoassay. 1980;1(2):229-49.
130. Morten Bo Johansen LKaSB. Analysis and prediction of mammalian protein glycation. Glycobiology. 2006;16(9):844-53.
131. Pundir S, Martin MJ, O'Donovan C. UniProt Tools. Current protocols in bioinformatics / editoral board, Andreas D Baxevanis [et al]. 2016;53:1.29.1-15.
132. White JS. Challenging the fructose hypothesis: new perspectives on fructose consumption and metabolism. Advances in nutrition (Bethesda, Md). 2013;4(2):246-56.
133. Raynor E, Robison WG, Garrett CG, McGuirt WT, Pillsbury HC, Prazma J. Consumption of a high-galactose diet induces diabetic-like changes in the inner ear. Otolaryngology--head and neck

surgery : official journal of American Academy of Otolaryngology-Head and Neck Surgery. 1995;113(6):748-54.
134. Szkudlarek A, Maciazek-Jurczyk M, Chudzik M, Rownicka-Zubik J, Sulkowska A. Alteration of human serum albumin tertiary structure induced by glycation. Spectroscopic study. Spectrochimica acta Part A, Molecular and biomolecular spectroscopy. 2015;153:560-5.
135. Cantero AV, Portero-Otin M, Ayala V, Auge N, Sanson M, Elbaz M, et al. Methylglyoxal induces advanced glycation end product (AGEs) formation and dysfunction of PDGF receptor-beta: implications for diabetic atherosclerosis. FASEB journal : official publication of the Federation of American Societies for Experimental Biology. 2007;21(12):3096-106.
136. Kuniyasu H, Oue N, Wakikawa A, Shigeishi H, Matsutani N, Kuraoka K, et al. Expression of receptors for advanced glycation end-products (RAGE) is closely associated with the invasive and metastatic activity of gastric cancer. The Journal of pathology. 2002;196(2):163-70.
137. Gupta NA, Mells J, Dunham RM, Grakoui A, Handy J, Saxena NK, et al. Glucagon-like peptide-1 receptor is present on human hepatocytes and has a direct role in decreasing hepatic steatosis in vitro by modulating elements of the insulin signaling pathway. Hepatology (Baltimore, Md). 2010;51(5):1584-92.
138. Perry T, Lahiri DK, Chen D, Zhou J, Shaw KT, Egan JM, et al. A novel neurotrophic property of glucagon-like peptide 1: a promoter of nerve growth factor-mediated differentiation in PC12 cells. The Journal of pharmacology and experimental therapeutics. 2002;300(3):958-66.
139. Engelbrecht B, Mattern Y, Scheibler S, Tschoepe D, Gawlowski T, Stratmann B. Methylglyoxal impairs GLUT4 trafficking and leads to increased glucose uptake in L6 myoblasts. Hormone and metabolic research = Hormon- und Stoffwechselforschung = Hormones et metabolisme. 2014;46(2):77-84.
140. Riboulet-Chavey A, Pierron A, Durand I, Murdaca J, Giudicelli J, Van Obberghen E. Methylglyoxal impairs the insulin signaling pathways independently of the formation of intracellular reactive oxygen species. Diabetes. 2006;55(5):1289-99.
141. Egan JM, Montrose-Rafizadeh C, Wang Y, Bernier M, Roth J. Glucagon-like peptide-1(7-36) amide (GLP-1) enhances insulin-stimulated glucose metabolism in 3T3-L1 adipocytes: one of several potential extrapancreatic sites of GLP-1 action. Endocrinology. 1994;135(5):2070-5.
142. Lapolla A, Fedele D, Seraglia R, Traldi P. The role of mass spectrometry in the study of non-enzymatic protein glycation in diabetes: an update. Mass spectrometry reviews. 2006;25(5):775-97.
143. Chen CY, Abell AM, Moon YS, Kim KH. An advanced glycation end product (AGE)-receptor for AGEs (RAGE) axis restores adipogenic potential of senescent preadipocytes through modulation of p53 protein function. The Journal of biological chemistry. 2012;287(53):44498-507.
144. Sabater D, Arriaran S, Romero Mdel M, Agnelli S, Remesar X, Fernandez-Lopez JA, et al. Cultured 3T3L1 adipocytes dispose of excess medium glucose as lactate under abundant oxygen availability. Scientific reports. 2014;4:3663.
145. Wang H, Meng QH, Gordon JR, Khandwala H, Wu L. Proinflammatory and proapoptotic effects of methylglyoxal on neutrophils from patients with type 2 diabetes mellitus. Clinical biochemistry. 2007;40(16-17):1232-9.
146. Wang X, Desai K, Clausen JT, Wu L. Increased methylglyoxal and advanced glycation end products in kidney from spontaneously hypertensive rats. Kidney international. 2004;66(6):2315-21.
147. Kilhovd BK, Giardino I, Torjesen PA, Birkeland KI, Berg TJ, Thornalley PJ, et al. Increased serum levels of the specific AGE-compound methylglyoxal-derived hydroimidazolone in patients with type 2 diabetes. Metabolism: clinical and experimental. 2003;52(2):163-7.
148. Anguizola J, Matsuda R, Barnaby OS, Hoy KS, Wa C, DeBolt E, et al. Review: Glycation of human serum albumin. Clinica chimica acta; international journal of clinical chemistry. 2013;425:64-76.

149. Bhat S, Jagadeeshaprasad MG, Patil YR, Shaikh ML, Regin BS, Mohan V, et al. Proteomic insight reveals elevated levels of albumin in circulating immune complexes in diabetic plasma. Molecular & cellular proteomics : MCP. 2016.
150. Festa R, Mosca A, Lapolla A, Paleari R, Foti D, Ferrai G, et al. Albumina glicata. Un indice di controllo glicemico da rivalutare. La Rivista Italiana della Medicina di Laboratorio - Italian Journal of Laboratory Medicine. 2012;8(2):71-83.
151. Neelofar KM, Ahmad J, Arif Z, Alam K. Elucidating the impact of glucosylation on human serum albumin: A multi-technique approach. International journal of biological macromolecules. 2016;92:881-91.
152. Raghav A, Ahmad J, Alam K. Impact of glycation on structural and antioxidant function of human serum albumin: Relevance in diabetic complications. Diabetes & metabolic syndrome. 2015.
153. Traldi P, Castilho G, Sartori CH, Machado-Lima A, Nakandakare ER, Correa-Giannella ML, et al. Glycated human serum albumin isolated from poorly controlled diabetic patients impairs cholesterol efflux from macrophages: an investigation by mass spectrometry. Eur J Mass Spectrom (Chichester, Eng). 2015;21(3):233-44.
154. Kuniyasu A, Ohgami N, Hayashi S, Miyazaki A, Horiuchi S, Nakayama H. CD36-mediated endocytic uptake of advanced glycation end products (AGE) in mouse 3T3-L1 and human subcutaneous adipocytes. FEBS letters. 2003;537(1-3):85-90.
155. Baraka-Vidot J, Planesse C, Meilhac O, Militello V, van den Elsen J, Bourdon E, et al. Glycation alters ligand binding, enzymatic, and pharmacological properties of human albumin. Biochemistry. 2015;54(19):3051-62.
156. Mio Hori MY, Keitaro Nomoto, Ryo Ichijo, Akihiko Shimode, Takahiro Kitano, Yonei Y. Experimental Models for Advanced Glycation End Product Formation Using:

Albumin, Collagen, Elastin, Keratin and Proteoglycan. Anti-Aging Medicine 2012;9(5):10.
157. Albrethsen J. Reproducibility in protein profiling by MALDI-TOF mass spectrometry. Clinical chemistry. 2007;53(5):852-8.
158. Amir Arasteh SF, Mehran Habibi-Rezaei and Ali Akbar Moosavi-Movahedi. Glycated albumin: an overview of the In Vitro

models of an In Vivo potential disease marker. Journal of Diabetes & Metabolic Disorders 2014;13(49):1-9.
159. Nativel B, Marimoutou M, Thon-Hon VG, Gunasekaran MK, Andries J, Stanislas G, et al. Soluble HMGB1 is a novel adipokine stimulating IL-6 secretion through RAGE receptor in SW872 preadipocyte cell line: contribution to chronic inflammation in fat tissue. PloS one. 2013;8(9):e76039.
160. Chawla D, Bansal S, Banerjee BD, Madhu SV, Kalra OP, Tripathi AK. Role of advanced glycation end product (AGE)-induced receptor (RAGE) expression in diabetic vascular complications. Microvascular research. 2014;95:1-6.
161. Wu CH, Huang HW, Huang SM, Lin JA, Yeh CT, Yen GC. AGE-induced interference of glucose uptake and transport as a possible cause of insulin resistance in adipocytes. Journal of agricultural and food chemistry. 2011;59(14):7978-84.
162. Leguisamo NM, Lehnen AM, Machado UF, Okamoto MM, Markoski MM, Pinto GH, et al. GLUT4 content decreases along with insulin resistance and high levels of inflammatory markers in rats with metabolic syndrome. Cardiovascular diabetology. 2012;11:100.
163. Chiu CY, Yang RS, Sheu ML, Chan DC, Yang TH, Tsai KS, et al. Advanced glycation end-products induce skeletal muscle atrophy and dysfunction in diabetic mice via a RAGE-mediated, AMPK-down-regulated, Akt pathway. The Journal of pathology. 2016;238(3):470-82.
164. Kirsi H. Pietilainen TR, Tuulikki Seppaanen-Laakso, Sam Virtue, Peddinti, Gopalacharyulu JT, Sergio Rodriguez-Cuenca, Arkadiusz Maciejewski, Jussi, Naukkarinen A-LR, ¨ PSN, Velagapudi SC,

Heli Nygren, Tuulia Hyo, Yki-Ja H, et al. Association of Lipidome Remodeling in the Adipocyte Membrane with Acquired Obesity in Humans. PLoS Biology. 2011;9(6).
165. Moraes-Vieira PM, Saghatelian A, Kahn BB. GLUT4 Expression in Adipocytes Regulates De Novo Lipogenesis and Levels of a Novel Class of Lipids With Antidiabetic and Anti-inflammatory Effects. Diabetes. 2016;65(7):1808-15.
166. Yore MM, Syed I, Moraes-Vieira PM, Zhang T, Herman MA, Homan EA, et al. Discovery of a class of endogenous mammalian lipids with anti-diabetic and anti-inflammatory effects. Cell. 2014;159(2):318-32.
167. Narayanaswamy P, Shinde S, Sulc R, Kraut R, Staples G, Thiam CH, et al. Lipidomic "deep profiling": an enhanced workflow to reveal new molecular species of signaling lipids. Analytical chemistry. 2014;86(6):3043-7.
168. Anne Barden PDTM, Ph.D. Measurement of lipid mediators of resolution of inflammation after ω-3 fatty acid supplementation in humans. CAYMAN CHEMICAL COMPANY. 2015(25):1-12.
169. Weijers RN. Lipid composition of cell membranes and its relevance in type 2 diabetes mellitus. Current diabetes reviews. 2012;8(5):390-400.
170. Pietilainen KH, Sysi-Aho M, Rissanen A, Seppanen-Laakso T, Yki-Jarvinen H, Kaprio J, et al. Acquired obesity is associated with changes in the serum lipidomic profile independent of genetic effects--a monozygotic twin study. PloS one. 2007;2(2):e218.
171. Hur KY, Lee MS. New mechanisms of metformin action: Focusing on mitochondria and the gut. Journal of diabetes investigation. 2015;6(6):600-9.
172. Ishibashi Y, Matsui T, Takeuchi M, Yamagishi S. Metformin inhibits advanced glycation end products (AGEs)-induced renal tubular cell injury by suppressing reactive oxygen species generation via reducing receptor for AGEs (RAGE) expression. Hormone and metabolic research = Hormon- und Stoffwechselforschung = Hormones et metabolisme. 2012;44(12):891-5.
173. Inzucchi SE, Lipska KJ, Mayo H, Bailey CJ, McGuire DK. Metformin in patients with type 2 diabetes and kidney disease: a systematic review. Jama. 2014;312(24):2668-75.
174. Viollet B, Guigas B, Sanz Garcia N, Leclerc J, Foretz M, Andreelli F. Cellular and molecular mechanisms of metformin: an overview. Clinical science (London, England : 1979). 2012;122(6):253-70.
175. Baruah MP, Kalra S, Ranabir S. Metformin; A character actor in the leptin story! Indian journal of endocrinology and metabolism. 2012;16(Suppl 3):S532-3.
176. Awan ARKaFR. Leptin Resistance: A Possible Interface Between Obesity and Pulmonary-Related Disorders. Int J Endocrinol Metab. 2016;1(14):1-6.
177. Adamia N, Virsaladze D, Charkviani N, Skhirtladze M, Khutsishvili M. Effect of metformin therapy on plasma adiponectin and leptin levels in obese and insulin resistant postmenopausal females with type 2 diabetes. Georgian medical news. 2007(145):52-5.
178. Litwinoff EM, Hurtado Del Pozo C, Ramasamy R, Schmidt AM. Emerging targets for therapeutic development in diabetes and its complications: The RAGE signaling pathway. Clinical pharmacology and therapeutics. 2015.
179. Tahara N, Yamagishi S, Takeuchi M, Tahara A, Kaifu K, Ueda S, et al. Serum levels of advanced glycation end products (AGEs) are independently correlated with circulating levels of dipeptidyl peptidase-4 (DPP-4) in humans. Clinical biochemistry. 2013;46(4-5):300-3.
180. Ueda S, Yamagishi S, Matsui T, Noda Y, Ueda S, Jinnouchi Y, et al. Serum levels of advanced glycation end products (AGEs) are inversely associated with the number and migratory activity of circulating endothelial progenitor cells in apparently healthy subjects. Cardiovascular therapeutics. 2012;30(4):249-54.
181. Sell H, Bluher M, Kloting N, Schlich R, Willems M, Ruppe F, et al. Adipose dipeptidyl peptidase-4 and obesity: correlation with insulin resistance and depot-specific release from adipose tissue in vivo and in vitro. Diabetes care. 2013;36(12):4083-90

APPENDIX

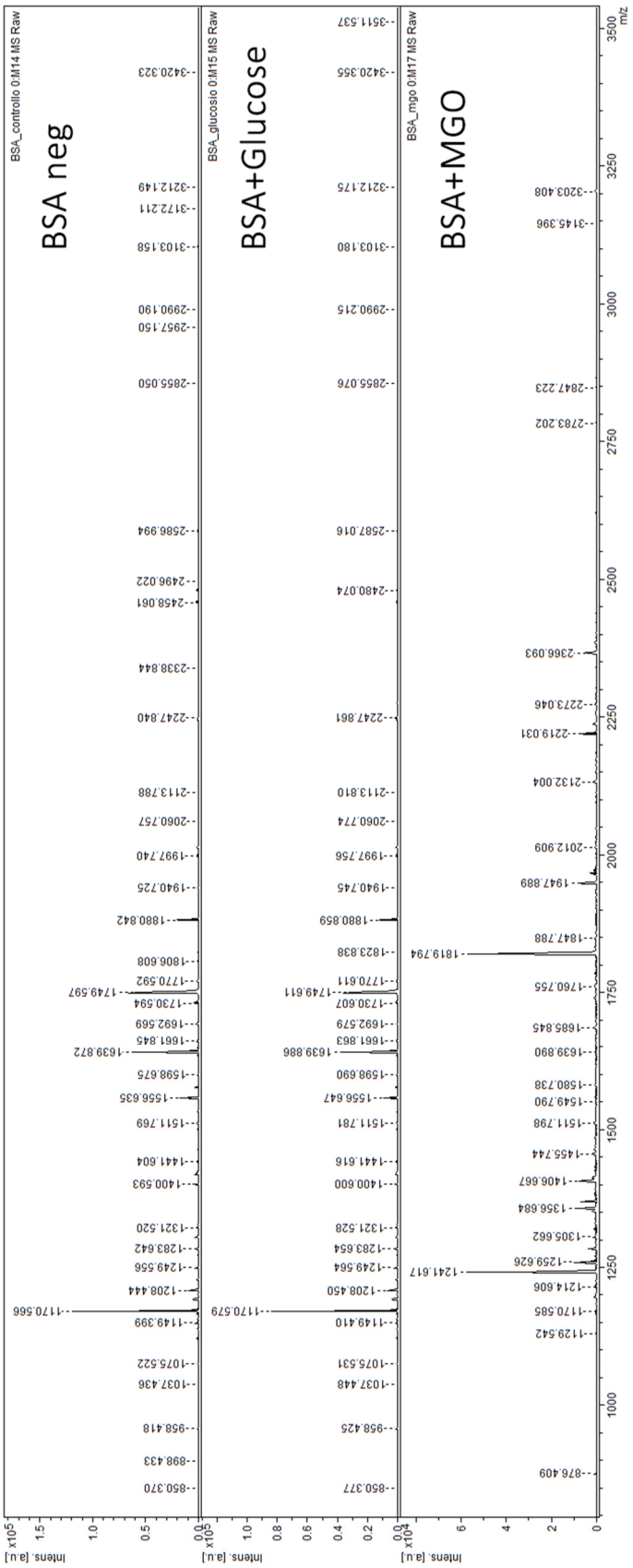

Figure 4.4

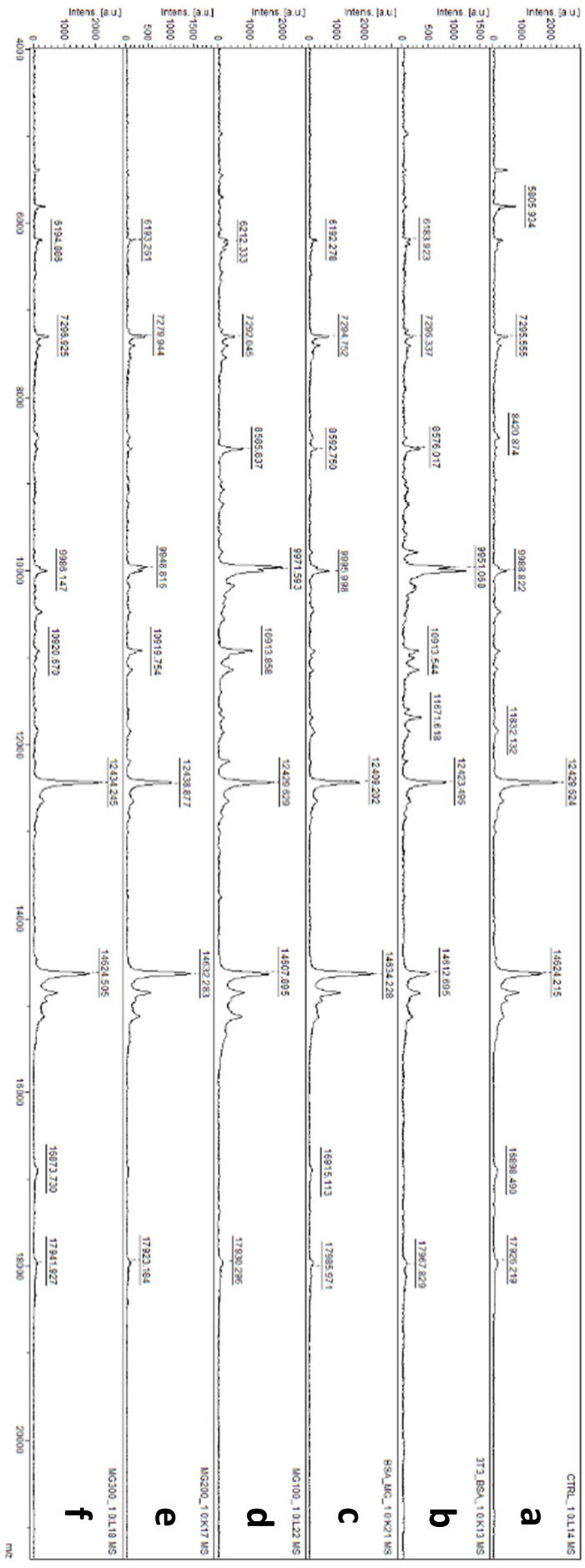
a
b
c
d
e
f
CTRL_1 0L14 MS
3T3_BSA_1 0K13 MS
BSA_MG_1 0K21 MS
MG100_1 0L22 MS
MG200_1 0K17 MS
MG300_1 0L19 MS
Intens. [a.u.]
m/z
5805.924
7295.655
8409.874
9851.059
9983.822
11832.132
12428.924
14624.215
16898.490
17926.219
6183.923
7286.337
8576.017
10913.544
11671.618
12423.495
14512.695
17967.829
6192.278
7284.702
8592.759
9996.938
12408.292
14534.228
16915.113
17985.971
6212.333
7292.845
8595.637
9971.593
10913.858
12429.829
14507.895
17930.286
6183.251
7279.944
9848.816
10619.754
12438.677
14632.283
17923.164
6194.889
7296.925
9988.147
10920.870
12434.245
14624.505
16873.730
17941.927

Figure 4.22